159757

U.S. GEOLOGICAL SURVEY LIBRARY

CLASS

(200) R29o

no.201,1952

USGS LIBRARY - RESTON
3 1818 00083486 9

(200)
R290
no. 201
1952

U. S. Geological Survey.
Reports open file.

U. S. GEOLOGICAL SURVEY
159757
LIBRARY
4 JAN 1957

200)
R29o
no. 201

U. S. Geological Survey
[Reports - Open file series

THE THEORY OF DIRECT CURRENT PROSPECTING IN THE PRESENCE OF CURVED BOUNDARY SURFACES

ROBERT G. VAN NOSTRAND, 1918-
U. S. GEOLOGICAL SURVEY

1952

This report and accompanying illustrations are preliminary and have not been edited or reviewed for conformity with Geological Survey standards and nomenclature.

U. S. GEOLOGICAL SURVEY
WASHINGTON
AUG 14 1953
LIBRARY

TABLE OF CONTENTS

Page

Part One - General Considerations

I Introduction 1

II Electrode Configurations 1

III Prior Theoretical Studies 4

IV Modes of Current Flow 8

V Object of the Present Paper 9

Part Two - Ellipsoidal Boundaries

VI Prolate Spheroidal Coordinates 11

VII Oblate Spheroidal Coordinates 14

VIII Solution of Laplace's Equation 16

IX Expansion of the Reciprocal Distance 19

X The Ellipsoidal Sink 26

XI The Equations Applied 29

XII The Hemispherical Sink 31

XIII Computations 35

Part Three - Buried Spheres

XIV Bipolar Coordinates 39

XV A Solution of Laplace's Equation in Bipolar Coordinates 42

XVI Special Case of Conducting Spheres 44

XVII Conclusions Drawn from the Conducting sphere problem 50

Part Four - The Cone Problem

XVIII A Solution of Laplace's Equation in Spherical Coordinates 55

XIX Expansion of the Reciprocal Distance in Cone Functions 57

XX Behavior of the Solution at the Origin 63

XXI Conal Boundaries 66

Part Five - Hyperboloidal Boundaries

XXII A Second Solution of Laplace's Equation in Prolate Spheroidal Coordinates 69

XXIII Orthogonality of the Hyperboloid Functions 71

XXIV Expansion of the Reciprocal Distance in Hyperboloid Functions 77

XXV A Buried Dome Structure 79

XXVI The Effect of Topography 85

Part Six - Investigation of a Geologic Problem

XXVII The Use of Horizontal Profiles 88

XXVIII The Use of Equiresistivity Maps 93

XXIX The Use of Depth Profiles 102

Bibliography 108

LIST OF ILLUSTRATIONS

		Page
1.	A Sketch of the Wenner Configuration	2
2.	Prolate Spheroidal Coordinates	12
3.	Oblate Spheroidal Coordinates	15
4.	Arbitrary Traverse over Hemispherical Sink	34
5.	Sample Computation Sheet	37
6.	Dipolar Coordinates	40
7.	Depth Profiles over Buried Conducting Spheres	52
8.	Cross-section of Double Cone	57
9.	Estimation of Depth Profile over a Buried Dome Structure	83
10.	Comparison of Horizontal Profiles Using the Lee Configuration with an Electrode Separation of 100 feet	91
11.	Geologic Section along Traverse 21500N	94
12.	Equiresistivity Map (Wenner Plotting) over Filled Sink ..	97
13.	Equiresistivity Map (Lee Plotting) over Filled Sink	98
14.	Theoretical Equiresistivity Map (Wenner Plotting) over Hemispherical Sink	100
15.	Theoretical Equiresistivity Map (Lee Plotting) over Hemispherical Sink	101
16.	Comparison of Depth Profiles over Various Filled Sinks ..	103
17.	Theoretical Depth Profiles over Hemispherical Sink	106

PART ONE - GENERAL CONSIDERATIONS

I

INTRODUCTION

It is generally conceded that direct current methods of geophysical prospecting had their start in a proposal by Frank Wenner in 1915.[1] However, this suggestion was not put to use until 1925 when Rooney and Gish[2] undertook resistivity measurements near Watheroo, Australia and Ebro, Spain. Since that time, the literature has been profuse with reports on a wide variety of field problems. Moreover, the hope for exact theoretical explanations has excited the imagination of geophysicists and a wealth of theoretical discussions supplement the reports on field work. A brief outline of the more important theoretical work is included here to provide a background for the development which is to follow.

II

ELECTRODE CONFIGURATIONS

Wenner[1] proposed four electrodes disposed in a line on the surface of the ground as shown in figure one; the distance between neighboring electrodes is "a" meters. A direct current of I amperes is supplied to the ground through two steel stakes at C_1 and C_2. By means of a potentiometer, the potential difference of V volts between the points P_1 and P_2 is measured. Wenner showed by elementary means that the potential due to a single point source of current, of strength I, on the

---

1. Wenner, 1915. See the bibliography for complete references.
2. Gish and Rooney, 1925.

surface of a homogeneous earth, is given by:

(1) $$U = \frac{I\rho}{2\pi R}$$

where R is the distance in meters from the source to the point at which the potential is to be determined and ρ is the uniform resistivity, given in meter-ohms, of the earth. Using this expression, it is found, in terms of the quantities given above, that the resistivity of the medium is:

(2) $$\rho_a = 2\pi a \frac{V}{I}$$

The derivation of this relationship is based upon the assumption of an isotropic, homogeneous earth. In practice, however, the earth under investigation is neither homogeneous nor isotropic. Therefore, the measured quantity represents an average effect; and, as such, it is called the apparent resistivity.

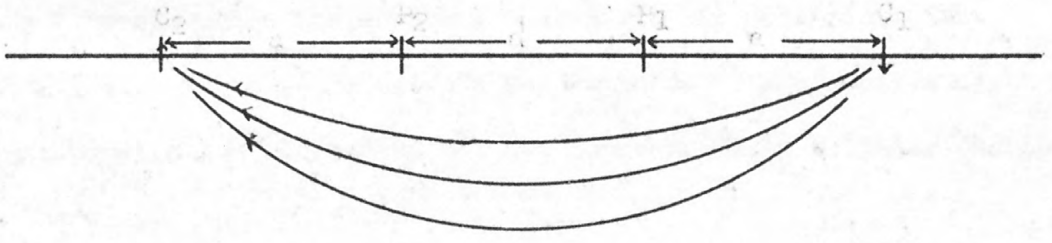

Figure One - A Sketch of the Wenner Configuration.

A second configuration of electrodes, for which curves will also be constructed in this paper, is the one proposed by Lee.[3] This

3. Lee, 1934.

"partitioning" configuration differs from the Wenner arrangement in that a third potential electrode, P_0, is placed midway between P_1 and P_2. The potential differences P_1-P_0 and P_0-P_2 are both measured. In this case, the apparent resistivity is given by:

$$(3) \quad \rho_a = 4\pi a \frac{V}{I}$$

where V is now one or the other of the two potential differences. The advocates of the Lee configuration use it to learn something about the symmetry -- or lack of symmetry - of the potential distribution in a given situation.

There are two standard techniques used to investigate the apparent resistivity of the earth in a given region. In horizontal profiling, or traversing, the electrode separation is maintained at an arbitrary value and the whole configuration is moved from point to point along a predetermined line or traverse; the line of electrodes is normally oriented in the direction of the traverse. In vertical or depth profiling, the center of the electrode configuration is fixed at a point on the traverse while the apparent resistivity is determined for systematically increased electrode separations. The effective depth of current penetration increases, but not necessarily in a linear fashion, with the electrode separation.

In horizontal profiling, measurements may be restricted rather successfully to horizontal changes in the earth's resistivity. However, it is to be noted that the apparent resistivities, as determined by vertical profiling, may be affected greatly by any horizontal changes in the actual resistivity as well as by the vertical changes which are being investigated.

III

PRIOR THEORETICAL STUDIES

The subject of the most extensive study has been in the field of horizontal bedding; several attempts have been made at quantitative interpretation in the case of a small number of beds. In each case, the main mathematical problem is one of deriving a suitable expression for the potential due to a point source of current in the presence of the geologic structure being investigated.

Hummel[1] has obtained a complete formulation for the simple case of two layers, the lower one of which extends infinitely downward. His method involves the use of an infinite series of images, whose strengths and positions are chosen in such a way as to satisfy the boundary conditions. In the same paper, he gave, without derivation, an incomplete expression for the three-layer case. Stefanesco and the Schlumberger brothers[2] have solved the latter problem completely through the methods of differential equations. The solutions were first obtained as sets of two or three infinite integrals whose integrands contained Bessel functions of zero order. The authors reduced each of these integrals to an infinite series and then proceeded to show that their solutions were equivalent to those of Hummel.

Roman[3] presented a complete treatment of the three-layer problem, each layer being of different resistivity from the others and the lower layer extending infinitely downward. In that paper, the author used the theory of images and gave an excellent background for the

---

1. Hummel, 1932.
2. Stefanesco et al., 1930.
3. Roman, 1933.

development of the method. Previously, Ehrenburg and Watson[4] had considered the problem of current flow through a medium composed of layers of equal thickness. The general method is indicated for an arbitrary number of layers, but explicit results are given only for those cases up to five equally thick layers.

Numerical calculations were accomplished only to a very limited extent in the above references. Tagg[5] was the first to prepare a major set of curves, these being for the two-layer case. His method of interpretation is essentially one of solving simultaneous equations graphically to determine the resistivity of the lower bed and the depth of the boundary. To use Tagg's method, one must prepare a field curve of apparent resistivity as a function of electrode separation at a given station. From this curve can be obtained the resistivity of the upper bed. This curve and Tagg's master curves are then used together to obtain a third set of curves whose intersection yield the desired results.

Roman[6] has proposed a somewhat simpler method of interpretation for the two-layer problem. He prepared a set of master curves, which he advises should be transferred to a transparent plastic sheet for field use. The necessary numerical tables are also given so that one may prepare his own reference curves. One plots his field curve to correspond to the master curves; after which, he determines directly the resistivities and the boundary depth by noting visually which of the standard curves most nearly matches his field plot.

---

4. Ehrenburg and Watson, 1931.
5. Tagg, 1934.
6. Roman, 1934 and 1941.

It should be noted that, except for scale, each of the above discussions applies equally well to both the Wenner and Lee configurations when employed in vertical profiling. However, care must be taken because this generalization is valid only if there are no horizontal changes in the earth's resistivity.

The mathematical methods of the above discussions may be applied directly to situations in which there are parallel, vertical boundaries between materials of different resistivities. However, no extensive work appears to have been accomplished along these lines; only the simplest case of a single boundary between materials of two different resistivities has been considered. Tagg[5] has published a series of curves of apparent resistivity, as determined by the Wenner configuration used in horizontal profiling, for various ratios of the two resistivities. Similar curves have been presented for the Wenner configuration for the case in which plane, vertical insulating and conducting sheets are imbedded in a material of otherwise uniform resistivity.[7]

The problem of dipping beds is more complicated. An attempt has been made by Aldredge[8] and others using the method of images to solve the case of a single, sloping boundary between two materials of different resistivities. It appears that the results may be considered only as an approximation at best, since the solution is restricted to the effect of a finite number of images, in analogy with the reflection of light, even for arbitrary angles. Moreover, the author cautions that the treatment is valid only when all electrodes are in the overlying material.

---

7. Hubbert, 1934.
8. Aldredge, 1937.

Complete solutions of the same problem are claimed by Russian workers. The first success consisted on solving an integral equation by means of successive approximations.[9] The results are applied to the important special case of layers differing considerably in resistivity; in which case, relatively simple, approximate formulae are obtained. An exact solution is obtained in the second instance[10] by transforming both the applicable differential equation and the boundary conditions and then by going on to solve the resulting equations. To accomplish the transformations, the author used a Bessel transform, analogous to the Fourier transform, in which the integrand is a Bessel function of imaginary order. The author goes on to apply his solution to special cases in which the dip is some simple angle such as 30 degrees, 45 degrees, etc., for which only elementary functions are involved. Although the author claims that his formulae in these special cases are convenient for numerical integration, no known curves have appeared in the literature to this writing.

Apparently, only Russian workers have offered a serious investigation of the effect of curved boundary surfaces. Tikhonov[11] has studied the distortion of the field of terrestrial currents caused by an infinite, horizontal cylinder buried in the earth. He presents a variety of curves of equipotential lines and apparent resistivities as a function of the position of the embedded body and its actual resistivity. Lipskaya[12] has worked out a similar problem concerning buried conducting

---

9. Tikhonov, 1946.
10. Skalskaya, 1948.
11. Tikhonov, 1942.
12. Lipskaya, 1949.

spheres. In his first article, he discussed the use of bipolar coordinates in electrostatic problems and presents some solutions for the case when the charge lies on the polar axis. In his second article, he uses the method of images to discuss the effect of a buried conducting sphere on a resistivity survey. Lipskaya's work partly parallels the discussion in Part Three of this paper. However, the present author has made additional calculations, has presented a new set of curves, and has used the results to draw pertinent conclusions concerning the limitations on the use of all resistivity methods of prospecting.

Other theoretical and empirical treatments occur throughout the journals. An extensive discussion of the whole subject has been prepared by Roman;[13] and, anyone wishing to study this field further should consult that paper, paying particular attention to its accompanying bibliography. Also, the two major reference texts[14,15] in geophysics present fairly complete backgrounds in the present subject.

IV

MODES OF CURRENT FLOW

Three means are available for the flow of current through the earth. Both direct and alternating current may flow by metallic and electrolytic conduction. The latter mode, in which the major transporting agent is normally ionized sodium chloride, is by far the most important at low frequencies.[16] Alternating current may also be carried by dielectric conduction - i.e., as displacement current.

In each of the theoretical studies mentioned in the previous

---

13. Roman, 1952.
14. Heiland, 1940.
15. Jakosky, 1950.
16. Heiland, p 26.

section, the authors have assumed the law of ohmic conduction which is obeyed by both metallic and electrolytic conduction. More recently, a modified theory of current flow in stratified earth has been advanced to explain certain phenomena.[17] It is suggested that, on some bedding planes, effectively there exists an electrical double layer. As the current is gradually increased,[18] this double layer acts as a barrier to the current until the potential due to the current at the boundary equals the potential barrier in magnitude; at which instance, the current breaks through the boundary. Obviously, the double layer offers no resistance to current returning to the surface of the earth. This phenomenon appears as an abrupt break in the curve formed by plotting the apparent resistivity against the current for a given electrode separation. When such a situation exists, the theoretical results based on Ohm's law are not strictly valid.

V

OBJECT OF THE PRESENT PAPER

It is the purpose of this paper to extend the theoretical treatment of surface potential methods of geophysical prospecting into the realm of curved surfaces of discontinuity. The most logical beginning for such an extension appears to lie in the family of geologic features which includes filled sinks and certain consolidated masses embedded in the earth. Accordingly, the use of elliptic coordinates and of bipolar coordinates is introduced in Parts Two and Three respectively. The first may be used to approximate filled sinks while the latter may

---

17. Lee, 1948, pp 14-16.
18. Refer to figure one.

serve satisfactorily to describe buried masses of spherical shape.

And, since elliptic coordinates may also be used to describe features which are approximated by hyperboloids of revolution, Part Five is devoted to a discussion of that class of structures.

The problem of conal boundaries has been given no direct application to geophysics. However, since it represents the limiting case of the corresponding hyperboloidal problem, the cone problem has been included and is made the subject of Part Four.

Several attempts are made to show various ways in which the present results may be used. In Part Three, some conclusions are drawn concerning the useful limits of direct current methods of prospecting. In Part Five, it is pointed out how one may approximate curves involving hyperbolic discontinuities from results in previous sections. And, the whole of Part Six is devoted to a discussion of application of the theory of resistivity surveys in the vicinity of filled sinks, with emphasis on field examples.

PART TWO

ELLIPSOIDAL BOUNDARIES

VI

PROLATE SPHEROIDAL COORDINATES

Consider figure two in which a set of confocal ellipses and hyperboloas are shown in the XZ-plane. The foci of both the ellipses and the hyperbolas are at $z = \pm b$. If these curves are rotated about the Z-axis, they will generate surfaces which, in cylindrical coordinates, can be expressed in the form:

$$(4) \qquad \frac{\rho^2}{u^2 - b^2} + \frac{z^2}{u^2} = 1$$

where u is the parameter determining which of the surfaces is being described.

If u^2 is greater than b^2, the equation represents the ellipsoids. Since the complete positive range of u covers all of the possible ellipsoids, it is not necessary to consider the negative values of u. As u becomes infinite, the surface approaches a spherical form; and, as u approaches b, the surface degenerates into that part of the Z-axis lying between plus b and minus b. Replacing u by $b\eta$, where $1 \leq \eta < \infty$, the equation for these ellipsoids becomes:

$$(5) \qquad \frac{z^2}{b^2\eta^2} + \frac{\rho^2}{b^2(\eta^2 - 1)} = 1$$

Similarly, if u^2 is less than b^2, the equation represents the hyperboloids. In this case, as u approaches b, the surface degenerates into that portion of the Z-axis for which z is greater than plus b or less than minus b - according as u is positive or negative. Replacing

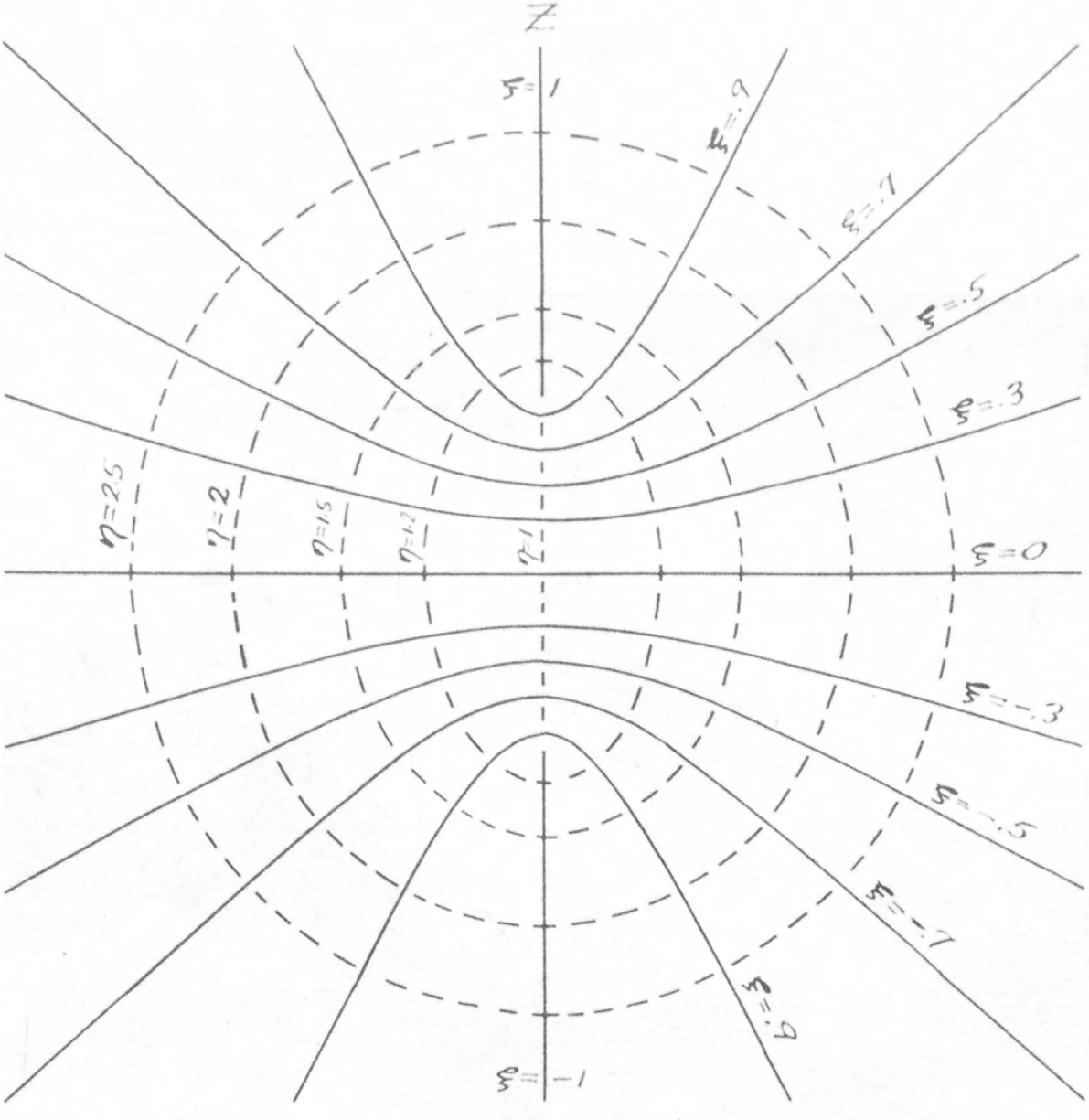

Figure Two - Prolate Spheroidal Coordinates.

u by $b\xi$, where $1 \geq \xi \geq -1$, the equation for the Hyperboloids becomes:

$$(6) \qquad \frac{z^2}{b^2\xi^2} - \frac{\rho^2}{b^2(1-\xi^2)} = 1$$

The third coordinate is identical with the angle φ from the cylindrical coordinates - which in turn corresponds to the longitudinal angle of spherical coordinates.

It may be necessary later to transform these coordinates to cylindrical coordinates. This transformation is indicated by solving equations 4 and 5 simultaneously for ρ and z. One gets:

$$(7) \qquad \begin{aligned} z &= b\eta\xi \\ \rho &= b\sqrt{(1-\xi^2)(\eta^2-1)} \end{aligned}$$

In terms of the variables η, ξ, and φ, Laplace's equation is written:[1]

$$(8) \qquad \nabla^2 u = \frac{\partial}{\partial\eta}\left[(\eta^2-1)\frac{\partial u}{\partial\eta}\right] + \frac{\partial}{\partial\xi}\left[(1-\xi^2)\frac{\partial u}{\partial\xi}\right] + \frac{(\eta^2-\xi^2)}{(1-\xi^2)(\eta^2-1)}\frac{\partial^2 u}{\partial\varphi^2} = 0$$

and the three components of the gradient are:

$$(9) \qquad \begin{cases} (\nabla u)_\eta = \dfrac{1}{b}\sqrt{\dfrac{\eta^2-1}{\eta^2-\xi^2}}\,\dfrac{\partial u}{\partial\eta} \\[2ex] (\nabla u)_\xi = \dfrac{1}{b}\sqrt{\dfrac{1-\xi^2}{\eta^2-\xi^2}}\,\dfrac{\partial u}{\partial\eta} \\[2ex] (\nabla u)_\varphi = \dfrac{1}{b\sqrt{(1-\xi^2)(\eta^2-1)}}\,\dfrac{\partial u}{\partial\varphi} \end{cases}$$

---

1. Smythe, pp 167-168.

VII

OBLATE SPHEROIDAL COORDINATES

In order to complete the range of possible ellipsoids of revolution which may be examined, it becomes necessary to introduce oblate spheroidal coordinates. In the previous system, the axis of revolution is the longest dimension of the ellipsoids; in the present case, the axis of revolution is the shortest dimension of the ellipsoids. Since the development closely parallels that of the prolate spheroidal coordinates, many of the details are omitted.

Consider figure three in which is shown the coordinate system as it appears in the meridian plane $\phi = 0$. The complete coordinate system is obtained if the curves shown are rotated about the Z-axis. The first variable is ζ which varies from zero to infinity and which forms the parameter in the family of oblate spheroids. The second variable is μ which varies between plus and minus one, and constitutes the parameter in the set of hyperboloids of one sheet. And, the third coordinate is again the longitudinal angle ϕ which varies from zero to 2π. It is seen that $\zeta = 0$ is represented by a circular disk of radius b, lying in the equatorial plane with its center at the origin; the remainder of the equatorial plane is described by $\mu = 0$. The Z- or polar axis is the line along which $\mu = \pm 1$. In relating these coordinates to cylindrical coordinates, it is found that the correct correspondence is given by:

$$(10) \begin{cases} z = b\zeta\mu \\ \rho = b\sqrt{(1+\zeta^2)(1-\mu^2)} \end{cases}$$

---

1. Smythe, pp 158-167.

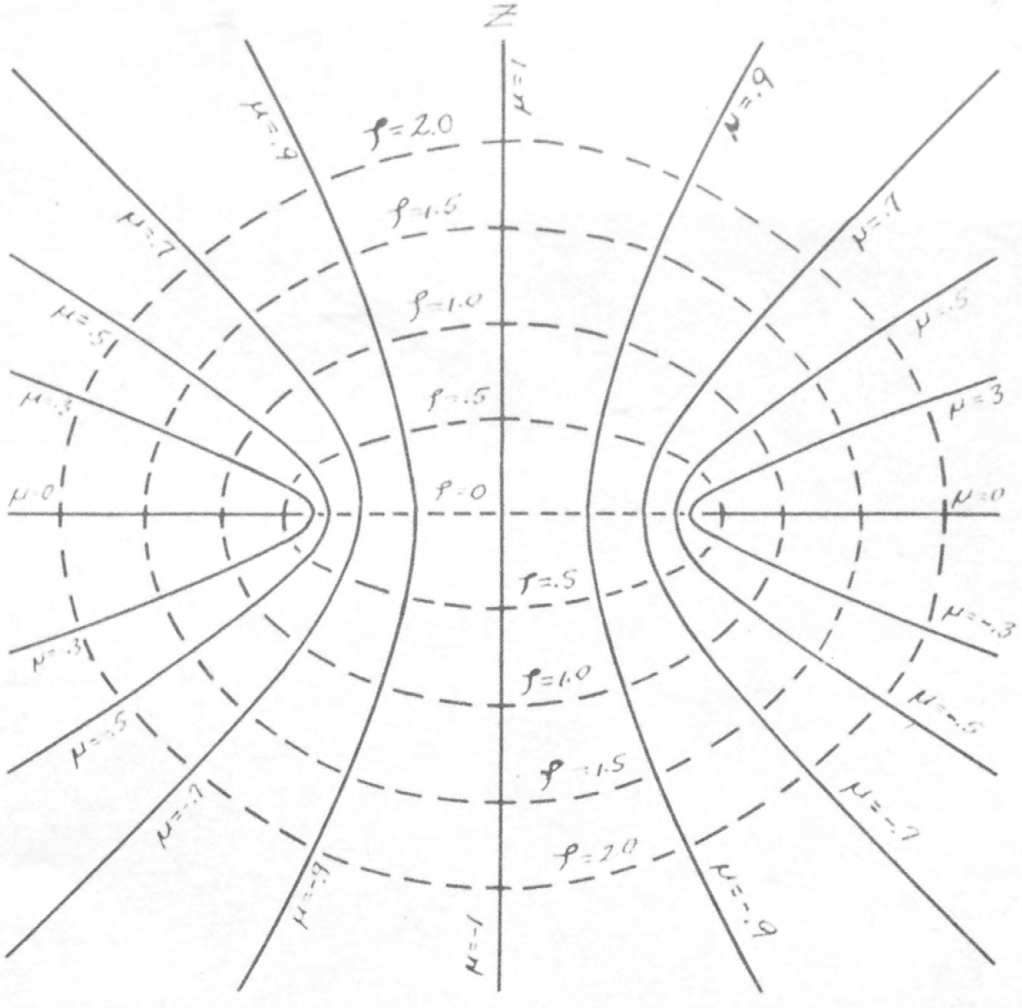

Figure Three - Oblate Spheroidal Coordinates.

while the angle φ is identical in both systems.

In terms of these variables, Laplace's equation becomes:

$$(11)\quad \frac{\partial}{\partial\mu}\left[(1-\mu^2)\frac{\partial u}{\partial\mu}\right]+\frac{\partial}{\partial\xi}\left[(1+\xi^2)\frac{\partial u}{\partial\xi}\right]+\frac{\mu^2+\xi^2}{(1+\xi^2)(1-\mu^2)}\frac{\partial^2 u}{\partial\varphi^2}=0$$

and the three components of the gradient are:

$$(12)\quad \begin{cases} (\nabla u)_\xi = \dfrac{1}{b}\sqrt{\dfrac{\xi^2+1}{\xi^2+\mu^2}}\,\dfrac{\partial u}{\partial\xi} \\[2ex] (\nabla u)_\mu = \dfrac{1}{b}\sqrt{\dfrac{1-\mu^2}{\xi^2+\mu^2}}\,\dfrac{\partial u}{\partial\mu} \\[2ex] (\nabla u)_\varphi = \dfrac{1}{b\sqrt{(1+\xi^2)(1-\mu^2)}}\,\dfrac{\partial u}{\partial\varphi} \end{cases}$$

VIII

SOLUTION OF LAPLACE'S EQUATION

Laplace's equation in prolate spheroidal coordinates is set down in equation 8 in section VI. The variables in this equation may be separated by the assumption of a solution in the form:

$$(13)\quad u = G(\xi)H(\eta)\Phi(\varphi)$$

In terms of the new dependent variables, equation 8 becomes:

$$(14)\quad \frac{1}{G}\frac{d}{d\xi}\left[(1-\xi^2)\frac{dG}{d\xi}\right]+\frac{1}{H}\frac{d}{d\eta}\left[(\eta^2-1)\frac{dH}{d\eta}\right]+\frac{(\eta^2-\xi^2)}{(1-\xi^2)(\eta^2-1)}\frac{1}{\Phi}\frac{d^2\Phi}{d\varphi^2}=0$$

The first step in the solution of the equation as it now stands is to set the term involving Φ equal to a constant so that:

$$(15)\quad \frac{d^2\Phi}{d\varphi^2}+m^2\Phi=0$$

whence the φ dependence of the solution is given by:

$$(16) \quad \Phi_m = A_m \cos m\varphi + B_m \sin m\varphi$$

When the relationship 15 is substituted back into equation 14, it is found that G and H both satisfy an equation of the same form. In the case of G, the equation is:

$$(17) \quad \frac{d}{d\xi}\left[(1-\xi^2)\frac{dG}{d\xi}\right] + \left[n(n+1) - \frac{m^2}{1-\xi^2}\right]G = 0$$

which is the associated Legendre equation. Thus, the dependence of the solution upon ξ and η is given by:

$$(18) \quad \begin{aligned} G &= C_{mn} P_n^m(\xi) + D_{mn} Q_n^m(\xi) \\ H &= E_{mn} P_n^m(\eta) + F_{mn} Q_n^m(\eta) \end{aligned}$$

where $P_n^m(\ )$ and $Q_n^m(\ )$ are the associated Legendre functions of the first and second kind respectively. In these expressions, both m and n must be integers; and, the absolute value of m can be no larger than the value of n.

It is necessary at this point to define the associated Legendre functions in the above solutions. One may define the Legendre polynomials by:[1]

$$(19) \quad P_n(x) = \frac{1}{2^n} \sum_{r=0}^{r=s} \frac{(-1)^r (2n-2r)!}{r!\,(n-r)!\,(n-2r)!} x^{n-2r}$$

where s is n/2 or (n - 1)/2, whichever is an integer. An alternate expression is Rodrigue's formula:[2]

---

1. Logan, p 1.
2. Smythe, p 135.

$$(20) \quad P_n(x) = \frac{1}{2^n n!} \frac{d^n (x^2-1)^n}{dx^n}$$

Either equation 19 or 20 is valid regardless of the range of x, providing m and n are integers.[2] If x lies between plus and minus one, the associated Legendre polynomial is defined as:

$$(21) \quad P_n^m(x) = (1-x^2)^{m/2} \frac{d^m P_n(x)}{dx^m}$$

which may be verified by substituting the expression on the right into equation 17 for example. If the absolute value of the argument of the function is greater than one, the associated Legendre polynomial is defined as:

$$(22) \quad P_n^m(x) = (x^2-1)^{m/2} \frac{d^m P_n(x)}{dx^m}$$

When results from other sources have been taken into this paper, or have been compared with results in this paper, definitions have been changed to conform to the above equations. For example, the expression on the right side of equation 21 differs from that given by Hobson[3] since he uses the expression in equation 22 to define $P_n^m(x)$ for all values of the argument.

For the Legendre function of the second kind, one may write:[2]

$$(23) \quad Q_n(x) = 2^n \sum_{s=0}^{\infty} \frac{(n+s)!\,(n+2s)!}{s!\,(2n+2s+1)!} x^{-n-2s-1}$$

The associated functions of the second kind may be defined by equations 21 and 22 if the P's are replaced by the corresponding Q's.

---

3. Hobson, p 90.

Since the most general solution is the sum of all possible solutions for the various values of m and n, one finally obtains:

$$U = \sum_{n=0}^{\infty} \sum_{m=-n}^{m=+n} \left[A_m \cos m\varphi + B_m \sin m\varphi\right] \cdots$$

(24)

$$\cdots \left[C_{mn} P_n^m(\xi) + D_{mn} Q_n^m(\xi)\right]\left[E_{mn} P_n^m(\eta) + F_{mn} Q_n^m(\eta)\right]$$

Equation 24 represents the general solution of Laplace's equation in prolate spheroidal coordinates. The functions in this solution are orthogonal over the ellipsoidal surfaces; which fact differentiates it from a second general solution which is presented in Part Five.

The separation of variables in Laplace's equation in oblate spheroidal coordinates, that is equation 11, follows the same line of reasoning as was presented in the case of equation 8, with one exception; the ζ -equation has the form of the associated Legendre equation in which the independent variable is $i\zeta$. It follows then that a general solution of Laplace's equation in oblate spheroidal coordinates is:

$$U = \sum_{n=0}^{\infty} \sum_{m=-n}^{m=n} \left[A_m \cos m\varphi + B_m \sin m\varphi\right] \cdots$$

(25)

$$\cdots \left[C_{mn} P_n^m(\mu) + D_{mn} Q_n^m(\mu)\right]\left[E_{mn} P_n^m(i\zeta) + F_{mn} Q_n^m(i\zeta)\right]$$

This solution, as does equation 24, contains functions which are orthogonal over the elliptical surfaces.

IX

EXPANSION OF THE RECIPROCAL DISTANCE

Before going on to apply the above solutions to specific physical problems, it is first useful to calculate the expressions for the field due to a point source of current in terms of the functions used in equations 24 and 25. From equation 1, it is readily seen that this

calculation amounts to an expansion of a reciprocal distance in terms of these functions.

In prolate spheroidal coordinates, let the coordinates of a source of strength I be ξ_0, η_0, and $\varphi = 0$. There is no loss of generality in choosing the meridian plane such that it contains the source; and, this choice is convenient in that it restricts the expression for the potential to even functions of φ. Therefore, the sine term may be discarded from equation 24.

It is now necessary to examine $P_n^m(\ )$ and $Q_n^m(\ )$ to learn whether they behave properly throughout the ranges of their arguments in this problem. Such relationships are well known;[1] both functions are continuous within the limits of their respective arguments. For argument zero, both functions remain finite; for argument unity, $P_n^m(\ )$ remains finite but $Q_n^m(\ )$ becomes infinite; and, at infinity, $P_n^m(\ )$ becomes infinite while $Q_n^m(\ )$ vanishes as the inverse $(n+1)$ power of the argument.

In view of the above facts, it becomes desirable to divide space into two regions, the first for which $1 \leq \eta \leq \eta_0$ and a second for which $\eta_0 \leq \eta < \infty$. Then, in the first region, where both ξ and η are sometimes unity, the potential has the form:

$$(26) \quad U_1 = \sum_{m,n} A_0 P_n^m(\eta) P_n^m(\xi) \cos m\varphi$$

where A_0 is an arbitrary function of m and n.

In the second region, where ξ is sometimes unity and η extends to infinity, the potential may be written as:

$$(27) \quad U_2 = \sum_{m,n} B_0 P_n^m(\xi) Q_n^m(\eta) \cos m\varphi$$

---

1. Smythe, pp 147-153.

where B_o is a second arbitrary function of m and n.

At the common boundary of these two regions, it is necessary that the potential be continuous; from which condition it is seen that:

$$(28) \quad B_o = A_o K_n^m(\eta_o)$$

where the symbol which has been introduced in this equation is defined as:

$$(29) \quad K_n^m(\eta_o) = \frac{P_n^m(\eta_o)}{Q_n^m(\eta_o)}$$

For a second boundary condition, consider the current which originates at the source. This source is now considered to be "smeared out" uniformly over a very small area on the surface $\eta = \eta_o$, keeping the average values of the coordinates as given above. If one now constructs a surface enclosing this area ΔS, the total current which flows outward through the enclosing surface is simply equal to I.

In order to enclose the source in the present problem, two non-intersecting surfaces are used, one being the spheroid $\eta = \eta_o - \varepsilon$ and the other being the spheroid $\eta = \eta_o + \varepsilon$. The increment ε is chosen to be so vanishingly small that it can be neglected in evaluating the various functions on the two surfaces. Using the expressions of equation 9, the current density, outward from the volume enclosed by the two spheroids, is calculated and found to be:

$$(30) \quad -\frac{1}{\rho}\left\{(\nabla u_2)_\eta - (\nabla u_1)_\eta\right\}_{\eta=\eta_o} = \frac{1}{b\rho}\sqrt{\frac{\eta_o^2-1}{\eta_o^2-\xi^2}} \sum_{m,n} A_o \Psi_n^m(\eta_o) P_n^m(\xi) \cos m\varphi$$

where the symbol introduced is given by:

$$(31)\quad \Psi_n^m(\eta_0) = P_n'^m(\eta_0) - K_n^m(\eta_0)\, Q_n'^m(\eta_0)$$

and the primes indicate differentiation with respect to the argument.

Following the reasoning applied elsewhere to ordinary Legendre polynomials,[2] the expression for $\Psi_n^m(\eta_0)$ may be somewhat simplified for computational purposes. The associated Legendre functions $P_n^m(\ )$ and $Q_n^m(\ )$ both satisfy the same equation so that we have:

$$(32)\quad \begin{aligned} &\frac{d}{d\eta}\left[(1-\eta^2)\frac{dP_n^m(\eta)}{d\eta}\right] + \left[n(n+1) - \frac{m^2}{1-\eta^2}\right]P_n^m(\eta) = 0 \\ &\frac{d}{d\eta}\left[(1-\eta^2)\frac{dQ_n^m(\eta)}{d\eta}\right] + \left[n(n+1) - \frac{m^2}{1-\eta^2}\right]Q_n^m(\eta) = 0 \end{aligned}$$

Multiplying the first equation by $Q_n^m(\ )$ and the second by $P_n^m(\ )$, subtracting the second from the first, and manipulating the terms, one finally arrives at the relationship:

$$(33)\quad \frac{d}{d\eta}\left[(\eta^2-1)\left\{Q_n^m(\eta)P_n'^m(\eta) - P_n^m(\eta)Q_n'^m(\eta)\right\}\right] = 0$$

from which it follows immediately that:

$$(34)\quad (\eta^2-1)\left[Q_n^m(\eta)P_n'^m(\eta) - P_n^m(\eta)Q_n'^m(\eta)\right] = C_n^m$$

This development has been general in the sense that it applies for all values of η. The value of C_n^m may be most easily determined by investigating the relationship in the limit as η becomes infinite. For this purpose, one must use the following relationships:[3]

---

2. MacRobert, pp 114-115.
3. Smythe, p 149.

$$
(35)\quad \begin{cases}
\lim\limits_{\eta\to\infty} P_n^m(\eta) \longrightarrow \dfrac{(2n)!}{2^n\, n!\,(n-m)!}\,\eta^n \\[2ex]
\lim\limits_{\eta\to\infty} P_n'^m(\eta) \longrightarrow \dfrac{(2n)!}{2^n (n-1)!\,(n-m)!}\,\eta^{n-1} \\[2ex]
\lim\limits_{\eta\to\infty} Q_n^m(\eta) \longrightarrow \dfrac{(-1)^m n!\,(n+m)!\,2^n}{(2n+1)!}\,\eta^{-(n+1)} \\[2ex]
\lim\limits_{\eta\to\infty} Q_n'^m(\eta) \longrightarrow \dfrac{(-1)^m (n+1)!\,(n+m)!\,2^n}{(2n+1)!}\,\eta^{-(n+2)}
\end{cases}
$$

Substituting these asymptotic values into equation 34, one gets for C_n^m:

$$
(36)\quad C_n^m = (-1)^m \frac{(n+m)!}{(n-m)!}
$$

Thus, the expression for $\Psi_n^m(\eta_0)$ is modified as follows:

$$
(37)\quad \Psi_n^m(\eta_0) = \frac{(n+m)!\,(-1)^m}{(n-m)!\,(\eta_0^2-1)\,Q_n^m(\eta_0)}
$$

The next step in the development is to multiply equation 30 by $P_{n'}^{m'}(\xi)\cos m'\varphi$ where the primes indicate specific integers in the sets of m and n. Consider now the integral of the left side of the equation over the whole surface of the spheroid $\eta=\eta_0$. The value of the integrand is zero everywhere on the surface except over the area ΔS. Thus, $P_{n'}^{m'}(\xi)\cos m'\varphi$ may be given its value at the coordinates of the source and removed from under the integral sign. Since the only contribution to the current flow out of the bounded region occurs in the immediate vicinity of ΔS, the remaining integral equals the total current I. Mathematically, this reasoning is represented by:

$$-\frac{1}{\rho}\int\left\{(\nabla u_2)_n-(\nabla u_1)_n\right\}_{\eta_0} P_{n'}^{m'}(\xi)\cos m'\varphi\, ds$$

(38)
$$= -P_{n'}^{m'}(\xi_0)\int_{\Delta S}\frac{1}{\rho}\left\{(\nabla u_2)_n-(\nabla u_1)_n\right\}ds = I\,P_{n'}^{m'}(\xi_0)$$

Integration of the right side of equation 30 over the surface of the spheroid is facilitated by the application of the orthogonality properties of the functions involved. These are:

(39)
$$\int_0^{2\pi}\cos m\varphi\,\cos m'\varphi\, d\varphi = \begin{Bmatrix}\pi\delta_{mm'} \text{ for } m'\neq 0\\ 2\pi\delta_{mm'} \text{ for } m'=0\end{Bmatrix} = \pi(1+\delta_{om'})\delta_{mm'}$$

(40)
$$\int_{-1}^{1}P_n^{m'}(\xi)P_{n'}^{m'}(\xi)\,d\xi = \frac{2}{2n'+1}\,\frac{(n'+m')!}{(n'-m')!}\,\delta_{nn'}$$

The correct element of area in this case is given by:

(41)
$$dS = b^2\sqrt{(\eta_0^2-1)(\eta_0^2-\xi^2)}\;d\xi\, d\varphi$$

First integrating with respect to φ to show that all terms for which m does not equal m' vanish, and then integrating with respect to ξ to eliminate all terms for which n does not equal n', one finds that:

(42)
$$\frac{b}{\rho}(\eta_0^2-1)\sum_{m,n}A_0\Psi_n^m(\eta_0)\int_{-1}^{1}\int_0^{2\pi}P_n^m(\xi)P_{n'}^{m'}(\xi)\cos m\varphi\cos m'\varphi\, d\xi\, d\varphi$$
$$= \frac{b}{\rho}(\eta_0^2-1)A_0\Psi_{n'}^{m'}(\eta_0)\,\pi(1+\delta_{om'})\,\frac{2(n'+m')!}{(2n'+1)(n'-m')!}$$

Equating the results of the operations in 38 and 42, dropping the primes on m and n, and solving the resulting equation for A_0, one finds that:

(43)
$$A_0 = \frac{I\rho}{2\pi}\;\frac{(2n+1)(n-m)!}{b(1+\delta_{om})(\eta_0^2-1)\,(n+m)!}\;\frac{P_n^m(\xi_0)}{\Psi_n^m(\eta_0)}\,,$$

Finally, the desired formula for the potential is obtained when equations 28, 29, 37, and 43 are all substituted into the original expressions:

$$(44)\quad U = \frac{I\rho}{4\pi}\sum_{m,n}\frac{(2-\delta_{om})(2n+1)}{b(-1)^m}\left[\frac{(n-m)!}{(n+m)!}\right]^2 P_n^m(\xi_0)P_n^m(\xi)\begin{matrix} Q_n^m(\eta_0)P_n^m(\eta) \\ P_n^m(\eta_0)Q_n^m(\eta)\end{matrix}\cos m\varphi$$

Note that equation 44 combines both equations 26 and 27; when two functions occur in a colum, the upper one applies when $\eta<\eta_0$ and the lower for $\eta>\eta_0$.

This result is consistent with the expression for the reciprocal distance in prolate spheroidal coordinates calculated elsewhere by an alternate procedure.[4]

The above considerations may likewise be applied to equation 25 in order to obtain a similar expansion of the reciprocal distance in oblate spheroidal coordinates. First, however, it is necessary to examine the new functions involved to learn their behavior.[5] It is found that $P_n^m(i\xi)$ is finite in all finite regions, but that it becomes infinite as ξ approaches infinity; $Q_n^m(i\xi)$ is finite everywhere. However, when $Q_n^m(i\xi)$ is contained in the potential function, the gradient becomes infinite along the circle for which $\xi=0$ and $\mu=0$.

Let a point source of current, of strength I, be located at ξ_0, μ_0, and $\varphi=0$ in a homogeneous and isotropic medium. It can then be shown that, analogous to equation 44, the potential is given by the expression:

$$(45)\quad U = i\frac{I\rho}{4\pi}\sum_{m,n}\frac{(2n+1)(2-\delta_{om})}{b(-1)^m}\left[\frac{(n-m)!}{(n+m)!}\right]^2 P_n^m(\mu_0)P_n^m(\mu)\begin{matrix} Q_n^m(i\xi_0)P_n^m(i\xi) \\ P_n^m(i\xi_0)Q_n^m(i\xi)\end{matrix}\cos m\varphi$$

---

4. Macrobert, pp 204-208.
5. Hobson, p 422.

X

The Ellipsoidal Sink

~~THE BOUNDARY VALUE PROBLEM~~

Consider a point source of current, either inside or outside of an ellipsoidal mass of material of resistivity ρ_2 embedded in a medium of resistivity ρ_1. The potential has the form given by either equation 24 or equation 25, as the case may be, where the constants must now be evaluated for each of the two media.

Throughout the remaining discussion, a uniform system of subscripts is used to label the various potential functions. The subscript "A" indicates that the source is in the region of resistivity ρ_1; while "B" means that the source is located in the second region. The subscript "1" labels the potential function in the first region; whereas "2" indicates the corresponding function in the second region. These subscripts are used in the appropriate combinations.

As in the previous instances, the type of boundary which can be described in prolate spheroidal coordinates are treated first; and, the results are carried over into oblate spheroidal coordinates without repeating the details of the argument. Let the boundary surface be the spheroid $\eta = \eta_1$; while, as in the previous section, the coordinates of the source are η_0, ξ_0, and 0. And, look first at the case in which the source is located outside of the spheroid; or, $\eta_0 > \eta_1$. Outside of the spheroid, in the region of resistivity ρ_1, the potential is given by:

$$(46) \quad U_{1A} = \sum_{m,n} \left\{ B_{mn} Q_n^m(\eta) + \begin{matrix} A_0 P_n^m(\eta) \\ B_0 Q_n^m(\eta) \end{matrix} \right\} P_n^m(\xi) \cos m\varphi$$

where A_0 and B_0 here have the same significance as they had in the previous section. B_{mn} is an arbitrary function of m and n. The various

terms in equation 24 have been discarded for reasons stated on page 20; and, the second term in equation 46 has been added to insure that the expression displays a pole of the correct strength at the position of the source.

Inside of the spheroid, the expression for the potential is:

$$(47) \quad U_{2A} = \sum_{m,n} A_{m,n} P_n^m(\eta) P_n^m(\xi) \cos m\varphi$$

The constants may now be determined by applying the boundary conditions. Over the surface of the spheroid, the potential must be continuous; which condition leads to the fact that:

$$(48) \quad B_{mn} Q_n^m(\eta_1) + A_0 P_n^m(\eta_1) = A_{mn} P_n^m(\eta_1)$$

By satisfying the condition that the normal component of the current density passing through the boundary surface must likewise be continuous, one arrives at the relationship:

$$(49) \quad \rho_2 \left[B_{mn} Q_n'^m(\eta_1) + A_0 P_n'^m(\eta_1) \right] = \rho_1 A_{mn} P_n'^m(\eta_1)$$

When the last two equations are solved simultaneously for A_{mn} and B_{mn}, the following expressions are derived:

$$(50) \quad \begin{cases} A_{mn} = A_0 \dfrac{\rho_2 [L_n^m(\eta_1) - K_n^m(\eta_1)]}{\rho_1 L_n^m(\eta_1) - \rho_2 K_n^m(\eta_1)} \\[2ex] B_{mn} = A_0 \dfrac{(\rho_2 - \rho_1) K_n^m(\eta_1) L_n^m(\eta_1)}{\rho_1 L_n^m(\eta_1) - \rho_2 K_n^m(\eta_1)} \end{cases}$$

where $K_n^m(\eta_1)$ has the meaning indicated in equation 29 and $L_n^m(\eta_1)$ is given by:

$$(51) \quad L_n^m(\eta_1) = \frac{P_n'^m(\eta_1)}{Q_n'^m(\eta_1)}$$

U. S. GEOLOGICAL SURVEY
LIBRARY

Finally, the correct expressions for the potential may be written as:

$$(52)\quad \begin{cases} U_{1A} = \sum_{m,n} A_0 \left\{ \dfrac{(\rho_2-\rho_1)K_n^m(\eta_1)L_n^m(\eta_1)}{\rho_1 L_n^m(\eta_1)-\rho_2 K_n^m(\eta_1)} Q_n^m(\eta) + \dfrac{P_n^m(\eta)}{K_n^m(\eta_0)Q_n^m(\eta)} \right\} P_n^m(\xi)\cos m\varphi \\ U_{2A} = \sum_{m,n} A_0 \dfrac{\rho_2[L_n^m(\eta_1)-K_n^m(\eta_1)]}{\rho_1 L_n^m(\eta_1)-\rho_2 K_n^m(\eta_1)} P_n^m(\eta) P_n^m(\xi)\cos m\varphi \end{cases}$$

Once again, it should be pointed out that A_0 has the value derived in the previous section - i.e., that given in equation 43.

When the source is located inside of the region of resistivity ρ_2, the same method of attack is applicable; and, one obtains for the potential functions in this case:

$$(53)\quad \begin{cases} U_{1B} = \sum_{m,n} A_0 \dfrac{\rho_1[L_n^m(\eta_1)-K_n^m(\eta_1)]}{\rho_1 L_n^m(\eta_1)-\rho_2 K_n^m(\eta_1)} K_n^m(\eta_0) Q_n^m(\eta) P_n^m(\xi)\cos m\varphi \\ U_{2B} = \sum_{m,n} A_0 \left\{ \dfrac{(\rho_2-\rho_1)K_n^m(\eta_0)P_n^m(\eta)}{\rho_1 L_n^m(\eta_1)-\rho_2 K_n^m(\eta_1)} + \dfrac{P_n^m(\eta)}{K_n^m(\eta_0)Q_n^m(\eta)} \right\} P_n^m(\xi)\cos m\varphi \end{cases}$$

In order to arrive at a conclusion concerning the case when the ellipsoid is oblate, it is useful to note the correspondence between equations 44 and 45. The former can be converted to the latter simply by multiplying by the imaginary number i and by making the following changes:

$$(54)\quad \begin{cases} \eta \to i\,\zeta \\ \xi \to \mu \end{cases}$$

together with identical substitutions for special values of these quantities.

Carrying the correspondence still further, analysis shows that all of the corresponding equations in oblate spheroidal coordinates

may be obtained from equations 52 and 53 by the same procedure. Therefore, the equations for this new case will not be written down explicitly. The same remarks apply equally well to any further equations which may be written down in prolate spheroidal coordinates.

XI

THE EQUATIONS APPLIED

In geoelectrical prospecting, both the current and potential electrodes are normally situated on the earth's surface which is assumed to be a horizontal plane; obviously, no current flows across this surface. Thus, in the above problems, any plane across which no current flows may be chosen to represent the surface of the earth. If such a plane is chosen to be the surface of the earth, all of the current I flows on one side of the separating plane; and, any of the above potential functions have to be increased by a factor of two when they are taken over into a geophysical problem.

Two planes which satisfy the above requirements are available in the prolate spheroidal case. The first is the meridian plane for which $\varphi = 0, \pi$. If this plane is oriented horizontally, and the upper half of space is then discarded, the resulting picture can be used to approximate a filled sink whose outcrop is elliptical in shape and whose long axis is roughly an axis of revolution.

If the potentials in equations 52 and 53 are doubled, they may be used as they are for calculations of data along an arbitrary traverse across the sink. But, a particularly simple case exists, at least from the standpoint of computations, when the traverse runs along the axis of revolution where $\xi = \pm 1$ or $\eta = 1$. In this instance, there is no dependence on the angle φ so that m can be made zero in equations 52

and 53; whence the double summations are now reduced to single summations. Remembering to introduce the factor of two, one can write the potentials as:

$$(55)\begin{cases} U_{1A} = 2\sum_n A_0 \left\{ \dfrac{(\rho_2-\rho_1)K_n(\eta_1)L_n(\eta_1)}{\rho_1 L_n(\eta_1)-\rho_2 K_n(\eta_1)} Q_n(\eta) + \dfrac{P_n(\eta)}{K_n(\eta_0)Q_n(\eta)} \right\} P_n(\xi) \\ U_{2A} = 2\sum_n A_0 \dfrac{\rho_2[L_n(\eta_1)-K_n(\eta_1)}{\rho_1 L_n(\eta_1)-\rho_2 K_n(\eta_1)} P_n(\eta) P_n(\xi) \end{cases}$$

and:

$$(56)\begin{cases} U_{1B} = 2\sum_n A_0 \dfrac{\rho_1[L_n(\eta_1)-K_n(\eta_1)]}{\rho_1 L_n(\eta_1)-\rho_2 K_n(\eta_1)} K_n(\eta_0) Q_n(\eta) P_n(\xi) \\ U_{2B} = 2\sum_n A_0 \left\{ \dfrac{(\rho_2-\rho_1)K_n(\eta_0)P_n(\eta)}{\rho_1 L_n(\eta)-\rho_2 K_n(\eta_1)} + \dfrac{P_n(\eta)}{K_n(\eta_0)Q_n(\eta)} \right\} P_n(\xi) \end{cases}$$

where the symbols used have their previous meanings when m equals zero.

The second possibility is to use the equatorial plane, for which $\xi = 0$, as the earth's surface. This yields the picture of a filled sink which is elliptical in section and whose maximum depth is greater than the radius of its circular outcrop. As above, equations 52 and 53 may be used to compute data for an arbitrary traverse in this plane. A slight simplification in the equations occurs in this special case because $P_n^m(0)$ vanishes whenever n plus m is odd.

It is to be noted that the intersection of the meridian and equatorial planes may be a traverse in either of the above two cases; this is the line $\xi = 0$ and $\varphi = 0, \pi$. If this traverse is used, an intrinsic ambiguity appears in the interpretation because the surveyor can not determine over which of the type sinks he is working. However, it is obvious that a second traverse rotated from the first, or otherwise removed from it, will in principle remove the ambiguity. Actually,

more than two traverses would be required since earth conditions never duplicate these idealized circumstances.

The same sort of remarks are valid in the consideration of oblate spheroids; the meridian and equatorial planes may be used to represent the earth's surface as outlined above. Further, any desired equation may be got from the corresponding one in prolate spheroidal coordinates by the procedure introduced on page 28. As pointed out in that discussion, the equations in the latter case will not be written down explicitly in this paper.

XII

THE HEMI-SPHERICAL SINK

In order to infer the validity of this development, as well as to introduce an important special case, the expressions in equations 55 and 56 will be reduced to the accepted ones in spherical coordinates by letting the parameter b go to zero. First, consider the limiting process in general.

In the meridian plane $\phi = 0, \pi$ as shown in figure two, consider the following limiting case of the ratio of z to ρ :

$$(57) \quad \lim_{\eta \to \infty} \frac{z}{\rho} = \lim_{\eta \to \infty} \frac{\eta \xi}{\sqrt{(1-\xi^2)(\eta^2-1)}} = \frac{\xi}{\sqrt{1-\xi^2}}$$

where ρ and z have the values stated in equation 7. Since the ratio approaches a constant which involves only ξ , it follows that a curve of constant ξ must approach an asymptote whose equation is $z = K\rho$ - and, thus which passes through the origin. Further, since the ratio of z to ρ is the slope of the asymptote, the assumption that ξ is the sine of the angle which that line makes with the X-axis is compatible with the facts. In the limiting case when b goes to zero, all of these hyper-

bolas become straight lines which pass through the origin. Hence, where θ is the polar angle of spherical coordinates, it is seen that:

$$(58) \quad \lim_{b \to 0} \xi = \cos\theta$$

From equation 7, it is seen that one can write:

$$(59) \quad \eta = \frac{z}{b\xi}$$

Therefore, as b is allowed to approach zero, η becomes infinite. Moreover, since ξ becomes $\cos\theta$ in the same limit, the ratio of z to ρ becomes the radius vector of spherical coordinates. Therefore:

$$(60) \quad \lim_{b \to 0} \eta = \frac{r}{b}$$

In order to study the limit of the potential as b approaches zero, it is necessary to use the asymptotic expressions for the Legendre functions which are obtained from equation 35 by setting m equal to zero.

The limiting process can best be illustrated by considering first only the part of the potential due to the point source. Multiplying equation 44 by two and equating m to zero, one gets for the potential due to a point source located on the axis of revolution in prolate spheroidal coordinates:

$$(61) \quad U_0 = \frac{I\rho}{2\pi} \sum_n \frac{2n+1}{b} P_n(\xi_0) P_n(\xi) \begin{matrix} Q_n(\eta_0) P_n(\eta) \\ P_n(\eta_0) Q_n(\eta) \end{matrix}$$

This equation could as easily be established by considering the second term in equation 55 and by making the necessary substitutions for A_0 and $K_n(\eta_0)$. When the limit in equation 60 is substituted into

equation 61 and the appropriate reductions are effected, one obtains:

$$(62)\quad \lim_{b\to 0} U_0 = \frac{I\rho}{2\pi} \lim_{b\to 0} \frac{1}{b} \sum_n \frac{\frac{1}{\eta_0}\left(\frac{\eta}{\eta_0}\right)^n}{\frac{1}{\eta}\left(\frac{\eta_0}{\eta}\right)^n} P_n(\xi)$$

which in turn, through the use of equations 58 and 60, can be reduced to the form:

$$(63)\quad \lim_{b\to 0} U_0 = \frac{I\rho}{2\pi} \sum_n \frac{\frac{1}{r_0}\left(\frac{r}{r_0}\right)^n}{\frac{1}{r}\left(\frac{r_0}{r}\right)^n} P_n(\cos\theta)$$

where the r in this expression is the radial distance of spherical coordinates. Comparing this equation with equation 1,[1] it is found that we have reproduced correctly the expansion in Legendre polynomials the reciprocal of the distance between a point on the polar axis and an arbitrary point.[2]

Now, if the limiting process is applied to equations 55 and 56, taken in their complete forms, it is easily verified that the following expressions for the potential result:

$$(64)\quad \begin{aligned} U_{1A} &= \frac{I\rho_1}{2\pi}\left\{\frac{1}{R} + \beta_{21}\sum_n \frac{n r_1^{2n+1}}{(n+\alpha_{21})(r_0 r)^{n+1}} P_n(\cos\theta)\right\} \\ U_{2A} &= \frac{I\rho_1}{2\pi}\,\frac{\alpha_{21}}{r_0}\sum_n\left[\frac{2n+1}{n+\alpha_{21}}\right]\left(\frac{r}{r_0}\right)^n P_n(\cos\theta) \\ U_{1B} &= \frac{I\rho_2}{2\pi}\,\frac{\alpha_{12}}{r}\sum\left[\frac{2n+1}{n+\alpha_{21}}\right]\left(\frac{r_0}{r}\right)^n P_n(\cos\theta) \\ U_{2B} &= \frac{I\rho_2}{2\pi}\left\{\frac{1}{R} + \beta_{12}\sum\left[\frac{n+1}{n+\alpha_{21}}\right]\frac{(r_0 r)^n}{r_1^{2n+1}} P_n(\cos\theta)\right. \end{aligned}$$

where the boundary surface is now the sphere $r = r_1$. Here the distance between the source and the point at which the potential is to be com-

---

1. From time to time, reference is made to equation 1 in comparison with a potential function based on the assumption that the current I flows outward in all directions. In such cases, the expression in equation 1 should be imagined to have an additional factor of two in the denominator.

puted is reduced to its closed form and is designated by R. The new constants, introduced in these equations, are given by:

$$(65) \quad \alpha_{ij} = \frac{\rho_i}{\rho_i + \rho_j} \; ; \; \beta_{ij} = \frac{\rho_i - \rho_j}{\rho_i + \rho_j}$$

Equations 64 have been verified by direct calculations in spherical coordinates by the present author. Also, the results may be checked against the corresponding electrostatic problem which is worked out by Stratton in spherical coordinates.[3]

In computations based on equations 64, it is necessary always to consider the source to lie on the polar axis; which assumption is made possible by the symmetry of the problem. If the traverse passes through the center of the hemisphere, there are no complications; instead, equations 64 actually assume a simplified form. On the other hand, if the traverse does not pass through the origin, a special procedure must be adopted in order to make the computations. Consider such a case, as

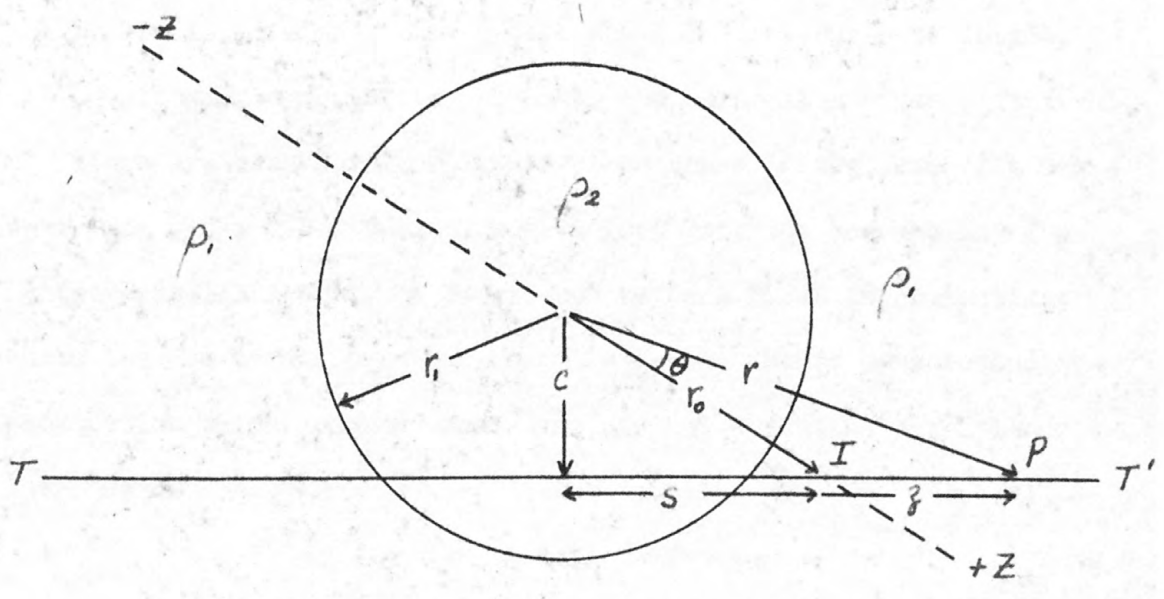

Figure Four - Arbitrary Traverse Over Hemispherical Sink.

---

2. Stratton, pp 172-174.
3. Idem, pp 201-205.

seen from above in figure four. If the polar axis is always considered to be the line joining the source and the center of the hemisphere, it is seen at once that the axis rotates as the source moves along the traverse T-T'. The problem is now resolved into one of determining r_o, r, and cos in terms of the other distances shown in the diagram. Note that z is the distance from the source to the point at which the potential is desired and is positive to the right of the source. From the simple trigonometric relationships, the following expressions are obtained:

$$(66)\quad \begin{cases} r = \sqrt{C^2+(s+z)^2} \\ r_0 = \sqrt{C^2+S^2} \\ \cos\theta = \dfrac{r^2+r_0^2-z^2}{2r_0 r} \end{cases}$$

In order to calculate the potentials at points along the traverse, the above substitutions must be made in equations 64. There is no distinction to be made in the substitutions as made for the cases when the source is outside of the sphere and when the source is inside.

Obviously, computations based on the assumption of an elliptical structure are much more complicated than those in the case of a hemispherical sink. In attacking a given problem, the assumption of a hemispherical shape may be considered to be a first approximation; while the use of a spheroidal shape is in the nature of a second approximation which, in many instances, is not worth the extra labor introduced.

XIII

COMPUTATIONS

It is not difficult to compute data from the expressions introduced to this point. However, in order to make the present discussion complete, a brief outline of the technique used to convert the poten-

tial formulae into resistivity curves is included.

As a vehicle to illustrate the method, consider a horizontal traverse across the center of a hemispherical sink, filled with a material of resistivity 1, in a country rock of resistivity 5; in which case, equations 64 are applicable as they stand. Let the electrode separation equal the radius of the hemisphere, which for simplicity may be assigned the value unity. Further simplification can be attained by letting the current be numerically 2π. The remaining constants required are computed to be:

$$(67)\quad \begin{cases} \beta_{12} = 2/3 & \beta_{21} = -2/3 \\ \alpha_{12} = 5/6 & \alpha_{21} = 1/6 \end{cases}$$

and the working equations become:

$$(68)\quad \begin{cases} U_{1A'} = 5\left[\frac{1}{R} - \frac{4}{r_0 r}\sum_n \left(\frac{1}{r_0 r}\right)^n \left[\frac{n}{6n+1}\right](\pm 1)^n\right] \\ U_{2A} = 5/r_0 \sum_n \left(\frac{r}{r_0}\right)^n \left[\frac{2n+1}{6n+1}\right](\pm 1)^n \\ U_{1B} = 5/r \sum \left(\frac{r_0}{r}\right)^n \left[\frac{2n+1}{6n+1}\right](\pm 1)^n \\ U_{2B} = 1/R + 4\sum_n (r_0 r)^n \left[\frac{n+1}{6n+1}\right](\pm 1)^n \end{cases}$$

where the upper sign in $(\pm 1)^n$ is to be used when the current and potential electrodes are on the same side of the center of the hemisphere and the negative sign applies when these two electrodes are separated by the origin.

The first step in the computation is to determine the value of r_0 and/or r for each electrode at each station which is to be considered

along the traverse. The station is normally chosen to be the position of P_0.

Next, for each station, it is necessary to compute the potential at each potential electrode due to each current electrode. For this purpose, if the current at C_1 is I, the current at C_2 is -I and allowance must be made for the change in sign. All of the operations up to this point may conveniently be organized into a work sheet which is too bulky to be included in this report. Finally, the computed potentials are transferred to a final work sheet, such as is shown in figure five, from which the resistivities are computed.

1	2	3	4	5	6	7	8	9	10	11	12	13	14	15	16	17	18	19	20
	Potentials due to C_2							Potentials due to C_1									Wenner $\rho_a = V/I$	Lee $\rho_a = 2V_{10}$	Lee $\rho_a = 2V_{02}$
		at P_2		at P_0		at P_1			at P_2		at P_0		at P_1						
x	r_0	r	U	r	U	r	U	r_0	r	U	r	U	r	U	V_{10}	V_{02}			
0	1.5	.5	4.02	0	3.33	.5	2.97	1.5	.5	2.97	0	3.33	.5	4.02	1.05	1.05	2.10	2.10	2.10
.1	1.4	.4	4.16	.1	3.47	.6	3.04	1.6	.4	2.85	.1	3.21	.6	3.89	1.06	1.05	2.11	2.12	2.10
.3	1.2	.2	4.52	.3	3.80	.8	3.40	1.8	.2	2.66	.3	3.01	.8	3.68	1.07	1.07	2.14	2.14	2.14
.5	1.0	0							0	2.50	.5							3.00	2.20
										2.37									

Figure Five - Sample Computation Sheet.

In this table, x is the distance of P_0 from the center of the sink. The necessary potential differences are obtained by combining correctly the appropriate potentials - remembering that the current at C_2 is negative. For example, V_{10} is the potential difference between P_1 and P_0, and is found by adding columns 6 and 15 and subtracting columns 8 and 13. V_{02} is obtained by adding columns 4 and 13, subtracting 6 and 11.

Now that the potential differences have been computed, equations 2 and 3 are applicable to compute the resistivities. Due to the simplifying choice of current and electrode separation, the last step is almost trivial. For the first branch of the Lee configuration, the apparent resistivity (column 19) is twice V_{10}; while, for the other branch, the apparent resistivity (column 20) is twice V_{02}. The apparent resistivity as determined by the Wenner configuration is actually the average of these two and is calculated most easily by adding columns 16 and 17.

The curves based on this computation are presented in Part Six.

PART THREE

BURIED SPHERES

XIV

BIPOLAR COORDINATES

In order to investigate situations in which a spherical mass of foreign material is completely enclosed by an otherwise homogeneous earth, it is necessary to resort to bipolar coordinates which are illustrated on the following page. If the right half of that diagram, consisting of two sets of coaxial circles, be rotated about the polar Z-axis, it will generate two orthogonal families of surfaces; the third family is the set of half planes whose common intersection is the polar axis. The azimuthal angle φ is the parameter in this set of planes.

The family of spheres whose centers lie on the Z-axis may be defined in cylindrical coordinates by the equation:

$$(69) \qquad (z - b \coth \sigma)^2 + p^2 = b^2 \operatorname{csch}^2 \sigma$$

At the point plus b, σ is positive and infinite; the spheres surrounding this point increase in radius as σ decreases until finally the equatorial plane represents the surface for which σ is zero. At the point minus b on the polar axis, σ is negatively infinite; and, the progressively larger spheres surrounding this point represent increasing values of σ. Thus, the range of σ is such that $-\infty < \sigma < \infty$.

The second family of orthogonal surfaces, being of the intersecting type, is somewhat more complicated than the first. In figure six, this family of circles is given by the equation:

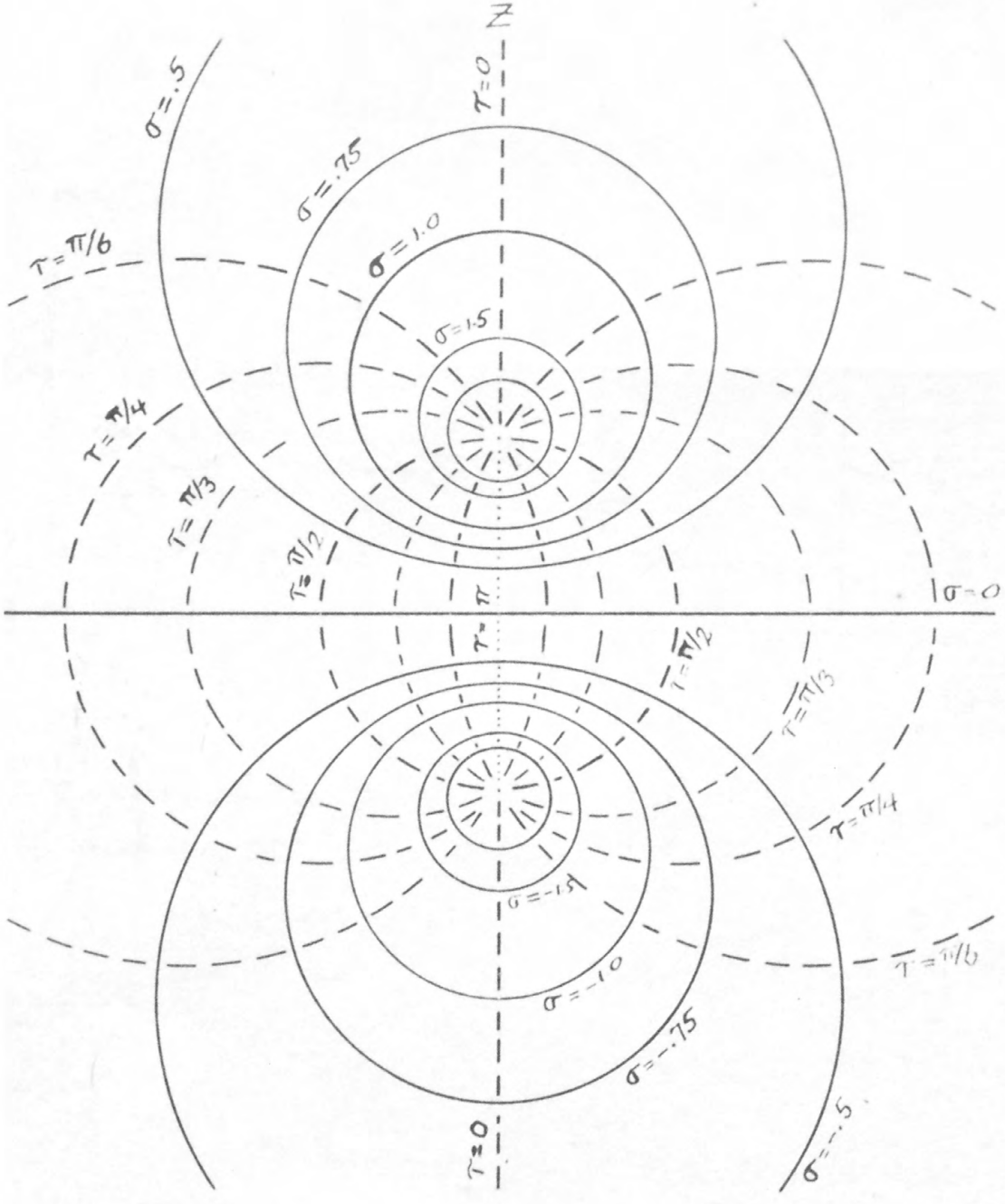

Figure Six - Bipolar Coordinates.

$$(70) \qquad z^2 + (\rho - b \cot \tau)^2 = b^2 \csc^2 \tau$$

Since only the right half of the diagram is rotated, the surfaces generated are not in general spheres, but are instead surfaces of degree four which Hobson designates as spindles.

The smallest sphere which can possibly pass through the two points for which z is plus and minus b respectively has its center at the origin and has the value $\tau = \pi/2$. The spindles of increasing radii represent decreasing values of τ while those inside the focal sphere $\tau = \pi/2$ have larger values of τ. Finally, the portion of the polar axis above plus b and below minus b is the two segment line $\tau = 0$, that part lying between plus and minus b being the locus of points for which $\tau = \pi$.

The following transformations from cylindrical coordinates to bipolar coordinates are sometimes useful:

$$(71) \qquad \begin{cases} z = \dfrac{b \sinh \sigma}{\cosh \sigma - \cos \tau} \\ \rho = \dfrac{b \sin \tau}{\cosh \sigma - \cos \tau} \end{cases}$$

which relationships can be got by solving equations 69 and 70 simultaneously for z and ρ.

In terms of the variables σ, τ, and φ, Laplace's equation is written as:[1]

$$(72) \qquad \frac{\partial}{\partial \sigma}\left[\frac{b \sin \tau}{\cosh \sigma - \cos \tau} \frac{\partial u}{\partial \sigma}\right] + \frac{\partial}{\partial \tau}\left[\frac{b \sin \tau}{\cosh \sigma - \cos \tau}\right] \frac{\partial u}{\partial \tau} + \frac{b}{\sin \tau (\cosh \sigma - \cos \tau)} \frac{\partial^2 u}{\partial \varphi^2} = 0$$

---

1. MacRobert, p 226.

and the three components of the gradient are:

$$(73)\quad \begin{cases} (\nabla u)_\sigma = \dfrac{\cosh\sigma - \cos\tau}{b}\,\dfrac{\partial u}{\partial \sigma} \\[2ex] (\nabla u)_\tau = \dfrac{\cosh\sigma - \cos\tau}{b}\,\dfrac{\partial u}{\partial \tau} \\[2ex] (\nabla u)_\varphi = \dfrac{\cosh\sigma - \cos\tau}{b\sin\tau}\,\dfrac{\partial u}{\partial \varphi} \end{cases}$$

XV

A SOLUTION OF LAPLACE'S EQUATION
in Bipolar Coordinates

A separation of variables in equation 72 can be effected through a change of the dependent variable.[1] To this end, let:

$$(74)\quad u = \sqrt{\cosh\sigma - \cos\tau}\; W$$

whence the differential equation assumes the form:

$$(75)\quad \frac{\partial^2 W}{\partial \sigma^2} + \frac{1}{\sin\tau}\frac{\partial}{\partial \tau}\left[\sin\tau\,\frac{\partial W}{\partial \tau}\right] + \frac{1}{\sin^2\tau}\frac{\partial^2 W}{\partial \varphi^2} - \frac{W}{4} = 0$$

The variables in this equation may now be seaprated by the assumption of a solution in the form of:

$$(76)\quad W = S(\sigma)\,T(\tau)\,\Phi(\varphi)$$

In terms of the component dependent variables, equation 75 becomes:

$$(77)\quad \frac{1}{S}\left[\frac{d^2 S}{d\sigma^2} - \frac{1}{4}\right] + \frac{1}{T\sin\tau}\frac{d}{d\tau}\left[\sin\tau\,\frac{dT}{d\tau}\right] + \frac{1}{\Phi\sin^2\tau}\frac{d^2\Phi}{d\varphi^2} = 0$$

An examination of equation 77 reveals that two parts of the equation may be equated to separate constants. The first of these is the part

---

1. MacRobert, p 226.

involving Φ which, when equated to a constant, leads to the equation:

$$(78) \quad \frac{d^2\Phi}{d\varphi^2} + m^2\Phi = 0$$

for which the solution is known to be:

$$(79) \quad \Phi = A_m \cos m\varphi + B_m \sin m\varphi$$

Now, the part of equation 77 which involves S may independently be equated to a second constant. This step leads to the equation:

$$(80) \quad \frac{d^2S}{d\sigma^2} - \left[n(n+1) + \tfrac{1}{4}\right]S = 0$$

which, through the methods of ordinary differential equations, leads to the solution:

$$(81) \quad S = C_n e^{(n+\frac{1}{2})\sigma} + D_n e^{-(n+\frac{1}{2})\sigma}$$

The solution, in the case of S, in terms of exponentials is preferred to the form involving hyperbolic sines and cosines because the former facilitates application of the solution to regions in which σ becomes positively or negatively infinite.

If the above constants are introduced into equation 77 through the relationships of equations 78 and 80, one obtains for T:

$$(82) \quad \frac{1}{\sin\tau}\frac{d}{d\tau}\left[\sin\tau\frac{dT}{d\tau}\right] + \left[n(n+1) - \frac{m^2}{\sin^2\tau}\right]T = 0$$

which is recognized as being the ordinary associated Legendre equation. Thus, the τ dependence of the solution is given by:

$$(83) \quad T = E_{mn} P_n^m(\cos\tau) + F_{mn} Q_n^m(\cos\tau)$$

Actually, all regions, in which this solution is useful, contain

points at which is zero or pi. Since the Legendre function of the second kind becomes infinite at such points, it may be excluded even from the general solution.

In the above solutions, the parameters n and m have their most common properties - i.e., n is an integer which may assume any positive value while m, also an integer, is restricted to values between and including plus n and minus n. When m appears explicitly in a function, only its absolute value is considered.

Finally, assembling the various component parts, one obtains for the general solution of equation 72:

$$U = \sqrt{\cosh\sigma - \cos\tau} \sum_{n=0}^{\infty} \sum_{m=-n}^{m=n} \left[A_m \cos m\varphi + B_m \sin m\varphi \right] \cdots$$

(84)

$$\cdots \left[C_{nm} e^{(n+1/2)\sigma} + D_{nm} e^{-(n+1/2)\sigma} \right] P_n^m(\cos\tau)$$

It is seen that the factor multiplying the series becomes infinite as the points $z = \pm b$, where σ becomes infinite, are approached. However, further examination shows that there is always a term in the summand which goes to zero, at the same time, in such a way that the solution remains finite but does not in general reduce to zero.

XVI

SPECIAL CASE OF CONDUCTING SPHERES

A simple, but very instructive case which can be treated in bipolar coordinates is that of a resistivity survey in the neighborhood of a buried conducting sphere. From a study of this situation, one is able to learn something of the limits of the electrical method of prospecting.

Before attacking the boundary value problem, it is necessary to

have an expression for the reciprocal distance in terms of the functions in equation 84. The desired expansion has been obtained by two independent methods elsewhere;[1,2] and we simply introduce the result at this point without proof. Substituting the expansion for 1/R in equation 1,[3] one gets for the potential due to a point source located at ($\sigma_0, \tau_0, 0$) in a homogeneous medium:

$$(85) \qquad U_0 = \sqrt{\cosh\sigma - \cos\tau} \sum_{n=0}^{\infty} \sum_{m=0}^{n} A_0 e^{\pm(n+1/2)\sigma} P_n^m(\cos\tau) \cos m\varphi$$

where the upper and lower signs in the exponential apply according as σ is less than and greater than σ_0 respectively. In this equation, A_0 is given by the expression:

$$(86) \qquad A_0 = \frac{I\rho}{4\pi} \frac{1}{b} \sqrt{\cosh\sigma_0 - \cos\tau_0}\; e^{\pm(n+1/2)\sigma_0} (2-\delta_{0m}) \frac{(n-m)!}{(n+m)!} P_n^m(\cos\tau_0)$$

Now consider the specific situation in which the material within the spheres $\sigma = \pm\sigma_1$ has comparatively low resistivity, which is assumed to be zero; while that exterior to both spheres has the uniform resistivity ρ. Further, let a point source of current of strength I be located at the point ($0, \tau_0, 0$). The symmetry of the problem is now such that the potential outside the spheres may be expressed as:

$$(87) \qquad U = \sqrt{\cosh\sigma - \cos\tau} \sum_{n=0}^{\infty} \sum_{m=0}^{n} \left\{ A_0 e^{\pm(n+1/2)\sigma} + A_{mn}\left[e^{(n+1/2)\sigma} + e^{-(n+1/2)\sigma} \right] P_n^m(\cos\tau) \cos m\varphi \right.$$

Within the spheres, the potential has some constant value, actually yet to be determined but which for the moment is considered to be zero. If the potential within the spheres were zero, as assumed, the potential function in equation 87 could be equated to zero at the surface $\sigma = \sigma_1$. From this condition, it is determined that:

---

1. Hobson, p 450.
2. MacRobert, pp 221-222.
3. See footnote 1, p 33.

$$(88) \quad A'_{mn} = -\frac{A_0}{1+e^{(2n+1)\sigma_1}}$$

where the prime indicates that the constant does not have its true value. Returning the reciprocal distance to its closed form, and introducing the value of A_0 as it is given by equation 86 for points on the boundary, the corresponding potential function is given by:

$$(89) \quad U' = \frac{I\rho}{4\pi}\left\{\frac{1}{R} - \frac{1}{b}\sqrt{(1-\cos\tau_0)(\cosh\sigma - \cos\tau)}\sum(2-\delta_{om})\frac{(n-m)!}{(n+m)!}\cdots\right.$$
$$\cdots\frac{\left[e^{(n+1/2)\sigma} + e^{-(n+1/2)\sigma}\right]}{1+e^{(2n+1)\sigma_1}} P_n^m(\cos\tau)\cos m\varphi\, P_n^m(\cos\tau_0)$$

In the geophysical problem of a buried sphere, the plane $\sigma = 0$ is considered to be the surface of the earth. Let our attention be further restricted to points along the line for which φ is zero or pi. Remembering to double the expression for reasons given in connection with equation 55, equation 89 in this case reduces to:

$$(90) \quad U' = \frac{I\rho}{2\pi}\left\{\frac{1}{R} - \frac{2}{b}\sqrt{(1-\cos\tau_0)(1-\cos\tau)}\sum_{m,n}(2-\delta_{om})\cdots\right.$$
$$\cdots\frac{(n-m)!}{(n+m)!}\frac{P_n^m(\cos\tau_0)\,P_n^m(\cos\tau)}{1+e^{(2n+1)\sigma_1}}(\pm 1)^m$$

The choice of positive or negative sign is to be made according as the point, at which the potential is to be computed, is on the same side or the opposite side of the origin from the source.

An expression will now be obtained for the apparent resistivity as measured by the Wenner configuration oriented along the line $\varphi = 0, \pi$ and symmetrically situated with respect to the buried sphere. Note that the value of τ_0 is the same for both current stakes as is the value of τ for

both potential electrodes. This symmetry permits one to use equation 90 without ever knowing explicitly the value of the constant potential within the conducting sphere. To explain this fact more fully, we resort to the electrostatic analogy - or, more exactly, to a series of electrostatic analogies.

Consider first a point charge in the vicinity of a grounded sphere. It is well known that a charge distribution is induced on the surface of the sphere, that the potential on that surface is zero, and that the effect of this induced charge on the potential in the exterior space may be described in terms of a single image located at the point within the sphere inverse to the postion of the true point charge. If the same situation exists but the sphere is not grounded, a second image must be introduced at the center of the sphere. This image has the same strength as the first, but with opposite sign, and its purpose is to maintain constant total charge on the sphere.

A point charge situated equidistant from two equal, grounded spheres presents a picture analogous to the above geophysical problem. In this electrostatic case, one may obtain an expression for the potential in the exterior region. Now, if the same problem be considered with insulated spheres, an additional expression must be provided to account for the fact that the total charge on each sphere must remain constant - or, in other words, to raise the potential of each sphere to its proper value in the field. A charge placed at the center of one sphere could produce the correct effect for that sphere; but, at the same time, it would adversely effect the second sphere. Therefore, as in the study of the effect of two charged spheres on each other,[4] one is compelled

---

4. Smythe, pp 118-122.

to use an infinite series of images. The point of the argument is that all of these images lie on the line joining the centers of the spheres, the net effect on the potential in the exterior region being symmetrical with respect to that axis.

If this argument is carried over into the direct current problem under consideration, it means that the term or terms, which have been omitted from equations 89 and 90 because the potential of the sphere was considered to be zero, have an equal effect on the two potential electrodes. The fact that such a term exists can not be determined by a measurement of the potential difference between these electrodes. Thus, the expression in equation 89 is usable in the present investigation as though it were the correct one. However, it is to be noted that this argument holds only in the present case and should not be carried over into situations in which the present symmetry does not exist.

In obtaining an expression for the apparent resistivity, it is seen in this symmetrical case that the potential difference between P_1 and P_2[5] due to C_2 is exactly the same as that due to C_1. Therefore, we consider only the potential difference due to C_1 and double the resulting expression. Further, since the coordinates of P_1 and P_2 are the same except for the angle φ, the potential difference between these two points is the difference between two summations which are alike except that one contains the factor $(-1)^m$. Thus, the terms for which m is even vanish and those for which m is odd appear with an additional factor of 2. If the distance between electrodes is given by a, the difference between $1/R_1$ and $1/R_2$ is given by $1/2a$. Thus, the potential difference, due to both current electrodes, is given by:

---

5. See the arrangement in figure one.

$$(91) \quad \bar{V} = 2\frac{I\rho}{2\pi}\left\{\frac{1}{2a} - \frac{8}{b}\sqrt{(1-\cos\tau_0)(1-\cos\tau)}\sum_{n=1}^{\infty}\sum_{\substack{m=1\\ odd}}^{n}\frac{(n-m)!}{(n+m)!}\,\frac{P_n^m(\cos\tau_0)P_n^m(\cos\tau)}{1+e^{(2n+1)\sigma_1}}\right.$$

The substitution of this expression into equation 2 yields the desired ratio of the apparent resistivity to the actual resistivity of the earth, which is:

$$(92) \quad \rho_a/\rho = 1 - \frac{2a}{b}\sqrt{(1-\cos\tau_0)(1-\cos\tau)}\sum_{n=1}^{\infty}\sum_{\substack{m=1\\ odd}}^{n}\frac{(n-m)!}{(n+m)!}\,\frac{P_n^m(\cos\tau_0)P_n^m(\cos\tau)}{1+e^{(2n+1)\sigma_1}}$$

As a reminder, it is pointed out that τ_0 is the coordinate of the current electrode; τ is the coordinate of the potential electrode; and, $\sigma = \sigma_1$ describes the surface of the buried sphere.

A certain complication exists in the computations, based on this equation, which is not present in such work as was described in section XIII. This difficulty arises chiefly from the non-linear transformation from τ in bipolar coordinates to ρ in cylindrical coordinates which, in this special case, is given by:

$$(93) \quad \rho = \frac{b\,(1+\cos\tau)}{\sin\tau}$$

Since the ratio of r_0 for the current electrode to r for the potential electrode is fixed at 3 in the present situation, it is not likely for a rational number to be chosen for both τ_0 and τ. Therefore, one is faced with the problem of interpolation. Here, we choose to make a single interpolation for each final result rather than to interpolate each time a Legendre function must be drawn from the tables. To this end, a graph based on equation 93 is prepared for each value of b used -- i.e., for each separate sphere treated. The desirable values of a and r_0 are chosen; and, from the graph, the corresponding values

of τ_0 to the nearest degree are calculated. The exact value of r corresponding to each rational τ_0 is computed; after which, the two nearest values of τ, in whole degrees, are found from the graph. Then, two apparent resistivities are computed for each value of τ_0, each based on a given value of τ. When the final results are obtained for each of these computations, the correct value of the apparent resistivity is computed by interpolating linearly between the two approximate values. In this way, four significant figures are obtained in the data although only three are of use in plotting curves.

In this work, the only available tables of the associated Legendre polynomials have been the National Bureau of Standards tables[6] which give values for all angles in whole degrees from 0 to 90 degrees. For all but one of the curves constructed, the series converge rapidly enough so that terms to $m=n=3$ are sufficient. However, in the last case, it is necessary to use terms up to $n=5$ and $m=3$.

XVII

CONCLUSIONS DRAWN FROM BURIED SPHERE PROBLEM

If a is allowed to vary in equation 92, a curve is obtained for a vertical profile over the buried sphere. Figure seven displays curves representing vertical profiles over a set of buried conducting spheres of constant unit radius at varied depths. Included is the limiting case of the hemispherical sink, the computations for which are based on equation 64. Although it is recognized that no such geologic situation as a conducting spherical body actually exists in nature, some interesting implications are present and some useful conclusions may be

---

6. Lowan, 1945.

drawn from these curves.

In figure seven, the ration $\frac{\rho_a}{\rho}$ is plotted against the ratio of the electrode separation to the radius of the spheres. The various curves are labelled with a depth which in reality is expressed as a factor times the radius of the spheres. Therefore, the whole diagram is dimensionless and may be applied to any specific case by introducing the correct scale.

When the sphere is definitely buried, the curve starts, for zero electrode separation, with $\frac{\rho_a}{\rho}$ equal to one. Each curve displays a minimum, which represents the electrode separation at which the sphere produces a maximum effect on the results; and, then each curve trends upward to approach one again asymptotically at large electrode separations.

On the other hand, if the sphere is truncated at all by the earth's surface, the corresponding curve starts at zero, at the electrode separation equal to the diameter of the circle of truncation, and then rises continuously to approach one asymptotically,. The curve for the hemispherical case, for which the depth of the sphere may be said to be zero, is one limiting example of this type. The curve representing the other limiting case - that in which the sphere is tangent to the surface of the earth - starts at the origin. This curve has been estimated and is shown in the diagram by a dashed line.

It should be noted that the first five curves in the diagram actually cross the "hemisphere" curve, in the range of the electrode separation between 3.5 and 6, but do not cross each other. This fact implies that the buried spheres have a greater effect at large electrode separations than does the hemisphere; which phenomenon is related to the

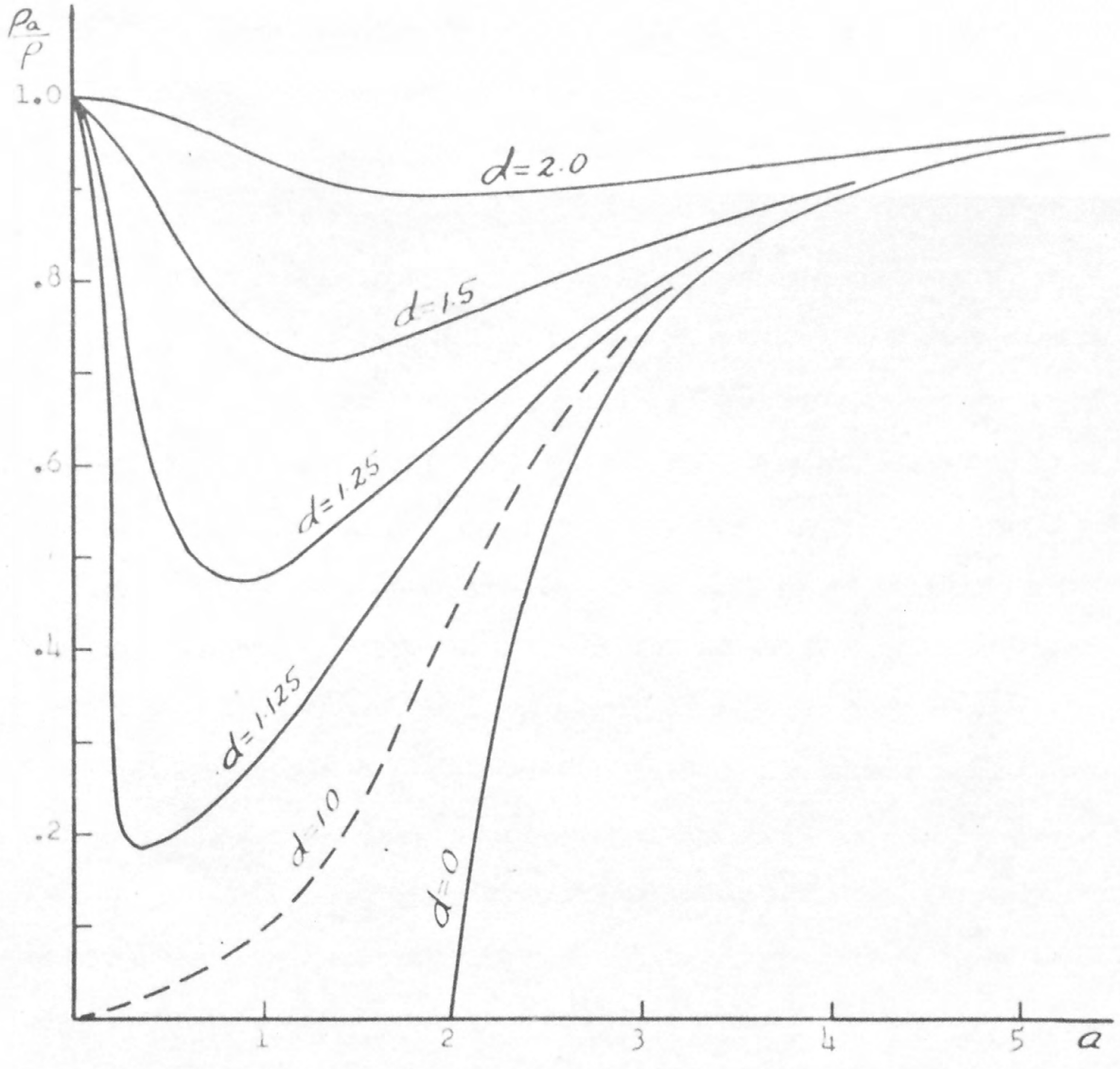

Figure Seven - Depth Profiles over Buried Conducting Spheres.

volume of foreign material which is present in the field and to the ratio of this volume to the volume of space in which the current density is arbitrarily appreciable.

The principal geophysical value of these curves stems from the fact that, for a given geometrical relationship, the body of zero resistivity has a maximum effect on the measurement of the apparent resistivity. This is a valid assumption at least if the resistivity of the disturbing body is smaller than that of the country rock.

The first useful implication lies in the maximum depth at which one can expect to locate a spherical mass of material by direct current methods. The fact that the curve, for which the depth to the center of the sphere is twice the radius of the sphere, has a minimum which is nine-tenths of its maximum leads one to the assumption that it would not be safe to depend on finding such a feature when its depth is greater than this value. This result, being in the nature of a guiding principle rather than a hard fact, may safely be extended to bodies of arbitrary shape provided that the variation between the maximum and minimum dimensions is not too extreme; a factor of two might well be permissible. In such a case, the maximum depth to the center of the body equal to the mean linear dimension of the body would appear to be in order. The rule may further be extended to cases in which the foreign body has higher resistivity than has the surrounding material. The curves for the case of higher resistivity spheres will have maxima corresponding roughly to the minima in the previous case; and, ~~it~~ as the variation in the apparent resistivity curve is small, the maxima will be of the same order of magnitude above one as the previous minima were below.

Because the maximum anomaly in a horizontal traverse occurs when the configuration is directly above the foreign mass, the above discussion applies in any direct current technique of prospecting.

A second use of these curves, applicable to horizontal profiling, is in choosing the proper electrode separation in a given situation. When one enters a region to perform a survey, he is generally advised by geologists as to the approximate depth at which he should find a certain geologic condition. Suppose, for example, that ore is known to be associated with clay filled sinks about 100 feet in diameter and 75 feet in vertical dimension, located in an ancient limestone surface which has later been overlain with lime and sandstone to a depth of 25 feet. Suppose further that the resistivity of the clay is normally much less than one fifth that of the other materials present. In the diagram on page 52, one imagines the curve for which the depth is about 1.3 times the radius and notes that the minimum occurs at an electrode separation about equal to the radius or one-half the average dimension of the body. Therefore, it would be concluded that a separation of 40 or 45 feet would be most useful.

In deciding on the appropriate spacing between traverses, one would conclude that the rule of permissible depth could be generalized to say that, if an anomaly is to be found along a given traverse, the traverse must pass within a distance from the center of the disturbing body roughly equal to the average dimension of the body. In the above example, this means 87.5 feet. Therefore, in order for the anomaly in this example to appear on at least two adjacent traverses, a traverse separation of no more than 55 feet could be tolerated.

If the disturbing mass actually outcrops, the above discussion must be altered accordingly.

PART FOUR

THE CONE PROBLEM[1]

XVIII

A SOLUTION OF LAPLACE'S EQUATION in Spherical Coordinates

Inasmuch as the limiting case of the hyperboloidal problem is a similar one in spherical coordinates wherein the boundary surfaces are cones, the latter problem will be treated first. In this way, an insight into the main issue will be gained.

The usual form of Laplace's equation in spherical coordinates is given by:

$$\frac{1}{r^2}\frac{\partial}{\partial r}\left[r^2\frac{\partial u}{\partial r}\right]+\frac{1}{r^2\sin\theta}\frac{\partial}{\partial\theta}\left[\sin\theta\frac{\partial u}{\partial\theta}\right]+\frac{1}{r^2\sin^2\theta}\frac{\partial^2 u}{\partial\varphi^2}=0 \tag{94}$$

where a general solution is normally stated in the form of:

$$u=\sum_{n=0}^{\infty}\sum_{m=-n}^{m=n}\left[A_m\cos m\varphi+B_m\sin m\varphi\right]\cdots$$

$$\cdots\left[C_n r^n+D_n r^{-n-1}\right]\left[E_{mn}P_n^m(\cos\theta)+F_{mn}Q_n^m(\cos\theta)\right] \tag{95}$$

If n is restricted to positive integers, the associated Legendre functions in this solution form a set of functions which are orthogonal over the spherical surfaces which have their centers at the origin. However, in the problem under consideration, a set of functions, which are orthogonal over the conal surfaces, for which the polar angle θ is the parameter, is required. Such a set of functions is obtained in the

---

1. Smythe, p 258, problem 57. The answer derived in this paper differs from that given by Smythe in the statement of his problem. In a personal communication, dated 24 March 1952, Smythe has acknowledged the error in his solution. Therefore, the present solution is considered to be correct.

radial part of the solution if n is chosen to be ip - 1/2.[2] Here, p is real but may assume any positive or negative value; and, the sum over n must be replaced by an integration over p. Further, although m is still a positive integer, it is no longer restricted in its range of values. Therefore, the summation over m runs from zero to infinity.

A valid definition of the Legendre function of this order in the region of cos θ is given by the hypergeometric series:[3]

$$(96)\quad P_{ip-1/2}(\cos\theta) = F\left(\tfrac{1}{2} - ip, \tfrac{1}{2} + ip, 1; \frac{1-\cos\theta}{2}\right).$$

And, because m is a positive integer in this problem, the associated Legendre function may be defined by equation 21.

Further, whenever n is not an integer, $P_n^m(x)$ and $P_n^m(-x)$ are two independent solutions of the associated Legendre equation. Therefore, instead of $Q^m_{ip-1/2}(\cos\theta)$, we use $P^m_{ip-1/2}(-\cos\theta)$ for the second independent function of θ. This function may be defined simply by replacing cos θ by -cos θ in equations 96 and 21 above.

An examination of equation 96, together with equation 21, reveals that $P^m_{ip-1/2}(\cos\theta)$ becomes infinite when cos θ approaches minus one; while $P^m_{ip-1/2}(-\cos\theta)$ does the same as cos θ approaches plus one. Both functions behave properly throughout the remainder of the range of cos θ.

Finally, equating n to ip - 1/2 in equation 95, and making the changes indicated above, one gets for the correct general solution:

---

2. Smythe, pp 70 and 155.
3. Hobson, p 187.

$$U = \frac{1}{\sqrt{r}} \sum_{m=0}^{\infty} \left[A_m \cos m\varphi + B_m \sin m\varphi \right] \cdots$$

(97)
$$\cdots \int_{-\infty}^{\infty} \left[C_m(p) P^m_{ip-1/2}(\cos\theta) + D_m(p) P^m_{ip-1/2}(-\cos\theta) \right] e^{ip \ln r} dp$$

where A_m and B_m are arbitrary constants depending on m; and $C_m(p)$ and $D_m(p)$ are arbitrary functions of p, also depending on m.

XIX

EXPANSION OF THE RECIPROCAL DISTANCE in Cone Functions

The first step in the solution of the physical problem is the derivation of the expression for the potential due to a point source of current, situated in a homogeneous space, in terms of these functions. Let the source of strength I be located at $(r_0, \theta_0, 0)$ as is shown in the accompanying diagram; and consider for the moment that the region is one of uniform resistivity. The results are obtained by fol-

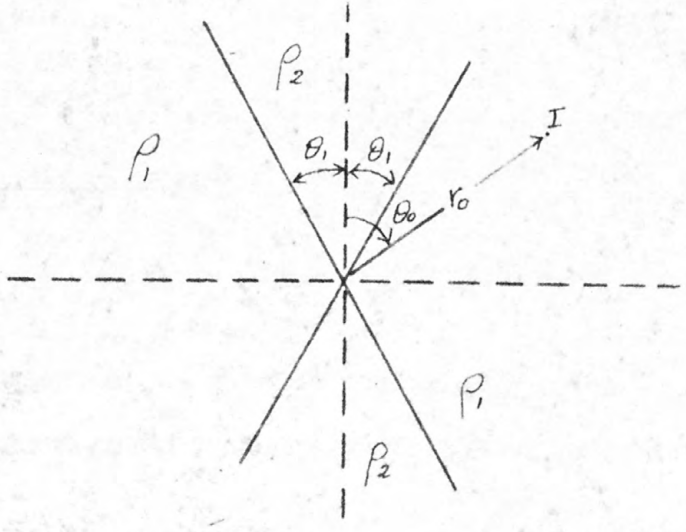

Figure Eight - Cross-section of a Double Cone.

lowing the same reasoning which was used in section IX.

The orientation of the coordinate system so that the source lies in the meridian plane permits the elimination of the sine term from the expression in equation 73. Further, due to the behavior of the associated Legendre functions being employed, it is convenient to divide space into those regions for which $\theta < \theta_0$ and $\theta > \theta_0$ respectively. In the first of these regions, which contains that part of the axis where $\theta = 0$, the potential has the form:

$$(98) \quad U_1 = \frac{1}{r^{1/2}} \sum_{m=0}^{\infty} \cos m\varphi \int_{-\infty}^{\infty} A_0 e^{-ip\ln r} P^m_{ip-1/2}(\cos\theta)\, dp$$

Similarly, in the second region where $\cos\theta$ may become equal to minus one, the potential is given by:

$$(99) \quad U_2 = \frac{1}{r^{1/2}} \sum_{m=0}^{\infty} \cos m\varphi \int_{-\infty}^{\infty} B_0 e^{ip\ln r} P_{ip-1/2}(-\cos\theta)\, dp$$

From the condition that the potential must be continuous across the surface of the cone $\theta = \theta_0$, it is seen at once that the relationship between A_0 and B_0 is:

$$(100) \quad A_0 = B_0 K^m_p(\cos\theta_0)$$

where $K^m_p(\cos\theta_0)$ is defined by:

$$(101) \quad K^m_p(\cos\theta_0) = \frac{P^m_{ip-1/2}(-\cos\theta_0)}{P^m_{ip-1/2}(\cos\theta_0)}$$

In order to determine the specific value of B_0, let us now examine the current density originating on the surface $\theta = \theta_0$ which is given by:

$$(102) \quad -\frac{1}{\rho}\left\{(\nabla U_2)_\theta - (\nabla U_1)_\theta\right\}_{\theta_0} = \frac{\sin\theta_0}{\rho r^{3/2}} \sum_m \cos m\varphi \int_{-\infty}^{\infty} B_0 e^{ip\ln r} \Psi^m_p(\cos\theta_0)\, dp$$

where, analogous to equation 31, $\Psi_p^m(\cos\theta_0)$ is defined as:

$$(103)\quad \Psi_p^m(\cos\theta_0) = -K_p^m(\cos\theta_0)\, P'^m_{ip-1/2}(\cos\theta_0) - P'^m_{ip-1/2}(-\cos\theta_0)$$

The primes in this expression indicate differentiation of a function with respect to its own argument.

The limiting process used on page 21 of section IX is omitted here; but it should be remarked that, in principle, the former procedure is still necessary.

If both sides of equation 103 are multiplied by $\frac{e^{-ip'\ln r}\cos m'\varphi}{r^{1/2}}$ and the resulting expressions integrated over the whole surface of the cone, the desired result is obtained. First, one has on the left side of the equation:

$$(104)\quad \begin{aligned} &-\int \frac{e^{-ip'\ln r}\cos m'\varphi}{r^{1/2}}\,\frac{1}{\rho}\left\{(\nabla u_2)_\theta - (\nabla u_1)_\theta\right\} dS \\ &= -\frac{e^{-ip'\ln r_0}}{r_0^{1/2}}\int_{\Delta S}\frac{1}{\rho}\left\{(\nabla u_2)_\theta - (\nabla u_1)_\theta\right\} dS = I\,\frac{e^{-ip\ln r_0}}{r_0^{1/2}} \end{aligned}$$

Introducing the appropriate element of area in spherical coordinates, the right side of equation 102 becomes:

$$(105)\quad \frac{\sin^2\theta_0}{\rho}\sum_m \cos m\varphi\,\cos m'\varphi \int_{-\infty}^{\infty} B_0\,\Psi_p^m(\cos\theta_0)\,dp \int_0^{\infty} e^{i(p-p')\ln r}\,\frac{dr}{r}$$

Integrating with respect to φ, and introducing the new variable $\nu = \ln r$, the expression is reduced to:

$$(106)\quad \frac{(1+\delta_{0m'})\pi\sin^2\theta_0}{\rho}\int_{-\infty}^{\infty} B_0\,\Psi_p^{m'}(\cos\theta_0)\,dp \int_{-\infty}^{\infty} e^{i(p-p')\nu}\,d\nu$$

This multiple integral may be evaluated through a knowledge of the Dirac delta function[4] which equals zero when its argument is not zero

---

4. Schiff, pp 50-51.

but becomes infinite as its argument approaches zero. This infinity is such that the definite integral of the delta function from negative to positive infinity is equal to one. As applied to the present problem, one means of expressing this function is given by:

$$(107) \quad \delta(p-p') = \frac{1}{2\pi}\int_{-\infty}^{\infty} e^{i(p-p')v}\,dv$$

A further property of the delta function is stated in the following form:

$$(108) \quad \int_{-\infty}^{\infty} f(p)\,\delta(p-p')\,dp = f(p')$$

Applying equations 107 and 108, one may finally reduce the expression in 106 to:

$$(109) \quad \frac{2(1+\delta_{om'})\pi^2 \sin^2\theta_0}{\rho} B_0 \Psi_{p'}^{m'}(\cos\theta_0)$$

Rejoining the two sides of equation 102 after these operations, dropping the primes on p and m, and solving the resulting equation for B_0, one gets:

$$(110) \quad B_0 = \frac{I p e^{-ip\ln r_0}}{2 r_0^{1/2}(1+\delta_{om})\pi^2 \sin^2\theta_0 \Psi_p^m(\cos\theta_0)}$$

The expression for $\Psi_p^m(\cos\theta_0)$ in equation 103 may be reduced to one of two convenient forms. The first may be deduced by reasoning similar to that used in obtaining equation 36. It can be shown by the previous procedure that:

$$(111) \quad \sin^2\theta\left[P_{ip-1/2}^m(-\cos\theta)\,P'^m_{ip-1/2}(\cos\theta) + P_{ip-1/2}^m(\cos\theta)\,P'^m_{ip-1/2}(-\cos\theta)\right] = C_m(p)$$

where $C_m(p)$ is indapendent of θ but may depend on m and p. This

constant is most easily evaluated at $\theta = \frac{\pi}{2}$ where it is found to be:

(112) $$C_m(p) = 2 P^m_{ip-1/2}(0) P'^m_{ip-1/2}(0)$$

Direct differentiation of equation 21 with respect to x establishes the following recursion formula:

(113) $$\sqrt{1-x^2}\, P'^m_n(x) = P^{m+1}_n(x) - m \frac{x}{\sqrt{1-x^2}} P^m_n(x)$$

which is valid for arbitrary n and integral, positive m. This recursion formula shows that $P'^m_{ip-1/2}(0)$ may be replaced in equation 112 by $P^{m+1}_{ip-1/2}(0)$. One then obtains:

(114) $$\Psi^m_p(\cos\theta_0) = -\frac{2 P^m_{ip-1/2}(0) P^{m+1}_{ip-1/2}(0)}{\sin^2\theta_0 P^m_{ip-1/2}(\cos\theta_0)}$$

The second expression for $\Psi^m_p(\cos\theta_0)$ is obtained through an alternate evaluation of the above constant $C_m(p)$. The new result is expressed as:[5]

(115) $$C_m(p) = \frac{-2 \sin(ip - 1/2 - m)\pi}{\sin(ip - 1/2 + m)\pi\, \Gamma(1/2 - ip + m)\Gamma(1/2 + ip - m)}$$

which, since m is an integer, reduces to:

(116) $$C_m(p) = \frac{-2}{\Gamma(1/2 - ip - m)\Gamma(1/2 + ip - m)}$$

By tedious, successive applications of the functional relationship:

(117) $$z\Gamma(z) = \Gamma(z+1)$$

which the gamma function satisfies, the expression may be changed to:

(118) $$C_m(p) = \frac{-2(-1)^m \Gamma(1/2 + ip + m)}{\Gamma(1/2 + ip)\Gamma(1/2 - ip)\Gamma(1/2 + ip - m)}$$

---

5. Snow, p 54.

This result may now be reduced by the relationship:[6]

$$(119) \quad \Gamma(\tfrac{1}{2}-z)\,\Gamma(\tfrac{1}{2}+z) = \pi \sec \pi z$$

whence one arrives at the expression:

$$(120) \quad C_m(p) = \frac{-2(-1)^m \Gamma(\frac{1}{2}+ip+m)\cosh \pi p}{\pi \Gamma(\frac{1}{2}+ip-m)}$$

Thus, the alternate expression for $\Psi_p^m(\cos\theta_0)$ is given by:

$$(121) \quad \Psi_p^m(\cos\theta_0) = \frac{2(-1)^m \Gamma(\frac{1}{2}+ip+m)\cosh \pi p}{\pi \Gamma(\frac{1}{2}+ip-m)\sin^2\theta_0\, P^m_{ip-\frac{1}{2}}(\cos\theta_0)}$$

Finally, the potential may be expressed in the form:

$$(122) \quad U = \frac{I\rho}{4\pi} \sum_m \frac{(2-\delta_{0m})}{2\sqrt{r_0 r}} \cos m\varphi \int_{-\infty}^{\infty} \frac{e^{ip\ln r_0/r}}{J_m(p)} \cdots \cdots P^m_{ip-\frac{1}{2}}(-\cos\theta_0)\, P^m_{ip-\frac{1}{2}}(\cos\theta)\, P^m_{ip-\frac{1}{2}}(\cos\theta_0)\, P^m_{ip-\frac{1}{2}}(-\cos\theta)\, dp$$

where, depending on whether one chooses to use equation 114 or 121, $J_m(p)$ may assume one of two forms. These are:

$$(123) \quad J_m(p) = -\pi P^m_{ip-\frac{1}{2}}(0)\, P^{m+1}_{ip-\frac{1}{2}}(0)$$

or:

$$(124) \quad J_m(p) = (-1)^m \frac{\Gamma(\frac{1}{2}+ip+m)}{\Gamma(\frac{1}{2}+ip-m)} \cosh \pi p$$

It may happen that one of these expressions is more convenient for computations under a given set of circumstances; while the other is more applicable at other times. The first is indicated (without the change introduced between equations 112 and 114) by the statement of Smythe's

---

6. Jahnke and Emde, p 12.

problem.[1] Further, the validity of the results is implied since the second form corresponds to the expansion of the reciprocal distance, in terms of the cone functions, given by Hobson in a more formal mathematical treatment.[7] It should be noticed that:

$$\frac{\Gamma(\frac{1}{2}+ip+m)}{\Gamma(\frac{1}{2}+ip-m)} = (-1)^m\left[p^2+\tfrac{1}{4}\right]\left[p^2+\tfrac{9}{4}\right]\cdots\left[p^2+\frac{(2m-1)^2}{4}\right] \tag{125}$$

If m is zero, the above ratio is one. This result may be of particular interest in computations based on the second form presented above.

Inasmuch as all of the quantities in equation 122 are even functions of p except the imaginary part of the exponential, this part of the exponential vanishes in the integration over p. On the other hand, the real part yields a result which is double that which would be obtained if the integration of the real part were taken between the limits of zero and infinity. Thus, an alternate form of the potential is:

$$U = \frac{I\rho}{4\pi}\sum \frac{(2-\delta_{om})}{\sqrt{r_0 r}}\cos m\phi \int_0^\infty \frac{\cos(p\ln r/r_0)}{J_m(p)} \tag{126}$$

$$P^m_{ip-\frac{1}{2}}(-\cos\theta)\,P^m_{ip-\frac{1}{2}}(\cos\theta) \cdots dp$$

$$P^m_{ip-\frac{1}{2}}(\cos\theta_0)\,P^m_{ip-\frac{1}{2}}(-\cos\theta)$$

XX

BEHAVIOR OF THE SOLUTION AT THE ORIGIN

The cone functions discussed above were introduced in connection with problems in electrostatics by Mehler;[1] but, because of the apparent

---

7. Hobson, p 447.
1. Mehler, 1868.

singularity in the consequent solutions at the origin, the actual validity of these solutions has ~~long been in doubt~~ sometimes been questionned.[2] It will be shown here, at least in a special case, that this objection is in fact unfounded.

Consider the expression for the reciprocal distance, as developed in the previous section:

$$\frac{1}{R} = \sum_{m=0}^{\infty} (-1)^m \frac{(2-\delta_{om})}{\sqrt{r_0 r}} \cos m\phi \int_0^{\infty} \frac{\cos(p \ln r/r_0)\,\Gamma(\frac{1}{2}+ip-m)}{\cosh \pi p\,\Gamma(\frac{1}{2}+ip+m)} \cdots$$

(127)

$$\cdots \frac{P^m_{ip-1/2}(-\cos\theta_0)\, P^m_{ip-1/2}(\cos\theta)}{P^m_{ip-1/2}(\cos\theta_0)\, P^m_{ip-1/2}(-\cos\theta)}\, dp$$

If the reference point be placed on the polar axis so that $\theta_0 = 0$, the expansion is independent of the angle ϕ and thus only the term for which m is zero need be retained. Since θ must now always be greater than θ_0, only the lower of the forms in equation 127 is used. If the situation is further restricted by the requirement that the variable point lie on the part of the polar axis where $\theta = \pi$, the expansion is finally reduced to:

(128) $$\frac{1}{R} = \frac{1}{\sqrt{r_0 r}} \int_0^{\infty} \frac{\cos(p \ln r/r_0)}{\cosh \pi p}\, dp$$

Note that $P^{m}_{ip-1/2}(\cos\theta_0)$ and $P^{m}_{ip-1/2}(-\cos\theta_0)$ have disappeared from the expression because they are both unity in this case.

It is now required to show that R reduces to r plus r_0 as a result of this expression, regardless of the point to which r is measured within the restrictions already imposed. The above integral may readily be evaluated and the desired result thus obtained.

---

2. Hobson, p 448.

Consider the contour integral:

$$(129) \qquad \oint \frac{\cos(z \ln r/r_0)}{\cosh \pi z} dz = \int_{-\infty}^{\infty} \frac{\cos(p \ln r/r_0)}{\cosh \pi p} dp + \int_{\infty}^{-\infty} \frac{\cos[(p+i) \ln r/r_0]}{\cosh \pi(p+i)} dp$$

where the path of integration encloses the infinite strip bounded by z equal to p and z equal to p plus i. The ends of the strip, where p is infinite, add no contribution to the integral. Introducing elementary relationships involving the trigonometric and hyperbolic functions of the sum of two quantities, reversing the limits of integration in the second term, and noting that the integrands are even functions of p so that the lower limit can be changed to 0 by doubling the resulting integral, it can be shown that:

$$(130) \qquad \oint \frac{\cos(z \ln r/r_0)}{\cosh \pi z} dz = 4 \cosh^2(\tfrac{1}{2} \ln r/r_0) \int_0^{\infty} \frac{\cos(p \ln r/r_0)}{\cosh \pi p} dp$$

The new integral on the right is identical to that required in equation 128. The integral on the left may be evaluated by Cauchy's integral theorem. Noting that there is only one pole enclosed by the path of integration, it occuring at z equal to i/2 where the residue is $\frac{\cosh(\frac{1}{2} \ln r/r_0)}{\pi i}$, the integral is seen to be:

$$(131) \qquad \oint \frac{\cos(z \ln r/r_0)}{\cosh \pi z} dz = 2 \cosh(\tfrac{1}{2} \ln r/r_0)$$

Consequently, the integral in equation 128 is found to equal:

$$(132) \qquad \int_0^{\infty} \frac{\cos(p \ln r/r_0)}{\cosh \pi z} dp = \frac{1}{2} \operatorname{sech}(\tfrac{1}{2} \ln r/r_0) = \frac{\sqrt{r_0 r}}{r + r_0}$$

and, as required:

$$(133) \qquad \frac{1}{R} = \frac{1}{r + r_0}$$

It is seen that this expression satisfies the requirements of the

problem whether r is zero or very large. It thus follows that the expansion in equation 128 must likewise be valid in spite of the apparent singularity at the origin.

~~Apparently, no one has ever questioned the validity of the expansion in equation 127 as r approaches infinity. It is reasoned here that, were enough known about the quantities in the expansion as functions of p, an integration could be carried out in the limits of the general case similar to the one above. And, thus, it could be shown by a single argument that the expansion vanishes at infinity as the order of 1/r and converges near the origin, approaching $1/r_0$ as r vanishes.~~

XXI

CONAL BOUNDARIES

Now, letting θ_0 become 90 degrees and considering the regions of different resistivities as shown in the diagram on page 57, one can investigate the potential due to a point source under those new circumstances. Due to the symmetry presented by the problem, it is necessary to set up expressions for the potential only within the upper cone and for the region exterior to both cones.

In the first region of resistivity ρ_2, where $\cos\theta$ becomes plus one, the potential has the form:

$$(134)\quad U_{2A} = \frac{1}{r^{1/2}} \sum_{m=0}^{\infty} \cos m\phi \int_{-\infty}^{\infty} A_m(p)\, P^m_{ip-1/2}(\cos\theta)\, e^{ip\ln r}\, dp$$

In the region of resistivity ρ_1, which contains no part of the polar axis, the potential may be written as:

$$(135)\quad U_{1A} = \frac{1}{r^{1/2}} \sum_{m=0}^{\infty} \cos m\phi \int_{-\infty}^{\infty} \left\{ B_m(p) \left[P^m_{ip-1/2}(\cos\theta) + P^m_{ip-1/2}(-\cos\theta) + \begin{matrix} A_0 P^m_{ip-1/2}(\cos\theta) \\ B_0 P^m_{ip-1/2}(-\cos\theta) \end{matrix} \right] \right\} e^{ip\ln r}\, dp$$

In the above expressions, $A_m(p)$ and $B_m(p)$ are arbitrary and have to

be determined from the boundary conditions; A_o and B_o have the values derived in section XIX.

From the condition that the potential must be continuous across the conal boundary $\theta = \theta_1$, it is seen that:

$$(136) \quad A_m(p) = B_m(p)\left[1 + K_p^m(\cos\theta_1)\right] + A_o$$

where $K_p^m(\cos\theta_1)$ has its value given in equation 101.

And, in order that the normal component of the current density be continuous across the same boundary, it is necessary that:

$$(137) \quad \rho_1 A_m(p) = \rho_2\left\{B_m(p)\left[1 - L_p^m(\cos\theta_1)\right] + A_o\right\}$$

where $L_p^m(\cos\theta_1)$ is defined by:

$$(138) \quad L_p^m(\cos\theta_1) = \frac{P'^m_{ip-1/2}(-\cos\theta_1)}{P'^m_{ip-1/2}(\cos\theta_1)}$$

and the primes indicate the differentiation of a function with respect to its own argument.

If these equations be solved simultaneously for $A_m(p)$ and $B_m(p)$, one arrives at the following expressions:

$$(139) \quad \begin{aligned} A_m(p) &= \frac{\rho_2\left[K_p^m(\cos\theta_1) + L_p^m(\cos\theta_1)\right]}{\rho_1 - \rho_2 + \rho_1 K_p^m(\cos\theta_1) + \rho_2 L_p^m(\cos\theta_1)} \\ B_m(p) &= \frac{\rho_2 - \rho_1}{\rho_1 - \rho_2 + \rho_1 K_p^m(\cos\theta_1) + \rho_2 L_p^m(\cos\theta_1)} A_o \end{aligned}$$

The correct expressions for the potential may now be written down by combining several of the above results. The reciprocal distance is returned to its closed form; A_o is given its value from equations 100 and 110; $\Psi_p^m(\cos\theta_0)$ is written according to equation 114; and, the inte-

gral is written in analogy with equation 126. Then, remembering that $\theta_0 = 0$, the potential functions become:

$$U_{2A} = -\frac{I\rho_1}{4\pi}\sum_{m=0}^{\infty}\frac{(2-\delta_{0m})}{\pi\sqrt{r_0 r}}\cos m\varphi \cdots$$

(140)

$$\cdots \int_0^{\infty}\frac{\rho_2[K_p^m(\cos\theta_1)+L_p^m(\cos\theta_1)]}{\rho_1+\rho_2+\rho_1 K_p^m(\cos\theta_1)+\rho_2 L_p^m(\cos\theta_1)}\cos(p\ln r/r_0)\frac{P^m_{ip-1/2}(\cos\theta)}{P^{m+1}_{ip-1/2}(0)}dp$$

and:

$$U_{1A} = \frac{I\rho_1}{4\pi}\left\{\frac{1}{R}+\sum_{m=0}^{\infty}\frac{(2-\delta_{0m})}{\pi\sqrt{r_0 r}}\cos m\varphi\int_0^{\infty}\frac{\rho_1-\rho_2}{\rho_1-\rho_2+\rho_1 K_p^m(\cos\theta_1)+\rho_2 L_p^m(\cos\theta_1)}\cdots\right.$$

(141)

$$\cdots\frac{\cos(p\ln r/r_0)}{P^m_{ip-1/2}(0)}\cdot\left[P^m_{ip-1/2}(\cos\theta)+P^m_{ip-1/2}(-\cos\theta)\right]dp$$

If it is desired to apply this solution to a geologic problem, only the second of these formulae need be considered. The plane $\theta = \pi/2$ is assumed to be the surface of the earth, in which case $\cos\theta$ is zero for all points at which the potential is to be measured. Doubling the value of the expression, for reasons explained at the beginning of section VI, one gets for the potential distribution over the surface of the earth:

$$U_{1A} = \frac{I\rho_1}{2\pi}\left\{\frac{1}{R}+\sum_{m=0}^{\infty}\frac{2(2-\delta_{0m})}{\pi\sqrt{r r_0}}\cos m\varphi\int_0^{\infty}\frac{\rho_1-\rho_2}{\rho_1-\rho_2+\rho_1 K_p^m(\cos\theta_1)+\rho_2 L_p^m(\cos\theta_1)}\cdots\right.$$

(142)

$$\cdots\cos(p\ln r/r_0)\frac{P^m_{ip-1/2}(0)}{P^{m+1}_{ip-1/2}(0)}dp$$

This equation is of some use later in computing the asymptotic behavior of curves constructed for the hyperboloidal problem.

PART FIVE

HYPERBOLOIDAL BOUNDARIES

XXII

A SECOND SOLUTION OF LAPLACE'S EQUATION in Prolate Spheroidal Coordinates

In this paper, there is interest only in hyperboloids of two sheets. Therefore, the discussion in Part Five is restricted to prolate spheroidal coordinates.

In section VIII, it was shown that Laplace's equation in prolate spheroidal coordinates yields a general solution[1] which contains functions orthogonal over the ellipsoidal surfaces. In the present section, we are looking for a general solution which contains functions orthogonal over the hyperbolic surfaces. The development of the solution is identical with the previous case, in section VIII, down to the point where the associated Legendre equation must be solved. Consider again the equation which $G(\xi)$ satisfies:

$$(17) \quad \frac{d}{d\xi}\left[(1-\xi^2)\frac{dG}{d\xi}\right] + \left[n(n+1) - \frac{m^2}{1-\xi^2}\right]G = 0$$

The previous choice of n as a positive integer stemmed from a knowledge of the orthogonality properties of the associated Legendre polynomials. However, the same orthogonality properties are no longer desired; and, consequently, n can no longer be taken to be an integer. On the other hand, the dependence of the solution on the angle φ has not changed from the previous case. Therefore, m is still an integer but with its range unrestricted.

It was shown at the beginning of section XII that a given hyper-

---

1. See equation 24.

boloid $\xi = \xi_1$ is asymptotic to a corresponding cone $\theta = \theta_1$ where the two parameters are related by $\xi_1 = \cos\theta_1$. Hence, it is implied that the dependence of the present solution upon ξ may be the same as the dependence upon $\cos\theta$ in the solution of the cone problem in section XVIII. Thus, as a solution of equation 17, we try:

$$(143) \qquad G = C_m(p)\, P^m_{ip-1/2}(\xi) + D_m(p)\, P^m_{ip-1/2}(-\xi)$$

The properties of these functions were discussed in the earlier section.

It was remarked in section VIII that $G(\xi)$ and $H(\eta)$ satisfy an equation of the same form - i.e., equation 17. In considering the appropriate solution for $H(\eta)$, it is noted that $P^m_{ip-1/2}(\eta)$ and $P^m_{ip-1/2}(-\eta)$ are independent solutions of the differential equation for the reasons given in the discussion of the cone functions. However, as it has previously been noted, $P^m_{ip-1/2}(-\eta)$ becomes infinite as η approaches plus one; and, since η equals plus one within any region bounded only by hyperboloids of the set for which ξ serves as the parameter, this function may be discarded from the solution at once. The function $P^m_{ip-1/2}(\eta)$ may be termed a "hyperboloid function" to distinguish it from the cone functions in which the argument is less than one.

Throughout the range of η, the hyperboloid function may be defined by:

$$(144) \qquad P_{ip-1/2}(\eta) = \left[\frac{1+\eta}{2}\right]^{ip-1/2} F\left(\tfrac{1}{2} - ip, \tfrac{1}{2} - ip, 1; \frac{\eta-1}{\eta+1}\right)$$

when m is equal to zero.

---

2. Magnus, p 56.

An integral expression for the same function is given by:[3]

$$P_{ip-1/2}(\eta) = \frac{2}{\pi} \cos \pi p \int_0^\infty \frac{\cos px}{(2\cosh x + 2\eta)^{1/2}}\, dx \tag{145}$$

Since m is a positive integer, the associated function may be defined by equation 22. There are many other valid definitions which may be adapted to the associated Legendre functions of order ip - 1/2 and for the present range of η.[4]

A general solution to Laplace's equation, in prolate spheroidal coordinates, may now be written down. It is necessary to sum over m from zero to infinity; and, because p may vary continuously, an integration is required over all positive values of p. Negative values of p are not required because the solution is an even function of p. The solution is:

$$U = \sum_{m=0}^{\infty} \left[A_m \cos m\varphi + B_m \sin m\varphi\right] \cdots$$

$$\cdots \int_0^\infty \left[C_m(p)\, P^m_{ip-1/2}(\xi) + D_m(p)\, P^m_{ip-1/2}(-\xi)\right] P^m_{ip-1/2}(\eta)\, dp \tag{146}$$

XXIII

ORTHOGONALITY OF THE HYPERBOLOID FUNCTIONS

In order to use the solution in the type of problems being considered, it is necessary to examine the orthogonality of the set $P^m_{ip-1/2}(\eta)$. One is led to suspect the orthogonality of the set because it has been shown that $P^m_{ip-1/2}(\eta)$ has an infinite number of zeros between $\eta = 1$ and $\eta = \infty$.[1]

---

3. Hobson, p 451.
4. Idem, pp 189, 195, 204, 209, 219, 272, etc.
1. Idem, p 402.

The end is accomplished in a straightfoward manner. Consider only two functions of the set and for simplicity let them be denoted by:

$$(147)\quad \begin{cases} H_1 = P^m_{ip_1-1/2}(\eta) \\ H_2 = P^m_{ip_2-1/2}(\eta) \end{cases}$$

Since each of these functions is a solution of an equation similar to equation 17, one may write:

$$(148)\quad \begin{aligned} &\frac{d}{d\eta}\left[(1-\eta^2)\frac{dH_1}{d\eta}\right] + \left[(ip_1-1/2)(ip_1+1/2) - \frac{m^2}{1-\eta^2}\right]H_1 = 0 \\ &\frac{d}{d\eta}\left[(1-\eta^2)\frac{dH_2}{d\eta}\right] + \left[(ip_2-1/2)(ip_2+1/2) - \frac{m^2}{1-\eta^2}\right]H_2 = 0 \end{aligned}$$

Multiplying the first equation by H_2, the second by H_1, subtracting the first from the second, and integrating from 1 to η, one gets:

$$(149)\quad \begin{aligned} (p_1^2-p_2^2)\int_1^\eta H_1H_2\,d\eta = &\int_1^\eta H_1\frac{d}{d\eta}\left[(\eta^2-1)\frac{dH_2}{d\eta}\right]d\eta \\ &- \int_1^\eta H_2\frac{d}{d\eta}\left[(\eta^2-1)\frac{dH_1}{d\eta}\right]d\eta \end{aligned}$$

which, by integration of both terms on the right side by parts, is easily reduced to:

$$(150)\quad (p_1^2-p_2^2)\int_1^\eta H_1H_2\,d\eta = \left[(\eta^2-1)\left\{H_1\frac{dH_2}{d\eta} - H_2\frac{dH_1}{d\eta}\right\}\right]_1^\eta$$

Since $P^m_{ip-1/2}(1)$ and $P'^m_{ip-1/2}(1)$ are finite, the expression on the right is zero at the lower limit. Therefore, the evaluation of the integral on the left is reduced to an investigation of the right side of equation 150 as a function of η.

Consider now the integral:

$$\lim_{\eta\to\infty}\int_{-\infty}^{\infty} f(p_2)\,dp_2\int_1^{\eta} H_1 H_2\,d\eta =$$

(151)

$$\lim_{\eta\to\infty}\int_{-\infty}^{\infty} f(p_2)\,dp_2\left\{\frac{\eta^2-1}{p_1^2-p_2^2}\left[H_1\frac{dH_2}{d\eta}-H_2\frac{dH_1}{d\eta}\right]\right\}$$

where the function $f(p_2)$ is assumed to be properly behaved.

Required in the development is the asymptotic expansion of the Legendre function for large values of the argument. This is:[2]

$$P^{m}_{ip-1/2}(\eta) = \left\{\frac{2^{ip-1/2}\Gamma(ip)}{\sqrt{\pi}\,\Gamma(ip+1/2-m)}\eta^{ip-1/2}\right.$$

(152)

$$\left.+\frac{2^{-ip-1/2}\Gamma(-ip)}{\sqrt{\pi}\,\Gamma(-ip+1/2-m)}\eta^{-ip-1/2}\right\}\left\{1+O\left(\frac{1}{\eta^2}\right)\right\}$$

which could as well be written in the form:

(153) $$P^{m}_{ip-1/2}(\eta) = \left\{\frac{1}{\eta^{1/2}}\left[A_m(p)\cos(p\ln\eta)+B_m(p)\sin(p\ln\eta)\right]\right\}\left\{1+O\left(\frac{1}{\eta^2}\right)\right\}$$

where the constants are given by:

(154) $$\begin{cases} A_m(p) = 2\,Re\left[\dfrac{2^{ip-1/2}\Gamma(ip)}{\sqrt{\pi}\,\Gamma(ip+1/2-m)}\right] \\ B_m(p) = -2\,Im\left[\dfrac{2^{ip-1/2}\Gamma(ip)}{\sqrt{\pi}\,\Gamma(ip+1/2-m)}\right] \end{cases}$$

Corresponding to equation 153, which is the form to be used throughout this discussion, is the following relationship:

$$\frac{dP^{m}_{ip-1/2}(\eta)}{d\eta} = -\frac{1}{2\eta^{3/2}}\left\{\left[A_m(p)-2pB_m(p)\right]\cos(p\ln\eta)\right.$$

(155)

$$\left.+\left[2p\,A_m(p)+B_m(p)\right]\sin(p\ln\eta)\right\}\left\{1+O\left(\frac{1}{\eta^2}\right)\right\}$$

---

2. Magnus, p 66.

Substituting expressions of the form of equations 153 and 155 into equation 151, one gets, after rearranging the terms:

$$\lim_{\eta\to\infty}\int_{-\infty}^{\infty} f(p_2)\,dp_2 \int_1^{\eta} H_1 H_2\,d\eta = \tag{156}$$

$$\lim_{\eta\to\infty}\int_{-\infty}^{\infty} f(p_2)\,dp_2\,\frac{(\eta^2-1)}{\eta^2}\,F(P_1,P_2,\eta)\left\{1+O\left(\frac{1}{\eta^2}\right)\right\}$$

where:

$$F(P_1,P_2,\eta) = \tag{157}$$

$$\frac{[P_1 A_m(P_1)B_m(P_2) - P_2 A_m(P_2)B_m(P_1)}{P_1^2-P_2^2}\sin(p_1\ln\eta)\sin(p_2\ln\eta)$$

$$+\frac{[P_2 A_m(P_1)B_m(P_2) - P_1 A_m(P_2)B_m(P_1)}{P_1^2-P_2^2}\cos(p_1\ln\eta)\cos(p_2\ln\eta)$$

$$+\frac{A(p_1)A(p_2)\sin(p_2\ln\eta)\cos(p_1\ln\eta) - B(p_1)B(p_2)\sin(p_2 p_1\ln\eta)\cos(p_2\ln\eta)}{}$$

$$+\frac{P_1}{P_1+P_2}\left[A(p_1)A(p_2)+B(p_1)B(p_2)\right]\frac{\sin[(P_1-P_2)\ln\eta]}{(P_1-P_2)}$$

The first point to be noted is that the factor $\frac{\eta^2-1}{\eta^2}$ may be removed from under the integral sign and becomes unity in the limit. The second point of interest is that the terms of the order of $1/\eta^2$ vanish in the limit; and, therefore, one is left with the sine and cosine terms to be investigated.

It has been shown that the Legendre functions are analytic functions of their order, in this case of ip - 1/2, within the ranges of their arguments for which the various definitions are valid.[3] It follows then that $A_m(p)$ and $B_m(p)$ are similarly analytic. It is further assumed

---

3. Hobson, 189.

that the products of $A_m(p)$, $B_m(p)$, and $f(p)$ are integrable.

On this basis then, except in the case for which p_1 equals p_2, it is apparent that $F(p_1, p_2, \eta)$ remains finite for all values of p_1 and p_2. It is now necessary to investigate, term by term, the exception if one exists. The first term in $F(p_1, p_2, \eta)$ leads to an indeterminancy, as p_2 approaches p_1, which may be evaluated by l'Hopital's rule:

$$\lim_{p_2 \to p_1} \frac{p_1 A_m(p_1) B_m(p_2) - p_2 A_m(p_2) B_m(p_1)}{p_1^2 - p_2^2} \tag{158}$$

$$= \lim_{p_2 \to p_1} \frac{p_1 A_m(p_1) B_m'(p_2) - A_m(p_2) B_m(p_1) - p_2 A_m'(p_2) B_m(p_1)}{-2 p_2}$$

The primes in equation 158 indicate differentiation with respect to p_2. Since $A_m(p)$ and $B_m(p)$ are analytic as explained above, it follows that the first term in $F(p_1, p_2, \eta)$ remains finite as p_2 approaches p_1. A similar argument may be applied to the second term in the expression. The third term requires no discussion of this kind. Now, during the integration over p_2, none of these terms adds any contribution, because of the integral theorem which states that:[4]

$$\lim_{\eta \to \infty} \int_a^b f(x) \begin{matrix} \sin \\ \cos \end{matrix} nx\,dx = 0 \tag{159}$$

The fourth term in the expression presents a somewhat different picture. The effect of this expression on the value of the integral is implied by one form of Dirichlet's integrals, which is:[5]

$$\lim_{\mu \to \infty} \int_0^\gamma f(x) \frac{\sin \mu x}{x}\,dx = \frac{\pi}{2} f(0) \tag{160}$$

Therefore, one finds that the net value of the integral in equa-

---

4. Carslaw, p 358.
5. Idem, p 219.

tion 156 is:

$$\lim_{\eta\to\infty}\int_{-\infty}^{\infty} f(p_2)\,dp_2\int_1^{\eta} H_1 H_2\,d\eta = +\frac{\pi}{2}\left[A_m^2(p_1)+B_m^2(p_1)\right]f(p_1) \tag{161}$$

It is now useful to evaluate explicitly the quantity in brackets in terms of m and p. This end is readily accomplished by noting from equation 154 that:

$$A_m^2(p)+B_m^2(p) = 4\left[\frac{2^{ip-1/2}\Gamma(ip)}{\sqrt{\pi}\,\Gamma(ip+1/2-m)}\right]\left[\frac{2^{-ip-1/2}\Gamma(-ip)}{\sqrt{\pi}\,\Gamma(-ip+1/2-m)}\right] \tag{162}$$

which reduces to:

$$A_m^2(p)+B_m^2(p) = \frac{2}{\pi}\,\frac{\Gamma(ip)\Gamma(-ip)}{\Gamma(ip+1/2-m)\Gamma(-ip+1/2-m)} \tag{163}$$

The expression in equation 163 may be further reduced by the relations:[5]

$$\Gamma(ip)\Gamma(-ip) = \frac{\pi}{p\sinh \pi p} \tag{164}$$

and:[6]

$$\frac{1}{\Gamma(1/2-ip-m)\Gamma(\frac{1}{2}+ip-m)} = \frac{(-1)^m\Gamma(\frac{1}{2}+ip+m)}{\pi\Gamma(\frac{1}{2}+ip-m)}\cosh \pi p \tag{165}$$

Finally, then, one may write:

$$A_m^2(p)+B_m^2(p) = \frac{2(-1)^m\Gamma(ip+1/2+m)}{\pi p\,\Gamma(ip+1/2-m)}\cosh \pi p \tag{166}$$

Replacing the H's with the corresponding associated Legendre functions, and substituting equation 166 into equation 161, one finds that:

---

5. Jahnke and Emde, p 12.
6. See equations 116-120 and 125.

$$\lim_{\eta\to\infty}\int_{-\infty}^{\infty} f(p_2)\,dp_2 \int_1^{\eta} P^m_{ip_1-1/2}\, P^m_{ip_2-1/2}\, d\eta =$$

(167)

$$+\frac{(-1)^m}{p_1}\,\frac{\Gamma(ip_1+1/2+m)}{(ip_1+1/2-m)}\coth \pi p_1 f(p_2)$$

As is customary, for example in the case of the orthogonality of the ordinary exponential function, we can now write the orthogonality property of the hyperboloid functions symbolically in terms of the Dirac delta function as follows:

(168) $$\int_1^{\infty} P^m_{ip_1-1/2}(\eta)\, P^m_{ip_2-1/2}(\eta)\,d\eta = \frac{(-1)^m}{p_1}\,\frac{\Gamma(ip_1+1/2+m)}{\Gamma(ip_1+1/2-m)}\coth \pi p_1\, \delta(p_1-p_2)$$

Or, employing the relationship found in equation 125, one could write alternately:

(169) $$\int_1^{\infty} P^m_{ip_1-1/2}(\eta)\, P^m_{ip_2-1/2}(\eta)\,d\eta = \frac{\coth \pi p_1}{p_1}\left[p_1^2+\frac{1}{4}\right]\left[p_1^2+\frac{9}{4}\right]\cdots$$

$$\cdots\left[p_1^2+\frac{(2m-1)^2}{4}\right]\delta(p_1-p_2)$$

XXIV

EXPANSION OF THE RECIPROCAL DISTANCE in Hyperboloid Functions

Using the results of the last section, it is now possible to expand the potential due to a point source of current, situated in a homogeneous space, in terms of the functions in equation 146. Since the same reasoning has been used in two previous cases, the present discussion is kept to a minimum.

As usual, let the source be located at the point $(\eta_0, \xi_0, 0)$. Due to the correspondence between this case and the cone problem with respect

to ξ and $\cos\theta$, and with respect to the angle φ, we assume the two corresponding expansions to have a similar functional dependence on these quantities. Therefore, we write down immediately the starting point of the present development, with the potential in the form:

$$(170)\quad U_0 = \sum_{m=0}^{\infty} \cos m\varphi \int_0^{\infty} C_m(p) \frac{P^m_{ip-1/2}(\xi) P^m_{ip-1/2}(-\xi)}{P^m_{ip-1/2}(-\xi_0) P^m_{ip-1/2}(\xi_0)} P^m_{ip-1/2}(\eta)\, dp$$

In order to evaluate $C_m(p)$, the flux condition is employed as before. We start with the expression for the current density originating on the surface $\xi = \xi_0$, which is given by:

$$(171)\quad -\frac{1}{\rho}\left\{(\nabla U_2)_\xi - (\nabla U_1)_\xi\right\}_{\xi_0} = \frac{1}{b}\sqrt{\frac{1-\xi_0^2}{\eta^2-\xi_0^2}} \sum_m \cos m\varphi \cdots$$

$$\cdots \int_0^{\infty} C_m(p) \frac{2 J_m(p)}{\pi(1-\xi_0^2)} P^m_{ip-1/2}(\eta)\, dp$$

The subscripts 1 and 2 indicate that $\xi > \xi_0$ and $\xi < \xi_0$ respectively - i.e., they indicate the use of the upper or lower form, as the case may be, in equation 170. Equations 103 and 121 have been used to eliminate the derivatives of the cone functions which appeared in the expression on the right; and $J_m(p)$ should have its value given by equation 124.

Equation 171 is now multiplied by $\cos m'\varphi\, P^{m'}_{ip'-1/2}(\eta)\, dS$, where the element of area is given by:

$$(172)\quad dS = b^2\sqrt{(1-\xi_0^2)(\eta^2-\xi_0^2)}\, d\eta\, d\varphi$$

and both sides are integrated over η and φ. Analogous to equations 104 and 106, one arrives at the result:

$$(173)\quad I P^{m'}_{ip'-1/2}(\eta_0) = 2b(1+\delta_{0m'}) \int_0^{\infty} C_{m'}(p) J_{m'}(p)\, dp \int_1^{\infty} P^{m'}_{ip'-1/2}(\eta) P^{m'}_{ip-1/2}(\eta)\, d\eta$$

Using the value of the second integral as given by equation 168,

and employing the property of the delta function introduced in equation 108, the expression on the right side of equation 173 is reduced to:

$$(174)\quad I P^{m}_{ip-1/2}(\eta_0) = \frac{2b}{\rho}(1+\delta_{0m})C_m(p)\,J_m(p)\,\frac{(-1)^m}{p}\,\frac{\Gamma(\frac{1}{2}+ip+m)}{\Gamma(\frac{1}{2}+ip-m)}\cdot\coth \pi p$$

where the primes on m and p have been dropped because they are no longer necessary. Solving for $C_m(p)$ and introducing the value for $J_m(p)$, one gets:

$$(175)\quad C_m(p) = \frac{I\rho}{4\pi}\,\frac{(2-\delta_{0m})\pi}{b}\,\frac{p\tanh \pi p}{\cosh \pi p}\left[\frac{\Gamma(ip+1/2-m)}{\Gamma(ip+1/2+m)}\right]^2 P^{m}_{ip-1/2}(\eta_0)$$

which, when returned to equation 170, yields the desired expression for the reciprocal distance or for the potential due to a point source.

XXV

A BURIED DOME STRUCTURE

The stage is now set to treat problems in two interesting geologic situations. The first is a buried dome structure in which the boundaries may be approximated by hyperboloids of revolution. We will commence as in previous cases by considering the field due to a point source located at $(\eta_0, 0, 0)$ in the presence of boundaries at $\xi = \xi_1$. The material in the region $-\xi_1 < \xi < \xi_1$ is assigned a resistivity ρ_1 while the resistivity of the material filling the rest of space is ρ_2.

Due to the symmetry which exists when the source is located on the plane $\xi = 0$, expressions for the potential need be established only for the regions $-\xi_1 \le \xi \le \xi_1$ and $\xi_1 \le \xi \le 1$ respectively. A consideration of the boundary conditions at the interface between these regions suffices to determine all of the arbitrary constants. Moreover, the geophysical application may be made immediately by considering the plane $\xi = 0$ the earth's surface and thus doubling the potential for reasons given earlier.

In the region of resistivity ρ_1, let the potential be:

$$U_{1A} = \sum_{m=0}^{\infty} \cos m\varphi \int_0^{\infty} \left\{ C_m(p) \begin{matrix} P^m_{ip-1/2}(\xi) \, P^m_{ip-1/2}(-\xi_0) \\ P^m_{ip-1/2}(-\xi) \, P^m_{ip-1/2}(\xi_0) \end{matrix} \right.$$

(176)

$$\left. + A_m(p) \left[P^m_{ip-1/2}(\xi) + P^m_{ip-1/2}(-\xi) \right] \right\} P^m_{ip-1/2}(\eta)\, dp$$

In the second region, the potential has the form:

(171) $$U_{2A} = \sum_{m=0}^{\infty} \cos m\varphi \int_0^{\infty} B_m(p) \, P^m_{ip-1/2}(\xi) \, P^m_{ip-1/2}(\eta)\, d\eta$$

In these expressions, $A_m(p)$ and $B_m(p)$ are arbitrary functions of p, also depending on m; while $C_m(p)$ has double its value given by equation 175. The following simultaneous equations, which are sufficient to determine $A_m(p)$ and $B_m(p)$, arise from the boundary conditions applied at the surface :

(178) $$\begin{cases} -A_m(p)\left[1 + K_p^m(\xi_1)\right] + B_m(p) = C_m(p) P^m_{ip-1/2}(-\xi_0) \\ -\rho_2 A_m(p)\left[1 - L_p^m(\xi_1)\right] + \rho_1 B_m(p) = \rho_2 C_m(p) P^m_{ip-1/2}(-\xi_0) \end{cases}$$

Here $K_p^m(\ )$ and $L_p^m(\ )$ have the values defined by equations 101 and 138. A solution of these equations for $A_m(p)$ and $B_m(p)$ gives the expressions:

(179) $$\begin{cases} A_m(p) = \dfrac{\rho_2 - \rho_1}{\rho_1 - \rho_2 + \rho_1 K_p^m(\xi_1) + \rho_2 L_p^m(\xi_1)} C_m(p) \, P^m_{ip-1/2}(-\xi_0) \\ B_m(p) = \dfrac{\rho_2\left[K_p^m(\xi_1) + L_p^m(\xi_1)\right]}{\rho_1 - \rho_2 + \rho_1 K_p^m(\xi_1) + \rho_2 L_p^m(\xi_1)} C_m(p) \, P^m_{ip-1/2}(-\xi_0) \end{cases}$$

Henceforth, we are interested only in equation 176, and in that only at points on the plane $\xi = 0$ which is used to represent the surface of the earth. A prime is used to denote that the potential function is

so restricted. Returning the reciprocal distance to its closed form and substituting for $A_n(p)$ and $C_n(p)$, one gets:

$$U'_{1A} = \frac{I\rho_1}{2\pi}\left\{\frac{1}{R} + 2\pi\frac{(\rho_1-\rho_2)}{b}\sum_{m=0}^{\infty}(2-\delta_{0m})\cos m\phi \int_0^{\infty}\frac{\left[P^m_{ip-1/2}(\theta)\right]^2}{\rho_1-\rho_2+\rho_1 K^m_p(\xi_1)+\rho_2 L^m_p(\xi_1)}\cdots\right.$$

(180)

$$\cdots\frac{p\tanh\pi p}{\cosh\pi p}\,\frac{\Gamma^2(ip+1/2-m)}{\Gamma^2(ip+1/2+m)}\,P^m_{ip-1/2}(\eta_0)\,P^m_{ip-1/2}(\eta)\,dp$$

Due to the obvious complexity of computations based on equation 180, especially since no tables exist for either the cone functions or the hyperboloid functions, it is of some interest to see what can be done in the way of approximating curves of traverses over dome structures. As an example of this sort of computation, we choose the simplest case in which a depth profile with the Wenner configuration symmetrically situated over the center of a dome whose resistivity is very much smaller than that of the country rock. As an approximation, let ρ_2 be zero in this calculation.

Before going on, it is useful to examine qualitatively the limiting cases of very small or very large electrode separations. The behavior at large separations is dictated by the asymptotic behavior of the hyperboloid. As the surface of the hyperboloid $\xi = \xi_1$ recedes from the origin, it approaches asymptotically the surface of a cone whose apex is at the origin. The cone and the hyperboloid are related such that $\xi_1 = \cos\theta_1$. Therefore, at large electrode separations, one would expect that the curve would behave like the corresponding curve for the conal boundary. This fact is true for all resistivity combinations, and is not restricted to the case being discussed here.

The behavior of the curve for small electrode separations is somewhat more elusive. It is certain, however, that the effect of the dome

on the apparent resistivity would always be less than the effect of a horizontal bed, of infinite depth, whose upper boundary was a horizontal plane tangent to the dome at its apex. This point is brought out better in the illustration to follow.

Consider figure nine in which are shown a set of depth profile curves and the cross-sections of the corresponding boundary surfaces. The depth to the top of each feature is the same in all cases and is arbitrarily chosen to be a unit distance.

The solid line represents a hyperbolic surface, whose flanks dip at an angle of 30 degrees, in the one case and the depth profile over that surface in the other case. The surface labelled "1" is a plane, horizontal boundary; "2" labels the conal asymptote; while "3" and "4" indicate spheres of radius 8 and 5 respectively. The corresponding curves bear the same numbers.

The data for curve 1 is taken from tables published by Roman.[1] Curves 3 and 4 are based on equation 88 and may be thought of as belonging to the set of curves presented in figure seven. The difference between the former curves and the present ones lies in the scale. In the previous case, the unit of distance was the radius of the sphere; while the unit distance in figure nine is the depth to the top of the dome. The resistivity scales are the same in both cases.

The computations for curve 2, based on equation 142, are more complicated. Making ρ_2 zero, and manipulating the potential functions as was done to obtain equation 92, it can be shown that:

$$(181)\quad \frac{\rho_a}{\rho} = 1 + \frac{32}{\pi\sqrt{3}} \sum_{\substack{m=1 \\ odd}}^{\infty} \int_0^{\infty} \frac{P^m_{ip-1/2}(\cos\theta_1)\, P^m_{ip-1/2}(0)\, \cos(p \ln 3)}{\left[P^m_{ip-1/2}(\cos\theta_1) + P^m_{ip-1/2}(-\cos\theta_1)\right] P^{m+1}_{ip-1/2}(0)}\, dp$$

It is noticed at once that the electrode separation "a" has been

---

1. Roman, 1934.

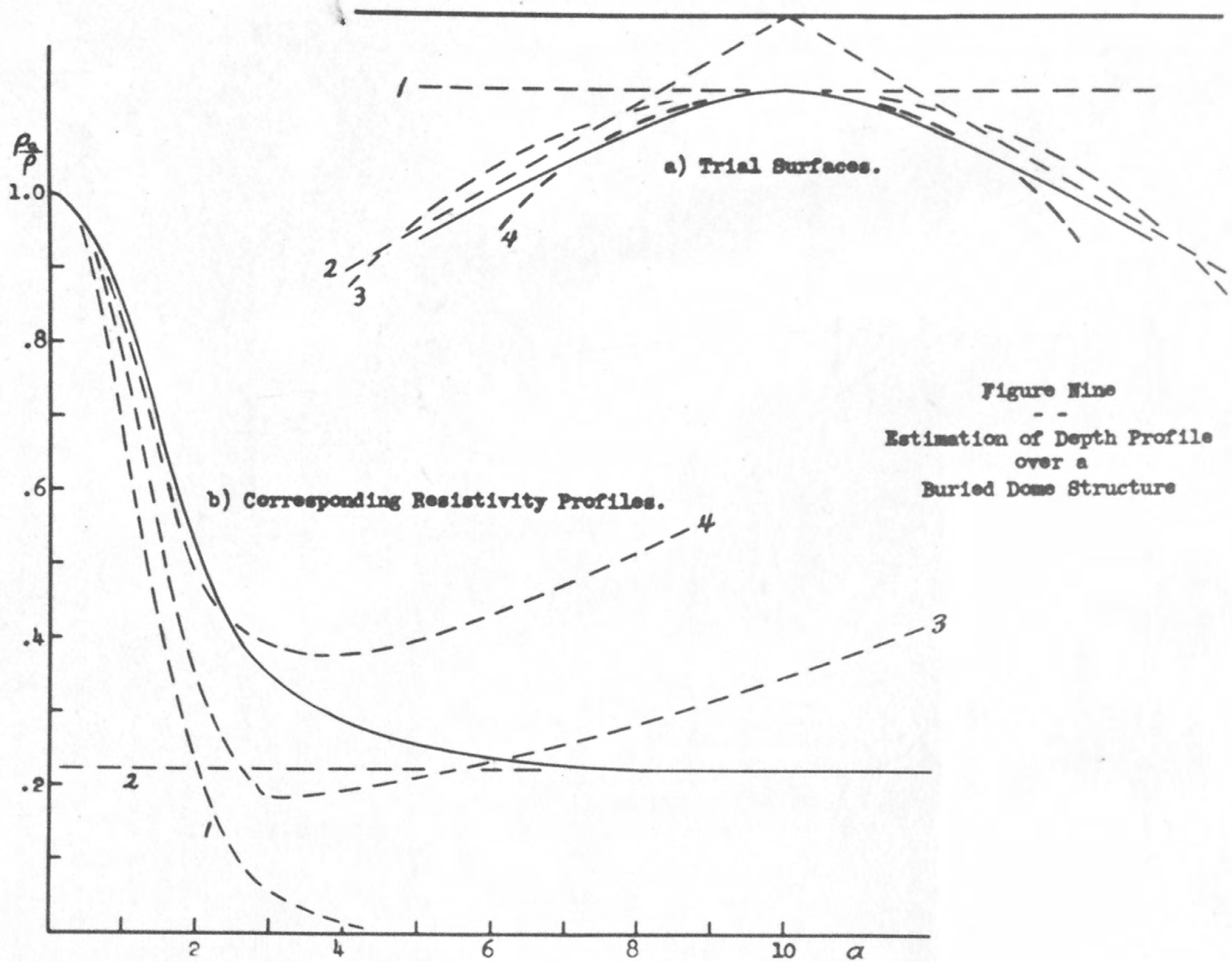

Figure Nine
- -
Estimation of Depth Profile
over a
Buried Dome Structure

eliminated from this expression so that the resulting curve is a horizontal line. That is as it should be since changing the electrode separation serves only to change the scale of the experimental situation.

Since no tables exist of the cone functions, the definitions given by equations 96 and 22 were substituted into equation 181 and as many simplifications as possible were effected before computations were commenced. Fortunately, it was found that only $m=1$ made any appreciable contribution and values of p, in steps of 1/2, up to 6 were more than adequate.

The results are best appreciated by an examination of the curves themselves. Surface 4 follows the hyperboloid closely until they cross at a horizontal distance of 3 from the center. Therefore, curve 4 is used as a basis for the initial behavior of the hyperboloid curve, making allowance for the inexact coincidence of the two surfaces. The next controlling point is furnished by curve 3. Note that surface 2 intersects surface 3 only slightly before surface 3 crosses the hyperboloid. Therefore, it is reasoned that curve 3 intersects the hyperboloid curve at a slightly larger electrode separation than it does curve 2. This fact is used to estimate how rapidly the hyperboloid curve approaches the cone curve. The results are shown in the diagram.

An interesting observation in connection with these curves involves a natural ambiguity which exists. The hyperboloid curve is very similar to the corresponding curve representing a horizontal bed with the same boundary as surface 1, but with a resistivity of about 1/6 that of the overlying material. And, in fact, the two curves approach the same asymptote for large electrode separations. Of course, this ambiguity is removed if the electrode configuration is moved appreciably from its position of symmetry.

XXVI

THE EFFECT OF TOPOGRAPHY

As a final item, we present a problem of some interest in geophysics - that of the situation in which a traverse is being run over ground of uniform resistivity but whose surface is irregular. The interest arises from the necessity of being able to sort out the anomalies due to geologic changes from those due to extraneous causes.

This problem can be illustrated within the framework of the present discussion if one returns to the general case and assumes a single discontinuity along the surface $\xi = \xi_1$ with material of resistivity ρ_1 below and of resistivity ρ_2 above the boundary. The source must then be allowed to enter the boundary; and, finally, ρ_2 is made to approach infinity so that the upper region represents the atmosphere. If ξ_1 is positive, the picture is one of a hyperboloidal bowl; while a negative ξ_1 presents the picture of the crest of a hyperboloidal hill. Let the source be located arbitrarily at $(\eta_0, \xi_0, 0)$ where $\xi_0 > \xi_1$. Then in the region of resistivity ρ_2, the potential is:

$$U_{2B} = \sum_{m=0}^{\infty} \cos m\varphi \int_0^{\infty} \left\{ C_m(p) \begin{matrix} P^m_{ip-1/2}(-\xi_0) P^m_{ip-1/2}(\xi) \\ P^m_{ip-1/2}(\xi_0) P^m_{ip-1/2}(-\xi) \end{matrix} + A_m(p) P^m_{ip-1/2}(\xi) \right\} P^m_{ip-1/2}(\eta)\, dp \tag{182}$$

In the region where $\xi < \xi_1$, the potential can be written as:

$$U_{1B} = \sum_{m=0}^{\infty} \cos m\varphi \int_0^{\infty} B_m(p) P^m_{ip-1/2}(-\xi) P^m_{ip-1/2}(\eta)\, dp \tag{183}$$

Here, as in previous cases, $A_m(p)$ and $B_m(p)$ are arbitrary functions of p, also depending on m; but, unlike the previous section, $C_m(p)$ has

exactly its value given in equation 175. Consideration of the boundary conditions yields the following simultaneous equations:

$$-A_m(p) + B_m(p) K_p^m(\xi_1) = C_m(p) P_{ip-1/2}^m(\xi_0) K_p^m(\xi_1)$$

(184)

$$\rho_1 A_m(p) + \rho_2 B_m(p) L_p^m(\xi_1) = \rho_1 C_m(p) P_{ip-1/2}^m(\xi_0) L_p^m(\xi_1)$$

where $K_p^m(\ )$ and $L_p^m(\ )$ are as given by equations 101 and 138. Solving these equations for $A_m(p)$ and $B_m(p)$, one gets:

$$A_m(p) = \frac{(\rho_1-\rho_2) K_p^m(\xi_1) L_p^m(\xi_1)}{\rho_1 K_p^m(\xi_1) + \rho_2 L_p^m(\xi_1)} C_m(p) P_{ip-1/2}(\xi_0)$$

(185)

$$B_m(p) = \frac{\rho_1 [K_p^m(\xi_1) + L_p^m(\xi_1)]}{\rho_1 K_p^m(\xi_1) + \rho_2 L_p^m(\xi_1)} C_m(p) P_{ip-1/2}^m(\xi_0)$$

From this point on, we need consider only equation 183. Substituting the correct values for $B_m(p)$ and $C_m(p)$, and letting $\xi_0 \to \xi_1$, one gets for the potential in the region of resistivity ρ_1 :

$$U_{1B} = \frac{I\rho_2}{4\pi} \frac{\pi\rho_1}{b} \sum_{m=0}^{\infty} (2-\delta_{0m}) \cos m\varphi \int_0^{\infty} \frac{p \tanh \pi p}{\cosh \pi p} \frac{\Gamma^2(1/2+ip-m)}{\Gamma^2(1/2+ip+m)} \cdots$$

(186)

$$\cdots \frac{K_p^m(\xi_1) + L_p^m(\xi_1)}{\rho_1 K_p^m(\xi_1) + \rho_2 L_p^m(\xi_1)} P_{ip-1/2}^m(\xi_1) P_{ip-1/2}^m(-\xi) P_{ip-1/2}^m(\eta_0) P_{ip-1/2}^m(\eta)\, dp$$

Now, if both the numerator and denominator in equation 186 are divided by ρ_2 and then ρ_2 is allowed to increase without limit, one gets the final result:

$$U = \frac{I\rho}{4\pi} \sum_{m=0}^{\infty} \frac{\pi(2-\delta_{0m})}{b} \int_0^{\infty} \frac{p \tanh \pi p}{\cosh \pi p} \frac{\Gamma^2(\frac{1}{2}+ip-m)}{\Gamma^2(\frac{1}{2}+ip+m)} \cdots$$

(187)

$$\frac{K_p^m(\xi_1) + L_p^m(\xi_1)}{L_p^m(\xi_1)} P_{ip-1/2}^m(\xi_1) P_{ip-1/2}^m(-\xi) P_{ip-1/2}^m(\eta_0) P_{ip-1/2}^m(\eta)\, dp$$

where the subscripts on the potential and resistivity have been dropped

because there is no longer need for them. By noting that part of this expression is nothing but the expansion of the reciprocal distance, one may write it as an alternate form:

$$U = \frac{I\rho}{4\pi}\left\{\frac{1}{R} + \sum_{m=0}^{\infty}\frac{\pi(2-\delta_{0m})}{b}\cos m\phi\int_0^{\infty}\frac{p\tanh\pi p}{\cosh\pi p}\,\frac{\Gamma^2(1/2+ip-m)\ldots}{\Gamma^2(1/2+ip+m)\ldots}\right.$$

(138)

$$\ldots\frac{K_p^m(\xi_1)}{L_p^m(\xi_1)}P_{ip-1/2}^m(\xi_1)P_{ip-1/2}^m(-\xi)P_{ip-1/2}^m(\eta_0)P_{ip-1/2}^m(\eta)\,dp$$

Either of these expressions may be used to calculate the potential distribution due to a point source of current located at the surface of the earth near the crest of a hill or near the bottom of a bowl shaped depression.

PART SIX

INVESTIGATION OF A GEOLOGIC PROBLEM

XXVII

THE USE OF HORIZONTAL PROFILES

In the Tri-State lead and zinc district, which consists of parts of Missouri, Kansas, and Oklahoma, ore occurs in a variety of deposits. In a certain part of the district, the main mode of occurrence is in connection with a slump structure, as it is called in that locality.

The geologic horizon which is of prime interest in this vicinity is the contact between the Mississippian and Pennsylvanian formations.[1] Underlying the whole of the area under consideration is the Mayes (Mississippian) limestone. The Cherokee (Pennsylvanian) shale lies unconformably upon the Mississippian in the western part of the region. There is a regional dip in the structure of some 15 to 20 feet per mile to the northwest. The outcrop of the contact between these two formations runs through the present region in a roughly northeasterly line. This discussion applies mostly to the part of the region which lies immediately to the southeast of the boundary outcrop.

In a broad sense, the steps followed in the deposition of the ore have been as follows.[2] At some time after the Mayes formation had been deposited, it was uplifted and became exposed at the surface of the earth. During this time, it was subject to unusual solution activity by percolating ground water. As a result, the limestone became

---

1. Martin et al., 1939.
2. Private communication from Dr. K.L. Cook, United States Geological Survey.

infested with solution channels and caverns. Eventually, as the process continued the roofs of some of the caverns failed, leading to the formation of sinks and probably to a moderate Karst topography.

With the subsequent encroachment of the sea, the Cherokee shales were laid down, first filling the sinks which at that time appeared as pockets in the bottom of the Pennsylvanian sea. Yet later, the area was once again uplifted and subjected to erosion. The result has been a re-exposure of the top of the Mayes formation southeast of the contact outcrop. And throughout much of the surface of the exposed limestone, there appears today a large number of shale filled sinks.

At some undetermined time during the above process, the water which was moving through the rock was rich in mineral content, including a comparatively high percentage of lead and zinc sulphides. It happened that many of the cracks and crevices which were left in the wake of the solution stage, and in some instances the solution channels themselves, presented conditions favorable to the deposition of the ore minerals. These include sphalerite, galena, etc. Since most of the fracturing occured near the periphery of the sinks, it is there that the ore is most likely to be found.

Therefore, the picture which is presented is one of a shale filled sink in limestone country rock. And usually, in such cases there exists considerable mineralization near the periphery of the sink, either inside or outside, or both. Since the resistivity of the shale is of the order of one-fifth that of the surrounding limestone, one of the most appropriate means of searching for such structures is a resistivity survey. Actually, this paper grew out of an obvious need, observed by

the present author in the field, for an increased knowledge of the behavior of resistivity profiles in the vicinity of the filled sinks.

In figure ten is shown a comparison of an actual field profile and a theoretical horizontal profile drawn by two different techniques. Information about the geology of the example chosen is meager.[3] At the present writing, only one hole has been drilled, that being on the line of the traverse shown and at station 1825k. The drilling indicated about 45 feet of shale, followed by massive limestone. A second hole has been located 75 feet to the east of the first. Drilling is in progress, but as yet no specific results have been reported. It is known that this feature exists in a position, of the order of one mile square, in which considerable ore has been recovered from shale plugs of the size indicated for the present one.

The field curve (b) is plotted in accordance with normal practice for treating Lee configuration data in the field. The solid line represents ρ_1 and the dashed line ρ_2. In each case, the value of the apparent resistivity is plotted against the position of the mid-point of the line connecting the two electrodes between which the appropriate potential difference is measured. Note that the apparent resistivities are not plotted against the station, which is the position of P_0, at which they are determined.

In order to approximate the field profile, it was first noted that the sharp peaks in that curve appear 200 feet apart. Previous calculations showed that the sharpest maxima occur 25 feet from the discon-

---

3. The present author assisted in the resistivity survey over this area as well as over the area of the second example to be presented later; and, further, he is in close contact with the progress of the drilling project which is based on the results of the survey.

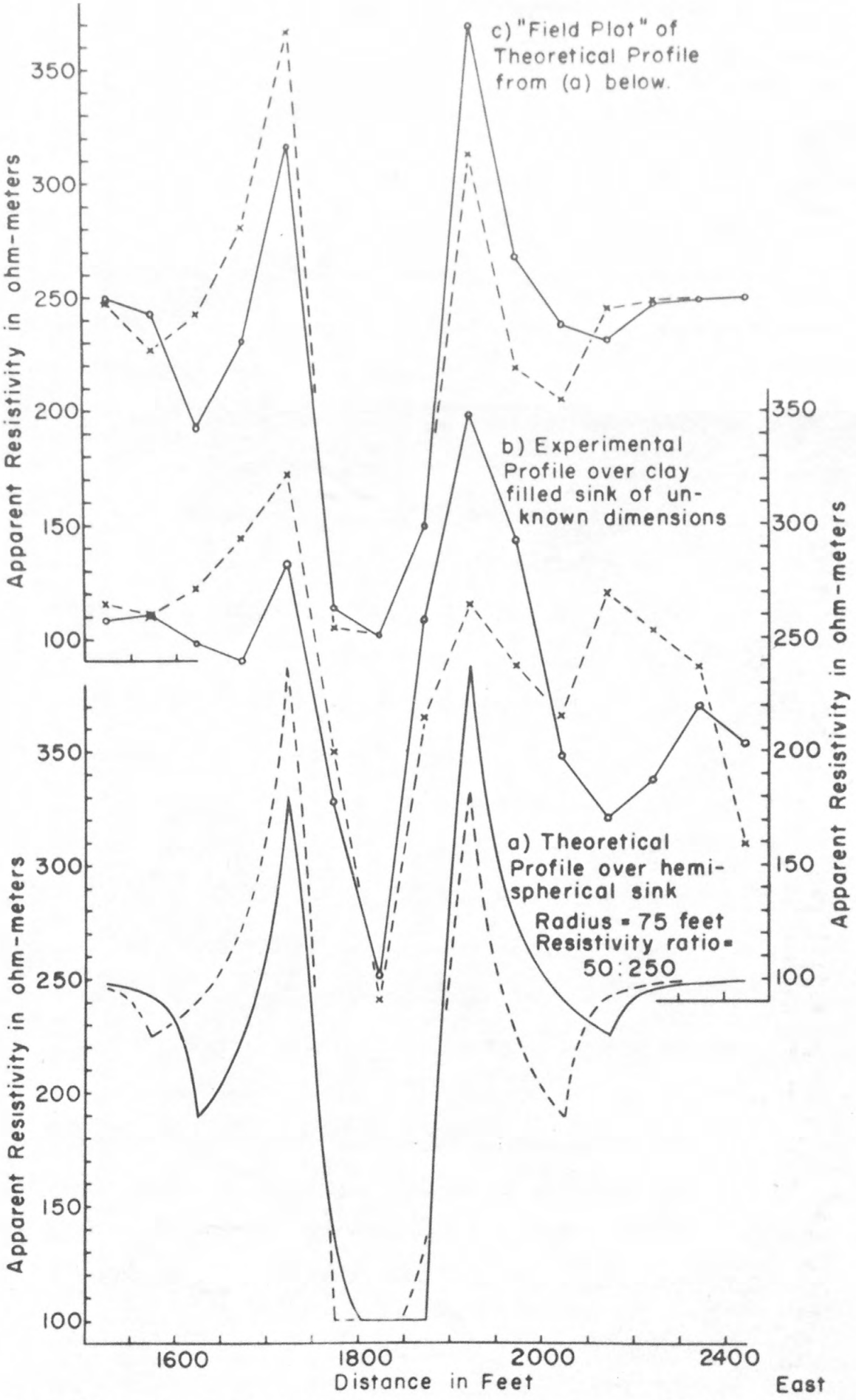

Figure Ten – Comparison of Horizontal Profiles using the Lee configuration with an electrode separation of 100 feet.

tinuity. Therefore, a hemispherical sink 75 feet in radius was chosen for trial computations. It also seemed appropriate, from field observations, to assume a ratio of 1:5 for the resistivity of the material within the sink to the resistivity of the material on the outside. After the calculations based on these assumptions were made, a choice of 50 ohm-meters as the constant of proportionality yields excellent agreement between the total anomaly observed and that calculated.

The results of the theoretical calculations are shown in (a) of figure ten. Obviously, one would not expect to find a field curve which possesses the smooth character of this theoretical curve. Therefore, an alternate means of presenting the theoretical data has been devised. Since points were taken every 50 feet, which is one-half the electrode separation of 100 feet, when the experimental data were obtained, points 50 feet apart on (a) have been selected and connected by straight lines. Such a procedure changes the appearance of the theoretical curve, even to the extent of destroying its symmetry. Curve (c) has been constructed in this manner. Although, by a variation in the set of points chosen, a large number of these curves may be constructed from (a), it is felt that this one serves its purpose in pointing out the possibility of plotting theoretical data by this new method.

One principal point is to be noted in this discussion. Still referring to the example in figure ten, one can see that any theoretical curve, corresponding to (c) and having been derived from (a), will have sharp maxima separated by a distance of 200 feet. In fact, one finds in general that, if the traverse crosses any inhomogeneity near its center, the highest peaks on the curve are separated by a distance equal to the

width of the disturbance (as measured along the traverse) plus the value of the electrode separation.

Thus, one concrete finding is that one may determine the width of an outcropping inhomogeneity by this technique although the exact position of the outcrop can not be determined within a possible error equal to one-half the electrode separation. It is possible, however, to eliminate this uncertainty by taking stations closer together in the region in which the resistivity curves indicate something of interest.

In trying to match field curves with theoretical curves, one must ever bear in mind the extreme heterogeneity of the earth. This explains for example the inexact correspondence between (b) and (c). The author has not been able to find any reasonable explanation of the strange separation of the two curves in (b) which is found at the eastern extremity of the diagram.

XXVIII

THE USE OF EQUIRESISTIVITY MAPS

A second common practice of presenting the results of field work is in the form of equiresistivity maps. For example, the Wenner resistivity is noted on a map at each station at which data was taken. Then, "contours" are drawn, at predetermined intervals, through points which have the same value of the resistivity. The method which one uses in drawing these contours is much the same as is used in drawing a standard topographic map. When hachures appear on a closed contour, they indicate that the apparent resistivity is decreasing in the direction in which the hachures point.

An alternate form of the equiresistivity map is constructed by using

Figure Eleven

Geologic Section Along Traverse 21500

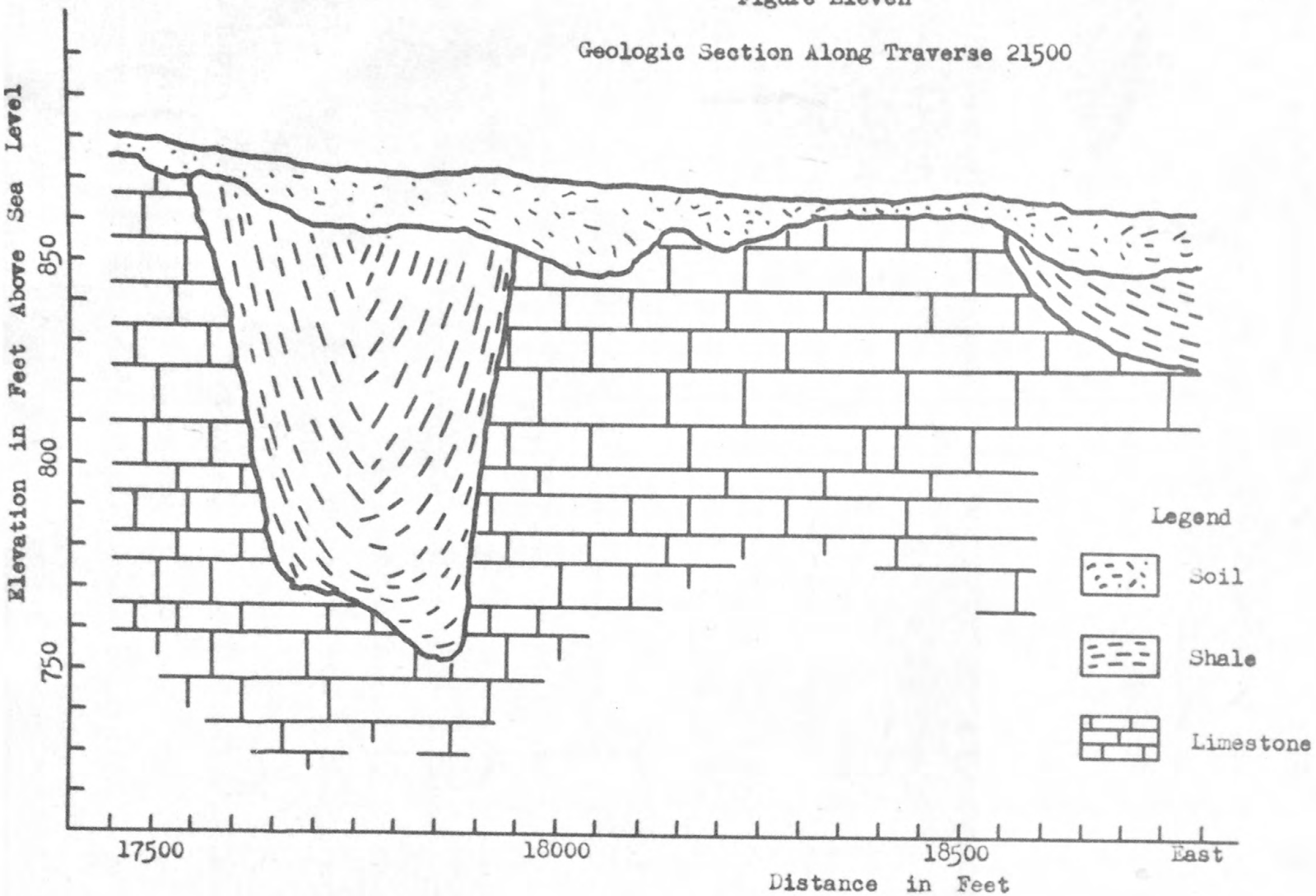

the data obtained through the Lee configuration. One takes a set of curves similar to (b) in figure ten. The first step is to draw a third broken line which represents the average value of the two resistivities as they are plotted in that diagram. These average values will, in general, differ somewhat from the value of the apparent resistivity as determined with the Wenner configuration. Finally, it is these average values which are plotted on the map and upon which the position of the contours is based. This map may be referred to as "Lee plotting" as differentiated from the "Wenner plotting" which was described in the previous paragraph.

The geologic structure, over which the present examples of resistivity surveys were taken, is shown in figure eleven on the previous page.[1] This cross-section is based on the findings of a drilling program which consisted of a line of holes 50 feet apart across the whole feature. It should be reported that, as the cross-section is drawn, the vertical scale is exaggerated 5 times over the horizontal scale.

The deeper of the shale pockets is postulated to be a true filled sink. Its actual shape however is unknown and it is one of the objects of this paper to reveal how the shape may be determined with a minimum of expensive drilling. This aspect of the question will be treated more fully in the following section.

The shallower of the shale features, which extends off the diagram to the east, is some 1000 feet wide and several times as long. It is thought to be the expression of an ancient solution valley which was

---

1. This diagram has been adapted from a cross-section prepared by the Salt Lake City office of the U.S.G.S. under the supervision of Dr. Cook.

filled with clay and shale when the Cherokee formation was laid down. And, as such, it presents a much less likely structure in which to find ore.

The Wenner and Lee plotting of the equiresistivity map are found in figures twelve and thirteen respectively. The data upon which the map is based were obtained from stations 50 feet apart along the traverses which run east-west; the traverses are separated 100 feet from each other in the north-south direction. The markers at the bottom and left of the diagrams refer to a convenient coordinate system. Note that the above cross-section was taken along traverse 21500N, which runs through the center of the feature upon which we are to focus our attention - the low area just west of the center of the map. However, the cross-section does not cover as much of the traverse as do the equiresistivity maps.

Since this area of resistivity low appears on the map in a roughly elliptical form, we have tried, as a first approximation, to duplicate this portion of the map by assuming that the sink has the form of a hemisphere. In units equal in magnitude to the electrode separation, the radius of the hemisphere was chosen to be 2; and, as in the previous example, the ratio of the resistivity of the material within the sink to that outside of the sink was chosen to be 1:5. A traverse was passed through the center of the hemisphere and was followed by parallel traverses at distances of 1, 1.73, 2 (tangent), 2.31, and 3 units from the center of the hemisphere. The irrational numbers which appear are the square roots of 3 and 4/3 and were chosen to facilitate computations.

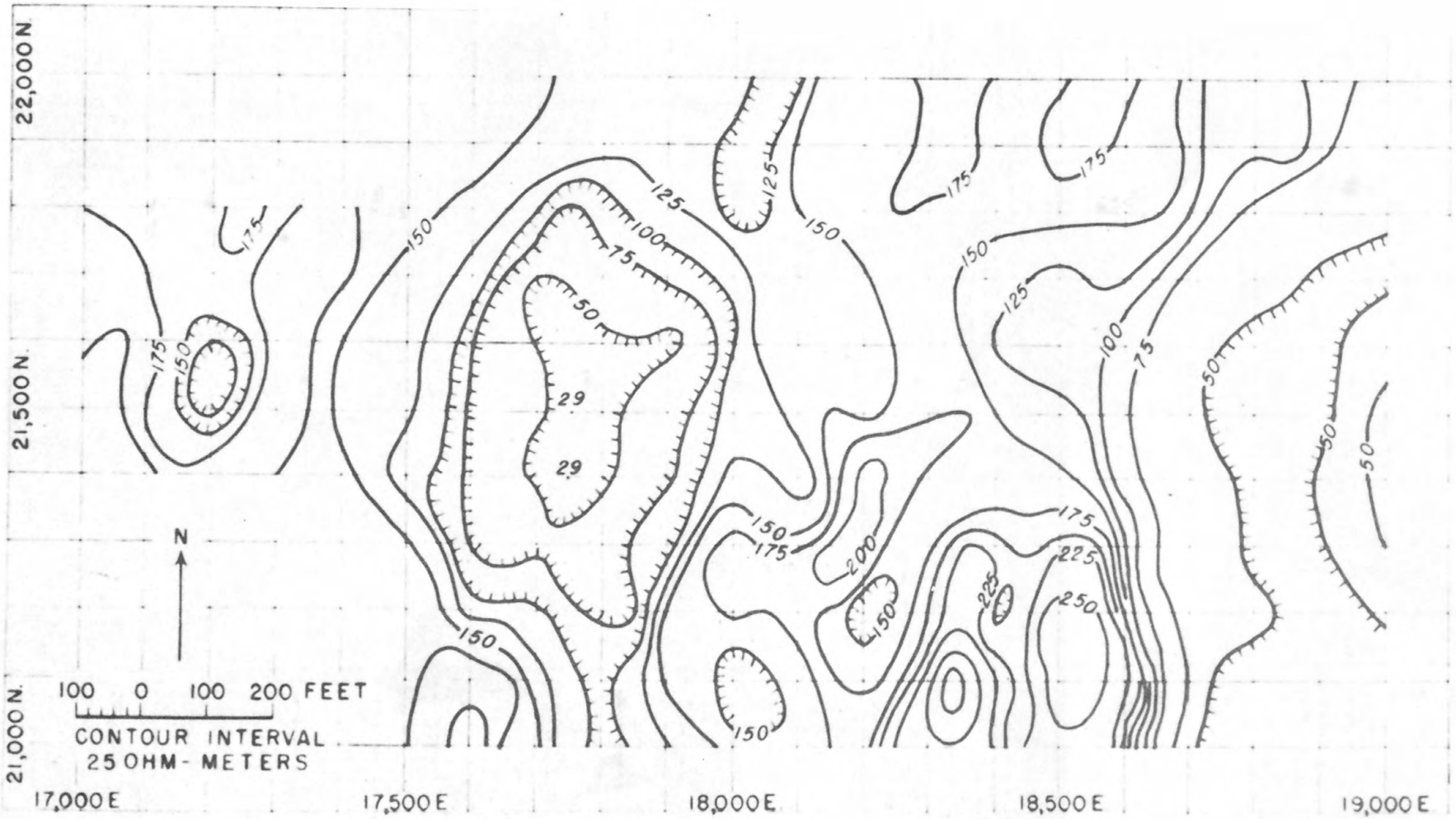

Figure Twelve - Equiresistivity Map (Wenner Plotting) over Filled Sink.

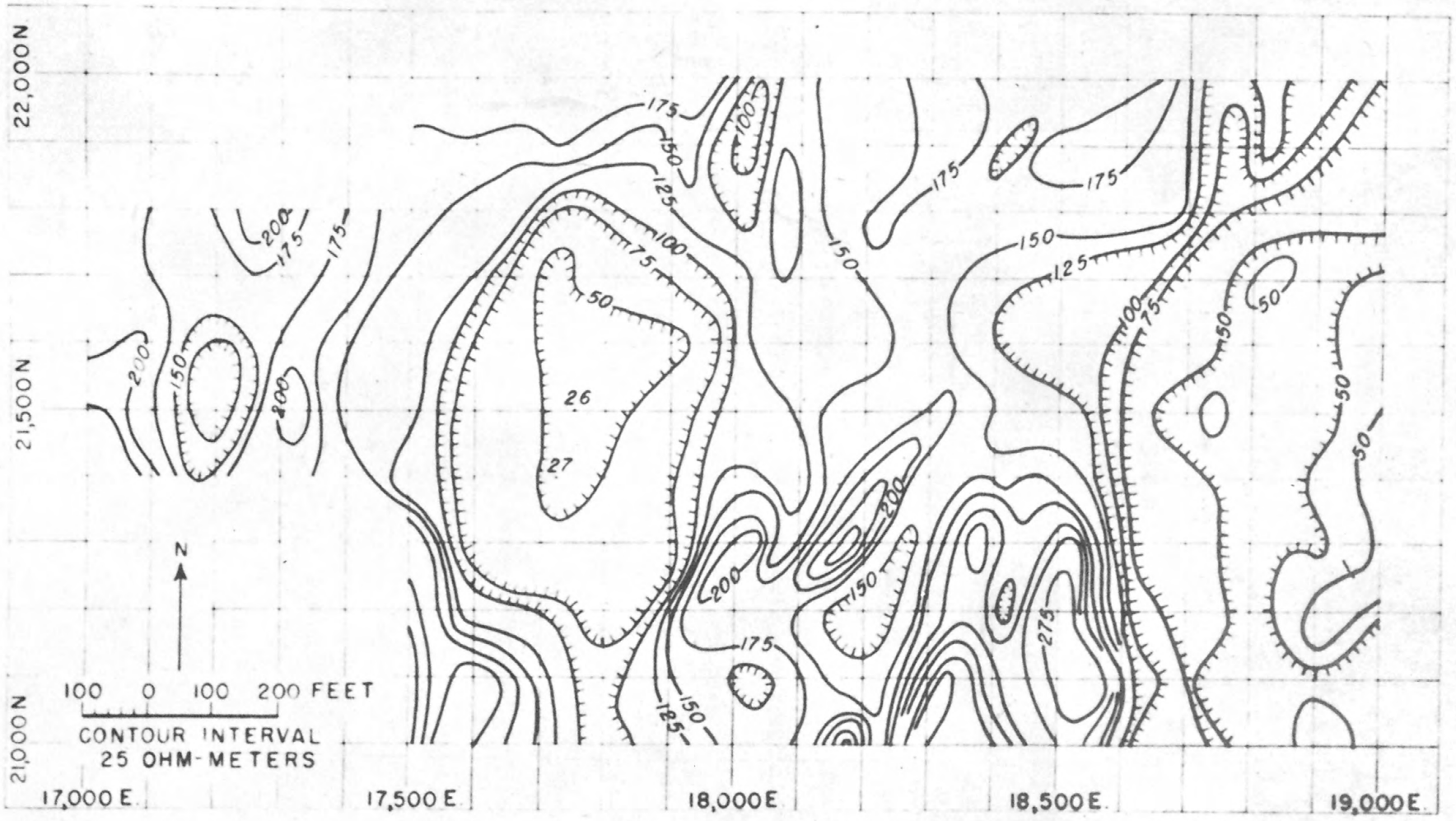

Figure Thirteen - Equiresistivity Map (Lee Plotting) over Filled Sink.

The Wenner and Lee plotting of the equiresistivity map based on the theoretical data are shown in figures fourteen and fifteen respectively. Care must be exercised in comparing these maps with the ones based on field data because they do not employ the same resistivity scale. In order to make an exact comparison, one should introduce a proportionality factor of about 38 ohm-meters in the theoretical data; after which, the contours should be re-drawn at 25 ohm-meter intervals as was done in the field maps.

However, even without these modifications, some conclusions may be drawn by comparing the two sets of maps. When the resistivity data is presented in this form, the hemispherical approximations appear to be wholly inadequate, although it may well be that the failure of the theory may be due in part to extraneous geologic inhomogeneities which exist immediately adjacent to this sink. The large shale feature in the east part of the section undoubtedly plays an important part; and it is known that there is a sandstone cap which outcrops just to the west of the slump. Further, there is a great possibility that there are fractures between the two shale outcrops which would alter the appearance of the resistivity curves and of these maps.

It is apparent that, of the two electrode configurations stressed in this paper, the Wenner configuration is the more simple and the less expensive. The additional central electrode and the necessary wire is eliminated; the instrumentation can be simplified; and at least one man can be dropped from the work party. In this connection, there is a perennial argument among geophysicists as to whether the Lee configuration yields enough additional data to warrant the extra expense.

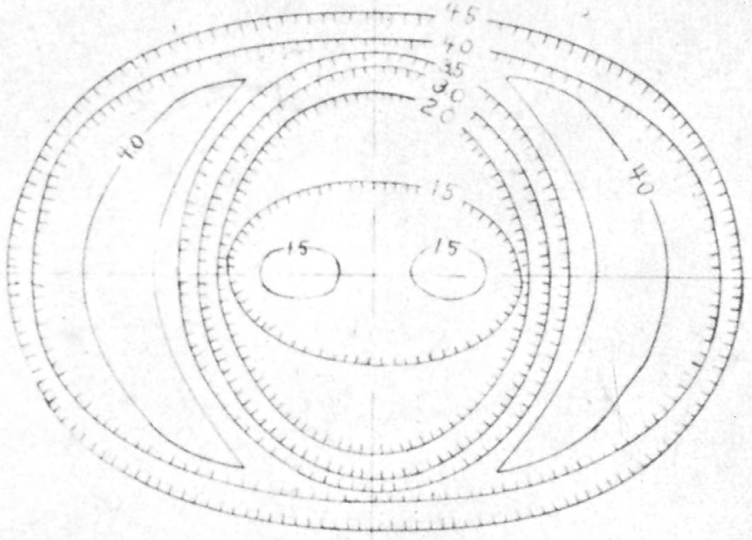

Figure Fourteen - Theoretical Equiresistivity Map (Wenner Plotting) over Hemispherical Sink.

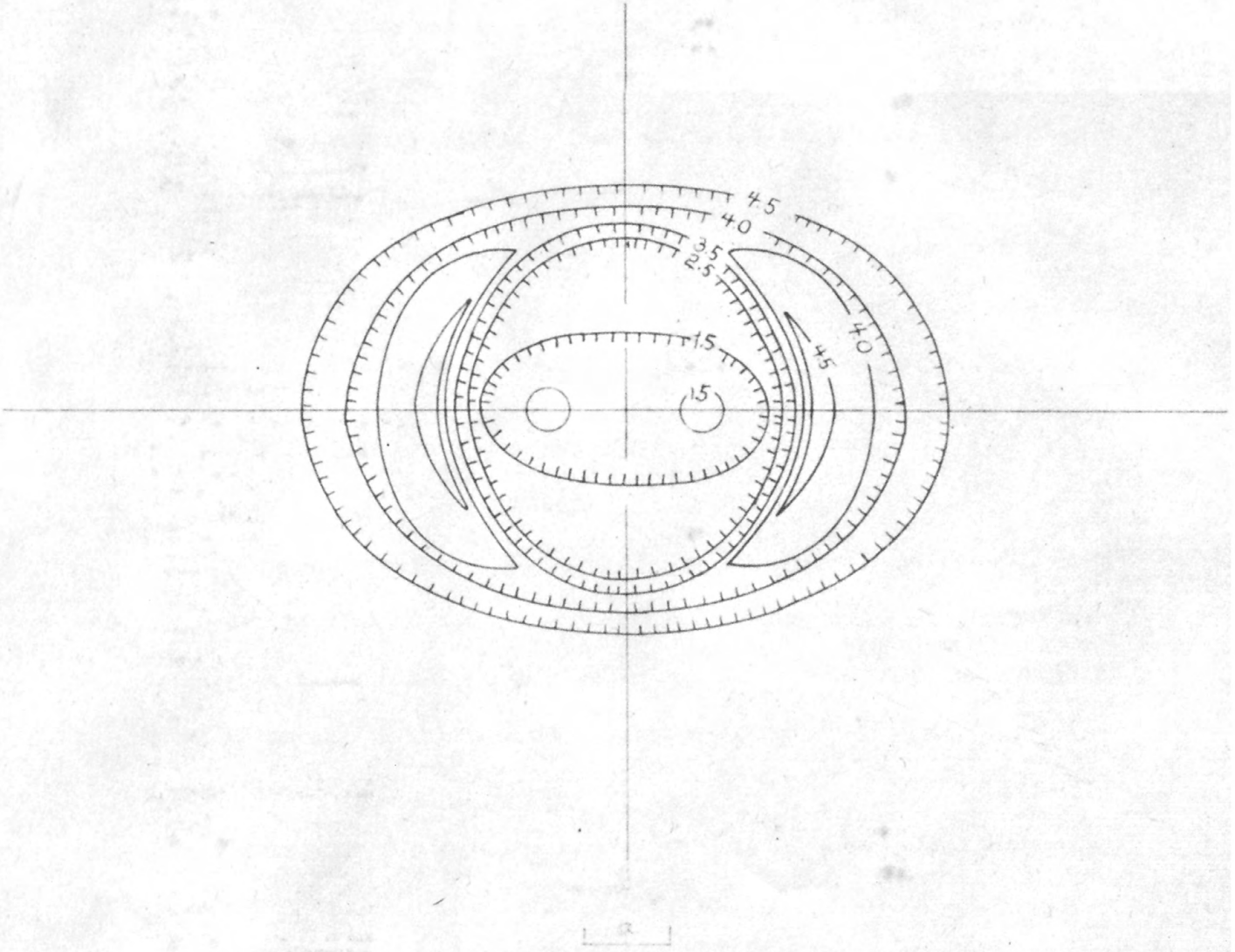

Figure Fifteen - Theoretical Equiresistivity Map (Lee Plotting) over Hemispherical Sink.

Part of the answer is to be found in the equiresistivity maps which have been presented, and in this one point the theory and practice seem to agree.

The gradients, as indicated by the density of contour lines in a direction normal to the lines themselves, are always steeper in the case of the Lee data. And the anomalies are definitely more pronounced in that case than they are in the Wenner plotting. Consider for example the high which occurs at about 21300N-10200E in figure thirteen. The apparent resistivity reaches a peak above 250 ohm-meters at this point. At the corresponding point, in figure twelve, only the 200 ohm-meter contour appears. The second closed contour which appears just to the west of the first in the Lee plotting, does not appear at all in figure twelve. Corresponding differences appear in the theoretical plots.

XIIA

THE USE OF DEPTH PROFILES

In current practice, depth profiles are normally associated with the determination of the depth to contacts between horizontal formations. In this section, it is suggested that depth profiles may well serve as an aid in outlining the outcrop of features other than horizontal beds.

In evidence for this argument, two sets of theoretical curves are presented. Figure sixteen shows depth profiles made over three separate bodies, together with cross-sections of the bodies. The solid line indicates the hemispherical sink, the dashed line one-half an oblate spheroid, and the dotted line one-half a prolate spheroid. The ratio of the radii of revolution are .5528:1:1.944, where the radius of the

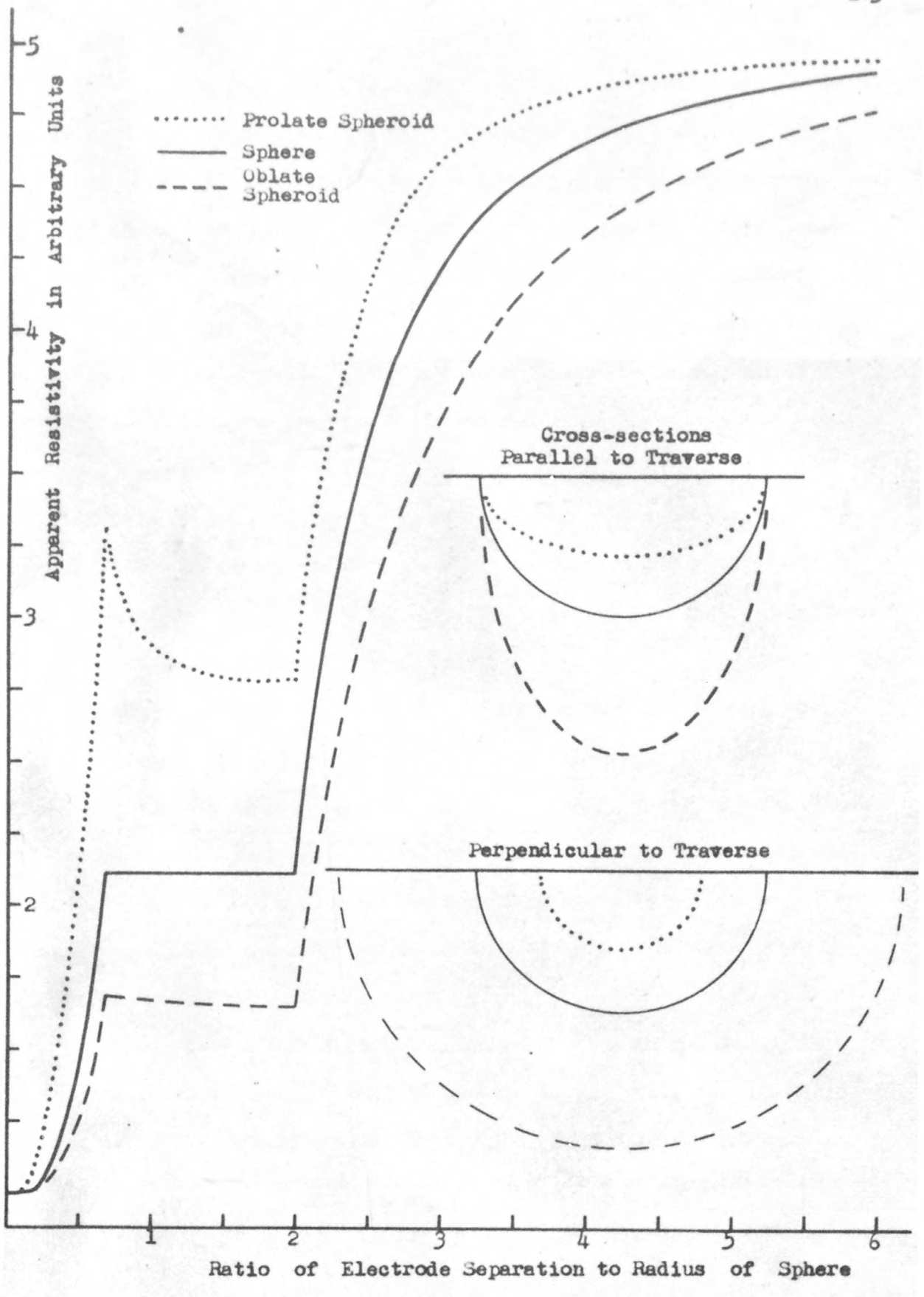

Figure Sixteen - Comparison of Depth Profiles Over Various Filled Sinks.

hemisphere is taken to be unity.

It should be noted that the upper cross-section may also be thought of as one-half of the plan view of the outcrop of the sink.

The traverse line, in each case coincides with the axis of revolution of the figure which is the reason the lower cross-sections appear as a series of concentric circles. The center of the electrode configuration is kept over the center of the body. Due to the symmetry in the theoretical case, there is no difference in the shape of the curves which one would get with the Lee configuration and those which would be obtained with the Wenner configuration.

It is surprising how much the curves resemble each other, considering the large variation in the volume of the foreign material involved. The ratio of the volumes is .3055:1:3.778, which is of course the square of the ratio of the radii given above.

It is noted that the average height of the plateau, in each of the above curves, above the value of the lowest resistivity (1) present is roughly inversely proportional to the corresponding radii of revolution. If the values of those average heights is chosen to be 1.90, 1.11, and .65, the ratio corresponding to the one given above is 1.7:1:.58. Obviously, considerably more work is required to establish a definite empirical relationship of this sort.

The most useful feature of these curves is the abrupt change in slope which occurs when the various electrodes pass over the boundaries of the sink. Starting from the origin, the first break occurs when the current electrode passes into the material outside of the sink. The curves all approach a horizontal orientation, the upper one actually

experiencing the most marked change in the slope. It is reasonable to assume that other prolate spheroids, which are smaller than the one shown, would present even sharper peaks than does the present one.

At the point where the potential electrode passes outside of the sink, the curve resumes its sharp upward trend, finally approaching the value of the resistivity of the material outside of the sink as an asymptote.

In figure seventeen, it is illustrated how a depth profile changes in its characteristics as the traverse line is removed from the center of the feature. The curve for traverse A is identical with that given for the hemisphere in the previous diagram, except that the scale has been changed slightly.

The curves for the traverses outside of the sink give some indication as to how close a traverse must be for an anomaly to be observed in connection with a sink of this type. The reasoning follows that in section XVII and will not be repeated at this point. It is simply observed that a traverse, which passes at a distance from the center equal to twice the radius, would scarcely be expected to indicate an anomaly. This result agrees closely with the conclusions drawn concerning the buried spheres in section XVII. Although similar curves have not been drawn for the ellipsoids, the general behavior of these other curves may easily be deduced if it is necessary.

It is proposed that the conduct of a survey over an area such as was described in the two preceding sections be organized roughly as follows. A reconnaissance survey using horizontal profiling should first be run with the traverses separated by appropriate intervals which

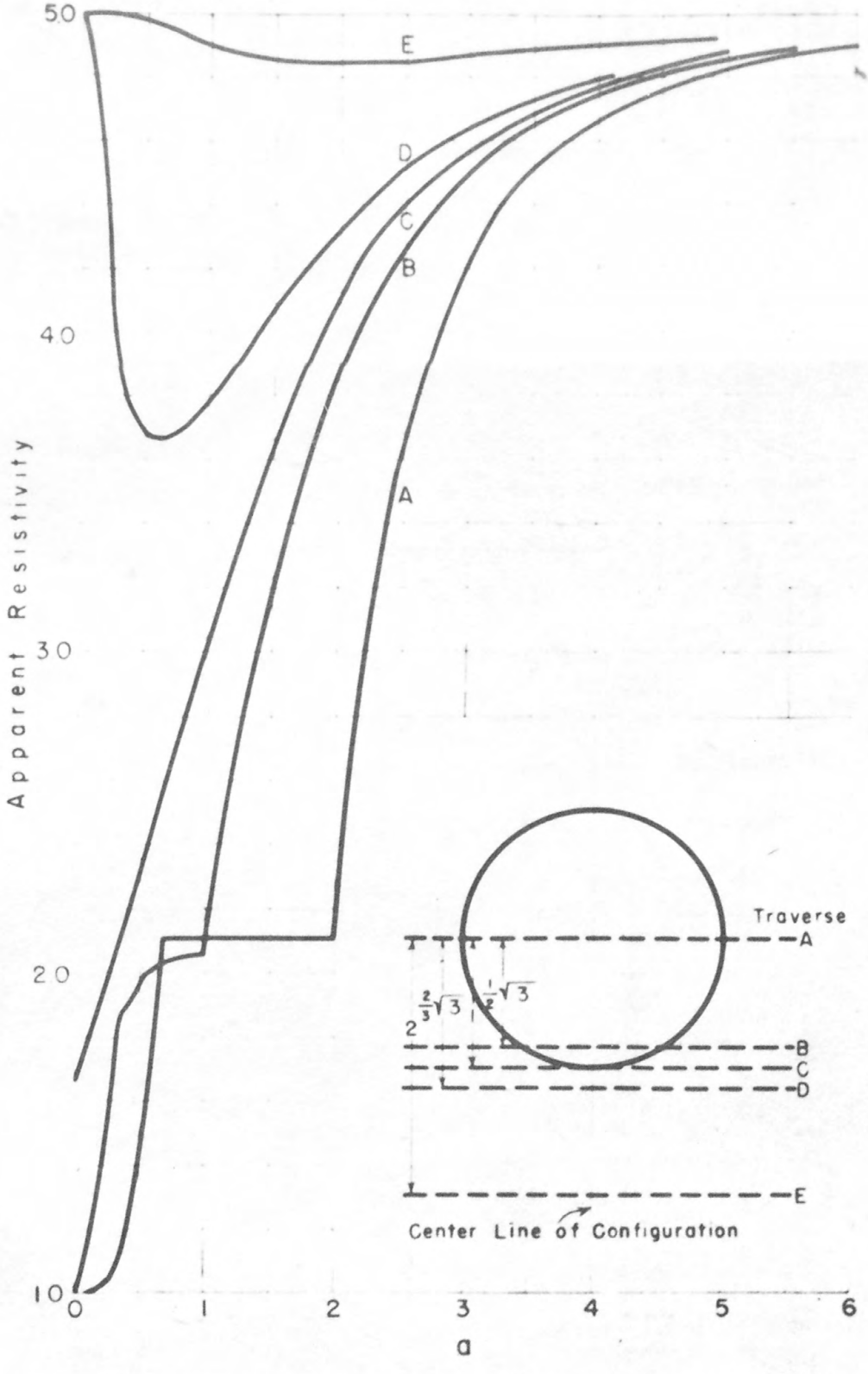

Figure Seventeen - Theoretical Depth Profiles over Hemispherical Sink.

will be governed largely by the amount of detail which is desired and by the amount of time and money which is available. If nothing is sought but the regions of resistivity lows, the Wenner configuration would be adequate. Equiresistivity maps may then be prepared and the likely areas outlined for further work.

In order to outline the outcrop of the sink as closely as possible, it is suggested that depth profiles be made over these areas of low resistivity, using traverses of varied orientation but with P_0 always kept at a fixed point which should be as close to the center of the feature as possible. Fortunately, as is seen in figure seventeen, the change in shape of the curve is small when the traverse is moved only a short distance from the center of the sink.

Although, in the theoretical case, there is no difference between the Lee and Wenner curves, it is conceivible that the Lee configuration would be of considerable value if the center of the configuration is not exactly at the center of the sink. In any case, the sinks are in general irregular in outline. So, as the different electrodes cross the boundaries, the two branches of the Lee curves would serve to give the desired information on the opposite sides of the sink.

In closing, it is remarked that this work has led to a second project, in this section of the Tri-state district, for which the field work probably will be completed early next year. Detailed resistivity work will be done following the recommendations of Dr. Cook and this author and based on the results of this dissertation. The worth of the above technique will be one of the things to be tested during this new project.

BIBLIOGRAPHY

Aldredge, M. F.; "The Effect of Dipping Strata on Earth Resistivity Determinations"; Colorado School of Mines Quarterly; XXXII (1937); 171-186.

Martin, R. S., et al.; "Contributions to a Knowledge of the Lead and Zinc Deposits of the Mississippi Valley Region"; U.S.G.S. Special Paper 24 (1939); 154 pp.

Bateman, H.; "Some Integral Equations of Potential Theory"; J. Math. Phys.; XVII (1946); pp. 91-102.

Carslaw, H. S.; Fourier Series and Integrals; New York; Dover Publications, Inc.; 1930; 368 pp.

Ehrenburg, W. G. and Watson, R. J.; "Mathematical Theory of Electrical Flow in Stratified Media;" N.Y.M.E. Tech. Publ. 309 (1931); 16 pp.

Gish, O. H. and Rooney, W. J.; "Measurement of the Resistivity of Large Masses of Undisturbed Earth"; Terr. Mag. and Atmos. Elec.; XXX (1925); 161-188.

Hall, R. H.; "The Application of Non-integral Legendre Functions to Potential Problems"; J. Math. Phys.; XX (1949); 925-931.

Heiland, C. A.; Geophysical Exploration; New York; Prentice Hall; 1940; 1013 pp.

Hobson, E. W.; The Theory of Spherical and Ellipsoidal Harmonics; Cambridge; The University Press; 1931; 500 pp.

Hubbert, M. King; "Results of Earth Resistivity Surveys on Various Geologic Structures in Illinois"; Trans. A.I.M.E.; CX (1934); 9-39.

Hummel, J. N.; "A Theoretical Study of Apparent Resistivity in Surface Potential Methods"; Trans. A.I.M.E.; XCVII (1932); 392-422.

Jahnke, Eugene and Emde, Fritz; Tables of Functions; New York; Dover Publications; 1943; 303 pp.

Jakosky, J. J.; Exploration Geophysics; Los Angeles; Trija Publishing Company; 1950; 1195pp.

Jakosky, J. J., Troyer, R. A. and Wilson, G. H.; "Geophysical Investigations in the Tri-State Zinc and Lead Mining District"; Kansas State Geological Survey Bull. 44; Dec. 1942; 151 pp.

Jeffreys, Harold and Bertha; Mathematical Physics; Cambridge; The University Press; 1950; 703 pp.

Klein, Felix; Vorlesungen Über die Hypergeometrische Funktion; Berlin; Julius Springer; 1933; 344 pp.

Lundquist, R.; "Associated Legendre Polynomial Approximations"; J. Ann. Math.; XXII (1951); 87-89.

Lee, F. S.; "Method of Conducting Geological Survey"; U. S. Patent 1,951,788; 20 March 1934.

Lee, F. S.; "Sand Extension Surveys in Southern Ohio"; R.R.C.A. Preliminary Report; 1948; 86 pp.

Lipskaya, N. V.; "The Disturbance of Electrical Fields by Spherical Inhomogeneities"; Akad. Nauk SSSR Izv., Ser. Geofiz. i Geofiz.; XIII (1949); 409-427.

Lipskaya, N. V.; "The Field of a Point Electrode Observed on the Earth's Surface near a Buried Conducting Sphere"; Akad. Nauk SSSR Izv., Ser. Geofiz. i Geofiz.; XIII (1949); 409-427.

Lowan, Arnold N. (Project Director); Tables of Associated Legendre Functions; New York; Columbia University Press; 1945; 291 pp.

MacRobert, T. M.; Spherical Harmonics; New York; Dover Publications; 1948; 372 pp.

Magnus, Wilhelm and Oberhettinger, Fritz; Formulas and Theorems for Special Functions of Mathematical Physics; New York; Chelsea Publishing Company; 1949; 172 pp.

Mehler, F. G.; "Über die Vertheilung der statischen Electricität in einem von zwei Kugelkalotten begrenzten Körper"; Crelle's Journal; LXVIII (1868); 134-150.

Mehler, F. G.; "Die Kugelfunktionen"; Math. Ann.; XVIII (1881); 161-194.

Neumann, C.; "Über die Mehler'schen Kugelfunktionen"; Crelle's Journal; LXVIII (1868); 195-236.

Noman, Irwin; "The Calculation of Electrical Resistivity for a Region Underlying Two Uniform Layers"; Geor. Inst. and Stud. Rep.; XXXVIII (1933); 185-202.

Noman, Irwin; "Resistivity Reconnaissance"; J. Geoph. Research; 1934. Manuscript (58 pp.) in hands of the editor.

Noman, Irwin; "Some Interpretations of Earth Resistivity Data"; Trans. A.I.M.E.; CX (1934); 135-147.

Noman, Irwin; "Superposition in Interpretation of Two-Layer Earth Resistivity Curves"; Geophys. Prob. 7(2); 1941.

Schiff, Leonard I.; Quantum Mechanics; New York; McGraw-Hill; 1949; 404 pp.

Skalskaya, I. F.; "Field of a Point Source of Current Situated on the Earth's Surface above an Inclined Stratum"; J. Tech. Phys. USSR; XVIII (1948); 1242-1254.

Smythe, William R.; Static and Dynamic Electricity; New York; McGraw-Hill; 1950; 615 pp.

Snow, Chester; The Hypergeometric and Legendre Functions with Application to Integral Equations of Potential Theory; National Bureau of Standards; 1942; 319 pp. (handwriting)

Stefanescu, S., Schlumberger, Conrad and Schlumberger, Marcel; "Sur la Distribution Electrique Potentielle autour d'une Prise de Terre Ponctuelle dans un Terrain a Couches Horizontales, Homogenes et Isotropes"; J. Phys. et Rad.; Ser. 7; I (1930); 132-141.

Stratton, J. A.; Electromagnetic Theory; New York; McGraw-Hill; 1941; 615 pp.

Tagg, G. F.; "Interpretations of Earth Resistivity Measurements"; Trans. A.I.E.E.; 53 (1934); 392-422.

Tallqvist, Rj.; "Sechsstellige Tafeln der 16 ersten Kugelfunktionen $P_n(x)$;" Acta Societatis Scientiarum Fennicae; Nova Ser. A; Tom II, No. 4 (1930); 43 pp.

Tallqvist, Rj.; "Sechsstellige Tafeln der 32 ersten Kugelfunktionen $P_n(\cos\ )$"; Acta Societatis Scientiarum Fennicae; Nova Ser. A; Tom II, No. 11 (1938); 43 pp.

Tikhonov, A. N.; "Concerning Electrical Sounding over an Inclined Layer"; Inst. Geofiz. Akademii (Moscow); I (1946); 110-136.

Watson, G. N.; The Theory of Bessel Functions; Cambridge; The University Press; 1945; 804 pp.

Wenner, Frank; "A Method of Measuring Earth Resistivity"; U. S. Bureau of Standards Scientific Paper 258; 11 October 1915; 469-478.

Whittaker, E. T. and Watson, G. N.; Modern Analysis; Cambridge; The University Press; 4th Edition (1927); 608 pp.

NOV 1956

USGS LIBRARY - RESTON
3 1818 00083486 9